

DRAFT

Black

52

Note: This is a reference cited in AP 42, *Compilation of Air Pollutant Emission Factors, Volume I Stationary Point and Area Sources*. AP42 is located on the EPA web site at www.epa.gov/ttn/chief/ap42/

The file name refers to the reference number, the AP42 chapter and section. The file name "ref02_c01s02.pdf" would mean the reference is from AP42 chapter 1 section 2. The reference may be from a previous version of the section and no longer cited. The primary source should always be checked.

0, #2

AIR POLLUTION TECHNOLOGY, INC.

Flux Force/Condensation Scrubber System

For Collection of Fine Particulate

Emissions from An Iron Melting Cupola

by

Richard B. Chmielewski and Seymour Calvert

Air Pollution Technology, Inc.
4901 Morena Blvd., Suite 402
San Diego, California 92117

Contract No. 68-02-2191

EPA Project Officer: Dale L. Harmon

4901 MORENA BLVD., SUITE 402 SAN DIEGO, CA 92117 (714) 272-0050

Notice

This document is a preliminary draft. It has not been formally released by EPA and should not at this stage be construed to represent Agency policy. It is being circulated for comment on its technical accuracy and policy implications.

DRAFT



P
3
6
8
29
34
38
39
40
41
43
49
51
→ 66
115
117
120
124
125

LIST OF FIGURES, Continued

<u>Figure</u>		<u>Page</u>
7-28	Predicted and Experimental Penetration Run 37/3	94
7-29	Predicted and Experimental Penetration Run 37/4	95
7-30	Predicted and Experimental Penetration Run 37/5	96
7-31	Predicted and Experimental Penetration Run 37/6	97
7-32	Predicted and Experimental Penetration Run 37/7	98
7-33	Predicted and Experimental Penetration Run 37/8	99
7-34	Predicted and Experimental Penetration Run 37/9	100
7-35	Predicted and Experimental Penetration Run 37/10	101
7-36	Predicted and Experimental Penetration Run 37/11	102
7-37	Predicted and Experimental Penetration Run 37/12	103
7-38	Predicted and Experimental Penetration Run 37/13	104
7-39	Predicted and Experimental Penetration Run 37/15	105
7-40	Predicted and Experimental Penetration Run 37/16	106
7-41	Predicted and Experimental Penetration Run 37/17	107
7-42	Predicted and Experimental Penetration Run 37/18	108
7-43	Predicted and Experimental Penetration Run 37/19	109
7-44	Predicted and Experimental Penetration Run 37/21	110
7-45	Predicted and Experimental Penetration Run 37/23	111
7-46	Predicted and Experimental Penetration Run 37/24	112
7-47	Predicted and Experimental Penetration Run 37/25	113
7-48	Predicted and Experimental Penetration Run 37/26	114

LIST OF FIGURES, Continued

<u>Figure</u>		<u>Page</u>
7-7	Predicted and Experimental Penetration Run 36/4	73
7-8	Predicted and Experimental Penetration Run 36/5	74
7-9	Predicted and Experimental Penetration Run 36/6	75
7-10	Predicted and Experimental Penetration Run 36/7	76
7-11	Predicted and Experimental Penetration Run 36/8	77
7-12	Predicted and Experimental Penetration Run 36/9	78
7-13	Predicted and Experimental Penetration Run 36/10	79
7-14	Predicted and Experimental Penetration Run 36/11	80
7-15	Predicted and Experimental Penetration Run 36/12	81
7-16	Predicted and Experimental Penetration Run 36/13	82
7-17	Predicted and Experimental Penetration Run 36/14	83
7-18	Predicted and Experimental Penetration Run 36/15	84
7-19	Predicted and Experimental Penetration Run 36/16	85
7-20	Predicted and Experimental Penetration Run 36/17	86
7-21	Predicted and Experimental Penetration Run 36/18	87
7-22	Predicted and Experimental Penetration Run 36/19	88
7-23	Predicted and Experimental Penetration Run 36/20	89
7-24	Predicted and Experimental Penetration Run 36/21	90
7-25	Predicted and Experimental Penetration Run 36/22	91
7-26	Predicted and Experimental Penetration Run 37/1	92
7-27	Predicted and Experimental Penetration Run 37/2	93

LIST OF FIGURES

<u>Figure</u>		<u>Page</u>
3-1	Particle Size Distribution Site One	9
3-2	Particle Size Distribution Site Two	10
3-3	Particle Size Distribution Site Three	11
4-1	F/C Demonstration Plant Flow Diagram Induced Draft	15
4-2	F/C Demonstration Plant Flow Diagram Forced Draft	16
4-3	Induced Draft System (Plan View)	17
4-4	Induced Draft System (Elevation View)	18
4-5	Forced Draft System (Plan View)	19
4-6	Forced Draft System (Elevation View)	20
4-7	Process Flow Sheet Induced Draft System	21
4-8	Process Flow Sheet Forced Draft System	22
4-9	Photograph of Saturator and Condenser	25
4-10	Settler	26
4-11	Condenser, Scrubber and Cooling Tower	26
4-12	Exhaust Fan Wheel	26
4-13	Fan Wheel Detail	31
5-1	Modified EPA Sampling System with In Stack Cascade Impactor	45
6-1	Simplified F/C Scrubber System	47
6-2	Example of Initial and Grown Size Distribution	55
6-3	Example of Condenser, Scrubber and Combined Penetration	56
7-1	Histogram of Condenser Inlet Mass Concentration	67
7-2	Average Condenser Inlet Size Distribution	68
7-3	Average Condenser Inlet Cumulative Size Distribution	69
7-4	Predicted and Experimental Penetration Run 36/1	70
7-5	Predicted and Experimental Penetration Run 36/2	71
7-6	Predicted and Experimental Penetration Run 36/3	72

LIST OF TABLES

<u>No.</u>		<u>Page</u>
3-1	Summary of Alternate Cupola Operations	7
4-1	Pump Specifications	33
4-2	Flow Measurement Specifications	40
6-1	Input Variables For Prediction Of Scrubber Performance	53
6-2	Example Calculation	54
7-1	F/C Scrubber System Operating Parameters For 36 Series	60
7-2	F/C Scrubber System Operating Parameters For 37 Series	61
7-3	Gas Flow Rates, Temperatures and Measured Condensation Ratio For 36 Series	62
7-4	Gas Flow Rates, Temperatures and Measured Condensation Ratio For 37 Series	63
7-5	Particulate Mass Concentrations	64
7-6	Particulate Mass Concentrations	65
8-1	Summary of Equipment Costs F/C Scrubber System	118
8-2	Summary of Equipment Losses Conventional Scrubber	119
8-3	Direct and Indirect Cost F/C System	121
8-4	Direct and Indirect Cost Conventional Scrubber	122
8-5	Summary of Power Requirements	123
8-6	Summary of Annual Operating Costs	123

TABLE OF CONTENTS

I.	INTRODUCTION	1
II.	SUMMARY, CONCLUSIONS, RECOMMENDATIONS.	3
III.	SITE SELECTION	6
IV.	SYSTEM DESIGN.	14
V.	PERFORMANCE TESTING.	40
VI.	SYSTEM PERFORMANCE MODEL	46
VII.	COMPARISON OF EXPERIMENTAL RESULTS AND PERFORMANCE MODEL.	59
VIII.	ECONOMIC ANALYSIS.	115

SECTION 1
INTRODUCTION

Flux force/condensation (F/C) scrubbing has been developed by Air Pollution Technology under EPA-sponsorship for the past several years. The objectives of (F/C) scrubbing involve reducing the power requirement for collection of fine particulate compared to conventional high energy scrubbers. The improvement in scrubber performance due to condensation effects is most apparent in the sub-micron size range where the mechanism of inertial impaction is difficult to apply economically.

There are three condensation effects which are utilized in F/C scrubbing. The condensation of water vapor from a hot saturated gas can be caused by contacting with a colder liquid. The suspended particles in the gas act as condensation nuclei resulting in growth of the particulate due to condensation of water vapor. The transfer of water vapor toward the cold liquid results in diffusiophoresis. This mechanism collects particles by movement of the condensing water vapor toward the cold surface. Simultaneously, the temperature gradient established in the condenser results in a thermal force which results in collection by thermophoresis. The particle growth due to condensation plus the flux forces of diffusiophoresis and thermophoresis enhance the particle collection efficiency of the F/C scrubber system.

This report presents the results of a demonstration project to verify the design methods and economics of flux force/condensation scrubbing on a large scale in an industrial environment. The F/C system was designed, built and tested on the total exhaust gas stream from a 12,500 Kg/hr iron melting cupola. The operating experience involved seven months of operation. This included summer, fall and winter in a demanding environment resulting in a

good test of the equipment design and materials selection.

Performance tests were made over a period of several months. The test results verified the design methods and showed that the F/C scrubber system could meet all emission limits at a lower power requirement than a conventional high energy scrubber. An economic analysis showed that a F/C scrubber system has a lower annual operating cost compared to a high energy scrubber.

SECTION 2

SUMMARY, CONCLUSIONS, and RECOMMENDATIONS

SUMMARY

The objectives of this program were to demonstrate the performance and economics of a flux force/condensation scrubber system in an industrial environment. The major tasks were:

1. Select a company in the iron and steel industry suitable for the demonstration scrubber.
2. Design the demonstration scrubber system for the chosen site.
3. Prepare a test plan.
4. Fabricate, install and start up F/C system.
5. Conduct test program.
6. Maintain laboratory capability to support test program.
7. ~~Engineering analysis of system performance.~~
8. ~~Site restoration, if needed.~~
9. Recommendations for a future demonstration plant.

All of the required tasks were completed. Since the system has been appraised and purchased by the host company, no site restoration was required.

A survey of three iron melting cupolas revealed that the main process parameters of exhaust gas temperature, flow rate and particulate concentration varied from site to site. Even for similar sized cupolas the gas flow rate, temperature, particle mass concentration, and size distribution varied. The site chosen had the largest production rate and uncontrolled mass emission rate of the three investigated.

The process weight limit required that the overall system penetration be less than 0.16 (16%) based on measured emission rates

after the spray saturator. The mass mean aerodynamic diameter was found to average about 1.2 μ m. The F/C scrubber system required a total power requirement of 233 Kw (299 HP) versus 345 Kw (462 HP) for a conventional high energy scrubber. This power savings was obtained by (1) reducing the necessary pressure drop for the F/C system and by (2) reducing the volumetric flow rate of the exhaust gas which occurs during the F/C process due to cooling.

The total annual operating cost for an F/C system operating on this source was estimated to \$84,400 compared to \$111,500 for a high energy scrubber.

CONCLUSIONS

The following conclusions can be drawn from the results of this study:

1. The performance data verified design methods developed by A.P.T. on previous EPA contracts.
2. The F/C scrubber system was built, operated for 6 months, and shown to be in compliance with all applicable air pollution regulations for that site.
3. The F/C scrubber system required only about 65% of the power requirement of a conventional high energy scrubber to achieve the same performance.
4. The emissions from the cupola varied in terms of particle mass concentration and size distribution during the charging cycle. In this regard continuous or semi-continuous charging operation with conveyor system would probably help reduce the variation in emissions which was observed.
5. The particle number concentration is very important in F/C scrubbing. For a given amount of condensation the number of particles which receive the condensed water determine the grown particle size.
6. The solids/liquid separation presented some maintenance problems and suggests that additional attention be given to equipment design, both to prevent settling in the scrubber equipment and to improve settling in the water

treatment system.

7. Corrosion can be a serious problem in this type of application. Sulfuric and sulfurous acids from the sulfur in the coke as well as carbonic acid must be neutralized in order to prevent significant deterioration of steel components in the system. Maintenance of the proper circulating water pH is also important if stainless materials are used because of the chloride content present.
8. Operation over a 6 month period showed that the F/C system is capable of performing well and without significant difficulty in the demanding conditions of a ferrous foundry. During the entire test period there were no production stoppages due to the F/C scrubbing system.
9. Incidental benefits for both plant operation and air pollution control came as a consequence of the detailed engineering study of the cupola operation.

SECTION 3

SITE SELECTION

ALTERNATIVE SITES

The site selection for the F/C demonstration plant involved preliminary investigation of three foundry operations. The first candidate was a foundry department in a shipyard which produced grey iron castings for use in the shipbuilding activities. The cupola had an internal diameter of 0.94 m and a melting rate of approximately 2,700 kg/hr (3 ton/hr). This cupola was operated with an iron to coke ratio which ranged from 5.6 to 7.2 depending upon the type of material being charged. The average iron to coke ratio was about 6.

This foundry operation produced a number of castings which required close attention to the composition of the metal produced. As a consequence each charge of coke, flux, iron and steel was weighed before charging and close control of melt rate and temperature was maintained.

Molten metal was taken from the cupola into a ladle which was used to pour the castings. This resulted in intermittent withdrawal of metal from the cupola, consequently the tuyere blower was operated in an on and off manner. The result was a wide variation in exhaust gas flows, temperature and particle concentration.

Table 3-1 summarizes the operating parameters for this foundry as well as two additional foundries which were evaluated. Particulate sampling tests were performed at a location downstream of the hot gas quencher.

The second foundry produced cast iron pipe and fittings. The cupola was significantly larger having an internal diameter

11/21 2:20P
 2:20P 10/25 7/2000

TABLE 3-1. SUMMARY OF ALTERNATE CUPOLA OPERATIONS

	<u>Site 1</u>	<u>Site 2</u>	<u>Site 3</u>
Cupola Diameter (m)	0.94	1.67	1.67
Charge Wt. (kg)	438	682	1,815
Melt Rate (kg/hr)	2,700	10,250	12,500
Iron to Coke Ratio	6	7	6
Tuyere Air (DNm ³ /s)	1.0	2.5	3.5
Exhaust Gas Flow (DNm ³ /s)	2.5	5.8	6.6
Exhaust Gas Temperature (°C)	600-950	350-1,050	350-1,100
*Exhaust Gas Particle Concentration (g/DNm ³)	1.0	1.5	1.8
	#/m 19.9	68.9	85.5
	#/ton (melt) 6.69	6.00	94.3
	9.36 #/ton	7.12	6.84
*Measured after quencher	8.02		8.21

1.0 g/DNm³ x 2.5 DNm³/s x 3600 s/hr
 = 9000 g/hr
 9 kg/hr
 / 2.700 Mg/hr
 3.3

2:20P 10/25

of 1.67 m and a melt rate of approximately 10,250 kg/hr. Table 3-1 shows the process conditions for this cupola. The iron to coke ratio for this cupola averaged about 7. The charges were weighed before being loaded into the cupola. The tuyere air flow rate was controlled with an orifice meter, damper and an automatic controller.

The molten metal from this cupola was withdrawn continuously into a holding ladle from which metal was taken for various casting operations. This continuous operation resulted in process conditions which were more uniform.

The third site investigated was a foundry which produced metal shot. The cupola had an internal diameter of 1.67 m. The production rate varied from about 8,200 kg/hr to 13,500 kg/hr depending upon the charging rate. The metal was withdrawn continuously from the cupola. Neither the charge weight nor the tuyere air flow rate was measured regularly by the foundry personnel.

PARTICULATE DATA FROM PRELIMINARY TESTS

Particulate sampling tests were performed at each of the three sites primarily to obtain particle size distribution data. Sampling was performed using the University of Washington cascade impactors. A few Method 5 total filter runs were made to determine particle concentration and mass flow rate. Figures 3-1, 3-2, and 3-3, show the particle size distribution measured with the U.W. impactors at the three sites. In each case the sampling was performed at a location downstream of the spray quenchers which were used to cool the hot cupola exhaust gas. The design of the quench systems varied from plant to plant, however, each of the quench systems utilized preformed sprays, which probably resulted in some collection of larger particulate matter.

The particle size distribution measurements at each site were found to be reasonably consistent from run to run. At the first site the average mass mean particle aerodynamic diameter was found to be about 0.45 μm . The average mass concentration

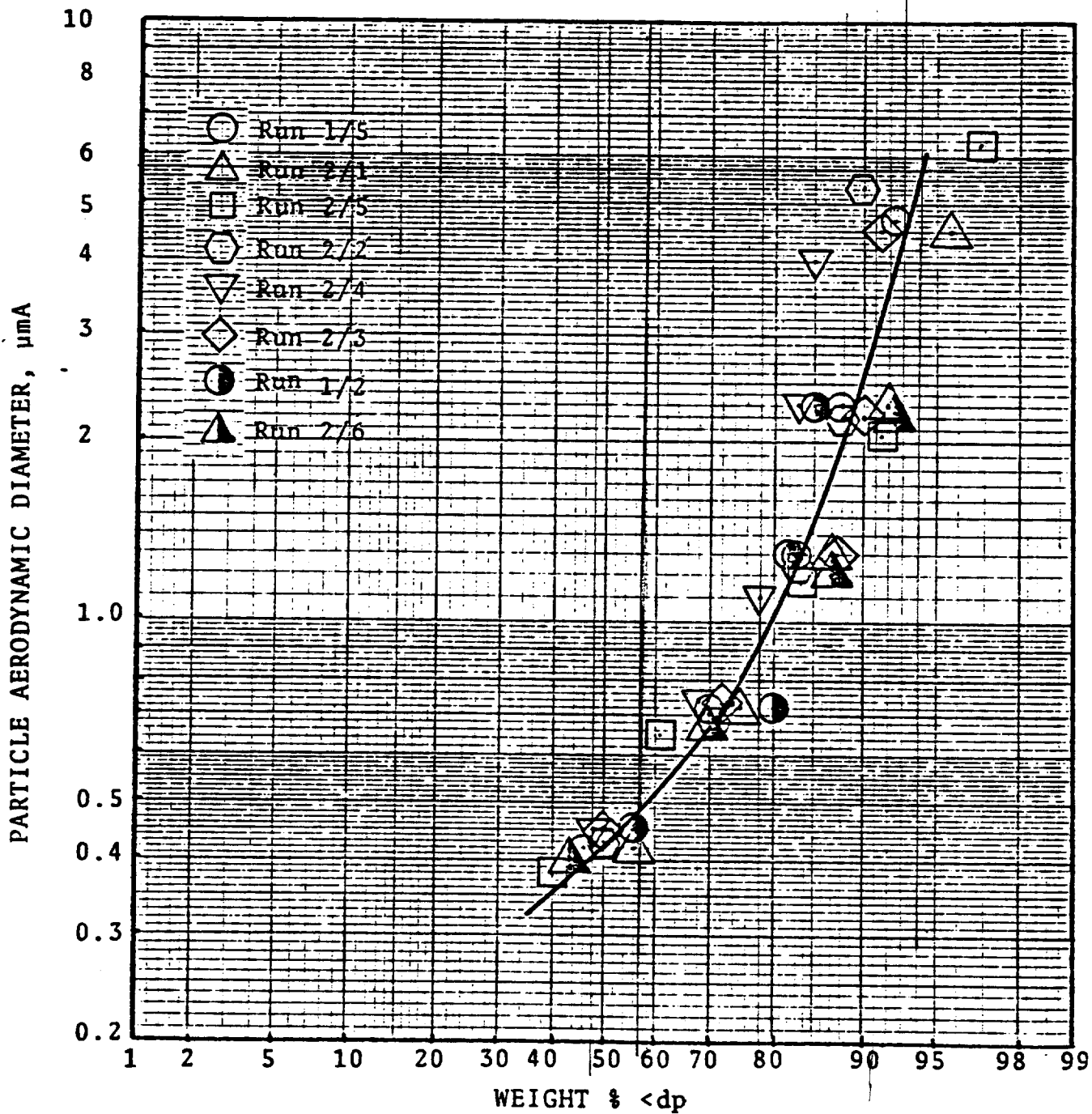


Figure 3-1. Particulate Size Distribution Site One

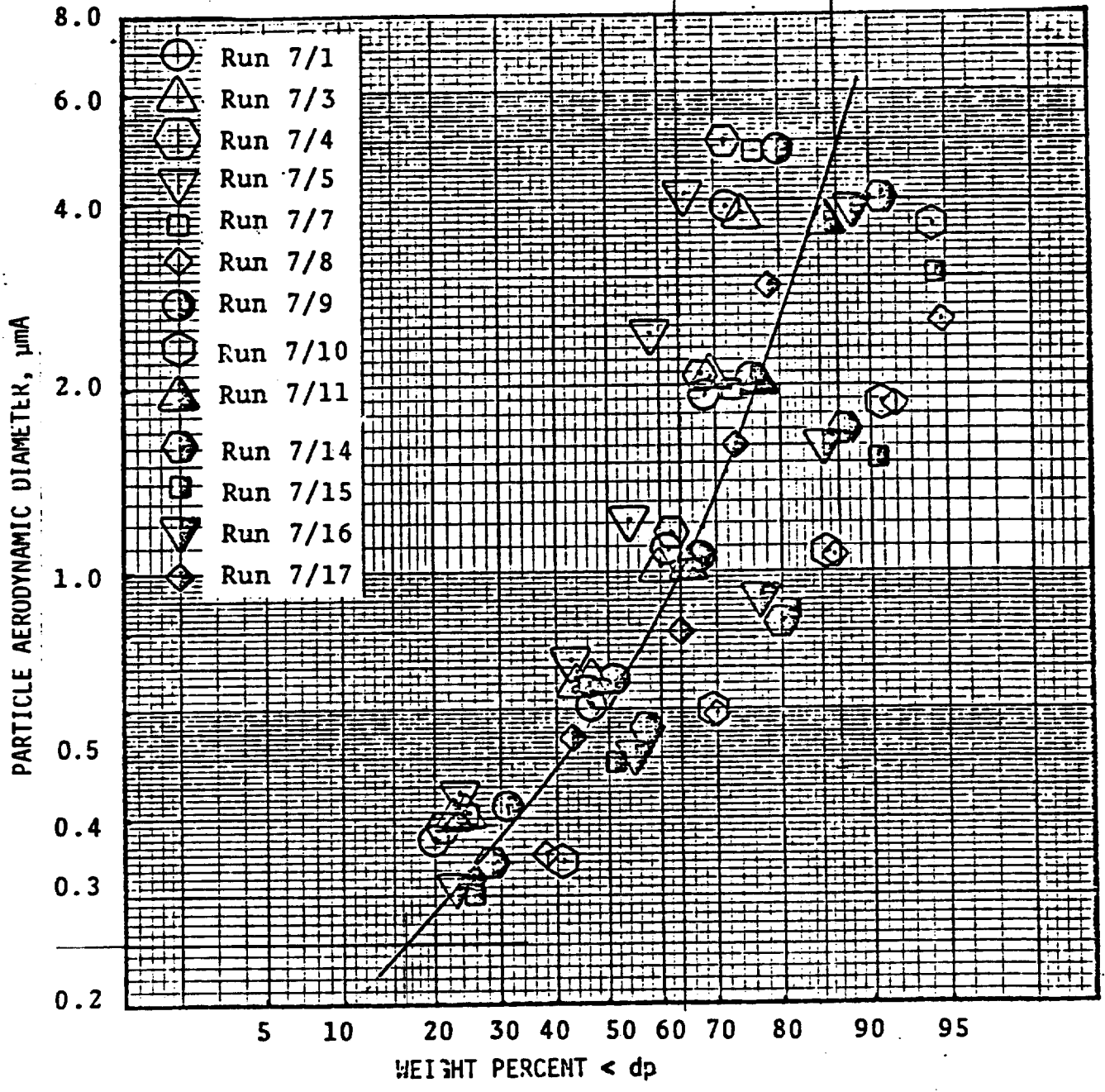


Figure 3-2. Particulate Size Distribution Site Two

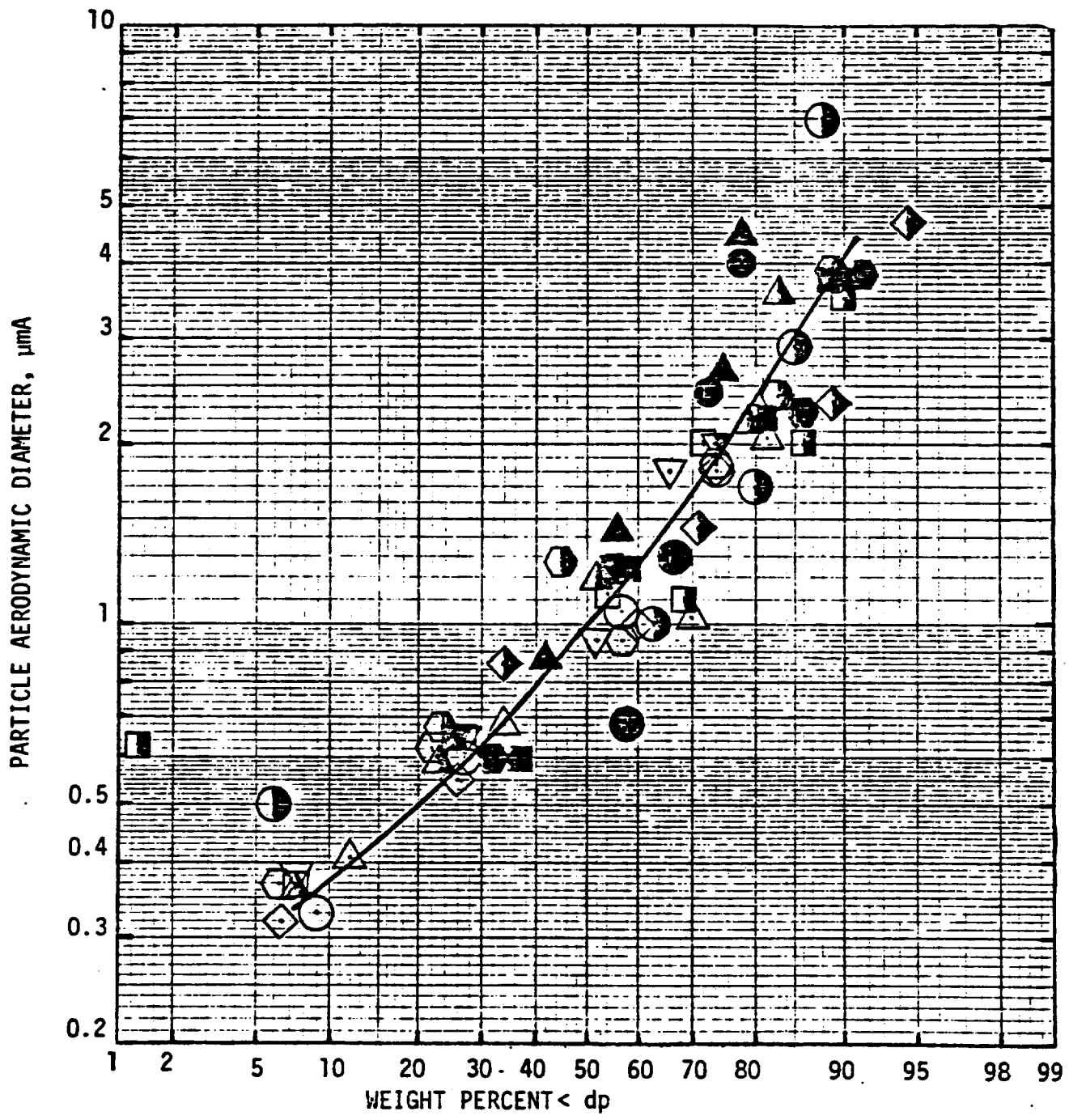


Figure 3-3 Particle size distribution site three

was 1.0 g/DNm³. This was the smallest cupola tested and the scrap charge was weighed very closely. The combination of small cupola and a closely controlled charge may contribute to the small particle size distribution measured. For the second site the average mass mean particle aerodynamic diameter was 0.60 μ m. The average particulate mass concentration was 1.5 g/DNm³. The third site was found to have a mass mean particle aerodynamic diameter which averaged 0.90 μ m. This large cupola had the highest particle concentration of 1.8 g/DNm³. No weighing of the charges was performed at this foundry. The third site had the largest charge weight as shown in Table 3-1.

SITE SELECTION

The site finally chosen for the demonstration plant was site 3. The first site proved to be unacceptable when the production schedule dropped to six hours per week. Discussion with the plant management indicated that while there was considerable interest in the project the production level was not expected to increase in the near future. The size of the cupola was relatively small and atypical of large industrial sources. These two factors resulted in a decision to seek an alternative host company.

The second site was a better candidate for the demonstration system. The cupola was significantly larger and the production schedule was five days per week. The management of the plant allowed preliminary testing in order to obtain design data, however, A.P.T. could not convince the owners of the foundry to continue with the demonstration project. The lack of available space for the proposed equipment was one contributing factor to the decision to reject the second site.

The third site was found and proved to be the better choice for building the demonstration plant. This site had a cupola which is representative of the larger cupolas in operation. The production schedule is normally three ten-hour days per week.

SECTION 4

SYSTEM DESIGN

INTRODUCTION

This section describes the system process design, the component design functions, and the structural details of the F/C scrubbing demonstration plant. The system flow diagrams are shown in Figures 4-1 and Figure 4-2 for the induced draft and forced draft configurations, respectively. Both configurations draw the hot gas from the cupola through the breeching and afterburner tank to the saturator and condenser vessels. In the induced draft system the blower is located downstream of the scrubber; while in the forced draft mode the blower is located between the condenser and the scrubber. Figures 4-3 and 4-4 show the system layouts for the induced draft system. Figures 4-5 and 4-6 show the layout for the forced draft system. Note that only the ducting is modified to switch from forced to induced draft; the remaining components remained stationary.

PROCESS DESCRIPTION

Figures 4-7 and 4-8 show the process flow sheet for both the induced draft and forced draft configuration. The flow rates and temperatures are shown for the design condition which would maximize the F/C effects.

The cupola converts scrap iron and steel to the molten state using heat generated by combustion of coke. The combustion air is supplied to tuyeres in the bottom of the cupola by a tuyere air blower. The cupola is a cylindrical vessel, brick lined internally and water cooled externally. The melting rate is determined by the charging rate and tuyere air flow rate. Raw materials are composed of scrap structural steel, engine blocks, metal stamping and turnings, cast iron pipe and fittings and other miscellaneous metal parts.

The foundry had an existing air pollution system consisting of an afterburner tank, quencher, scrubber and exhaust fan. The existing system was 12 years old and capable of only marginal performance. As a consequence the plant management had a keen interest in hosting the demonstration plant.

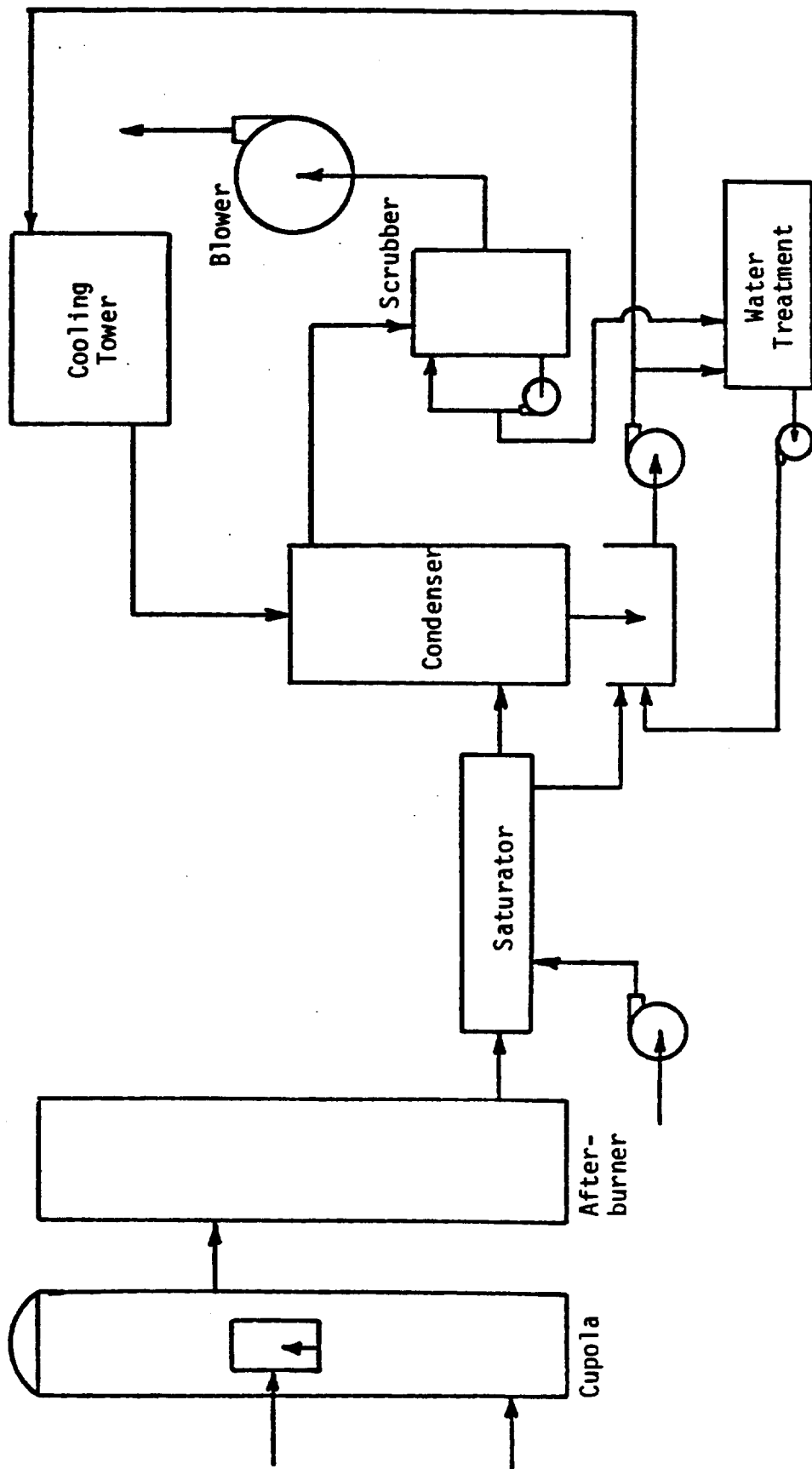


Figure 4-1. F/C demonstration plant flow diagram induced draft.

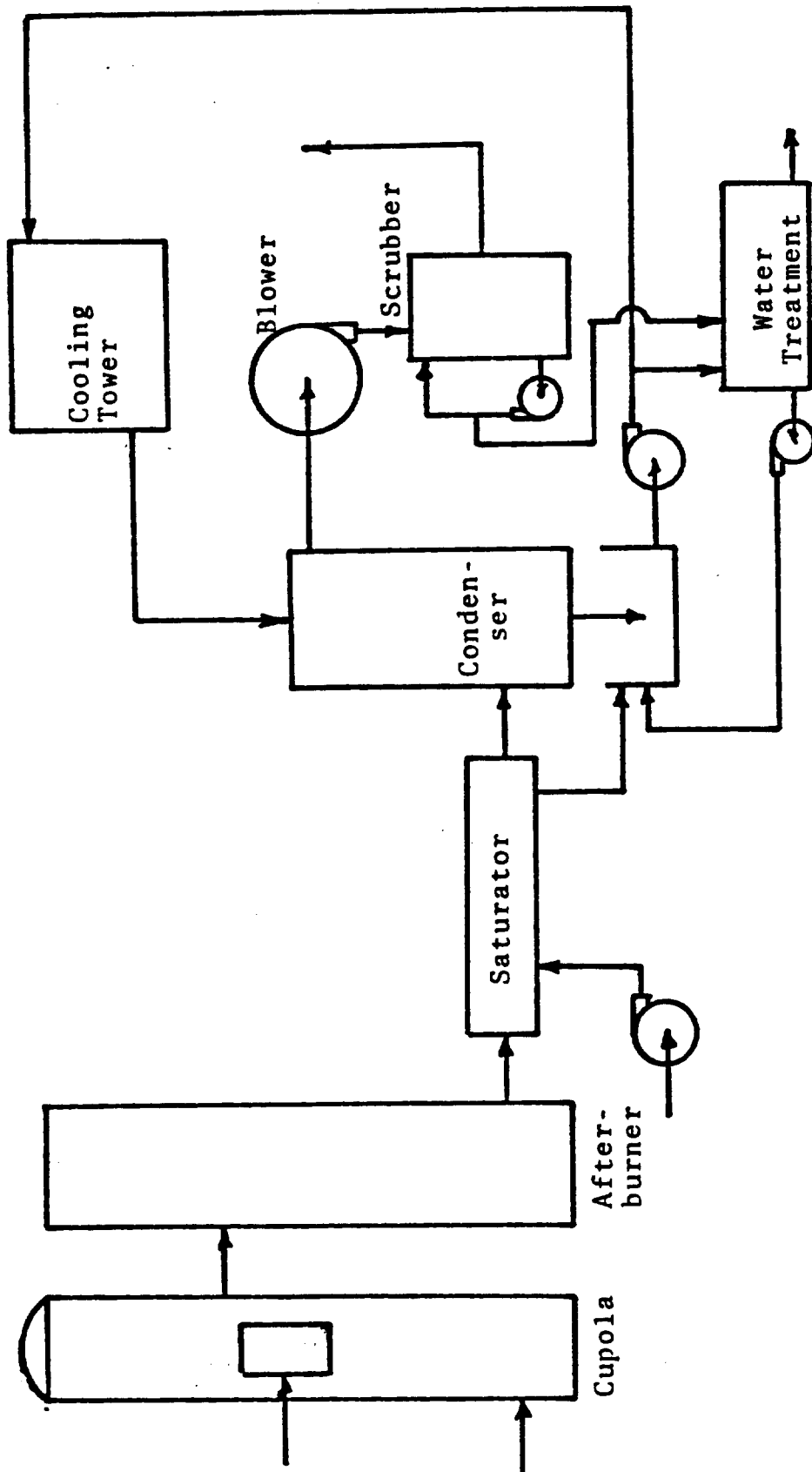
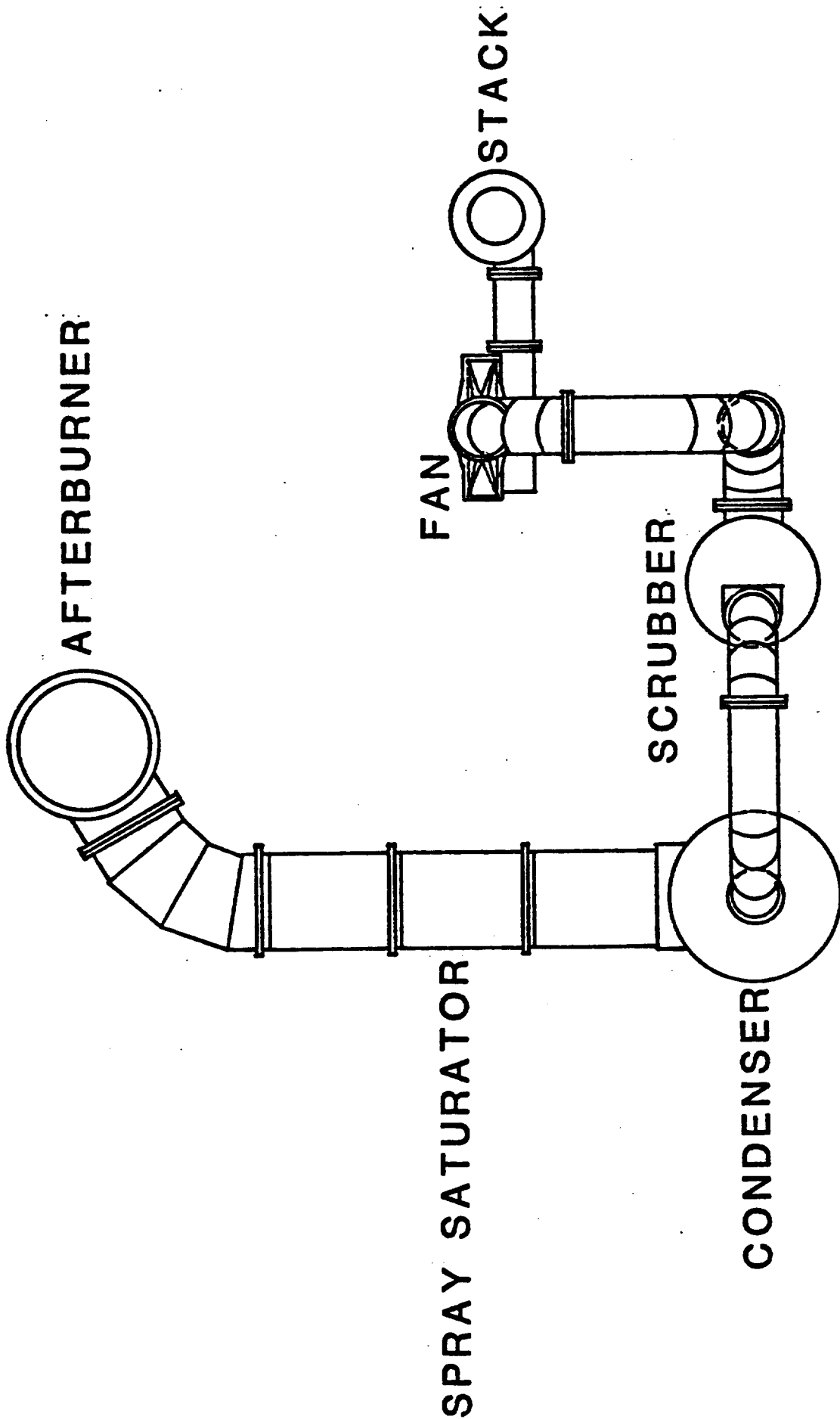
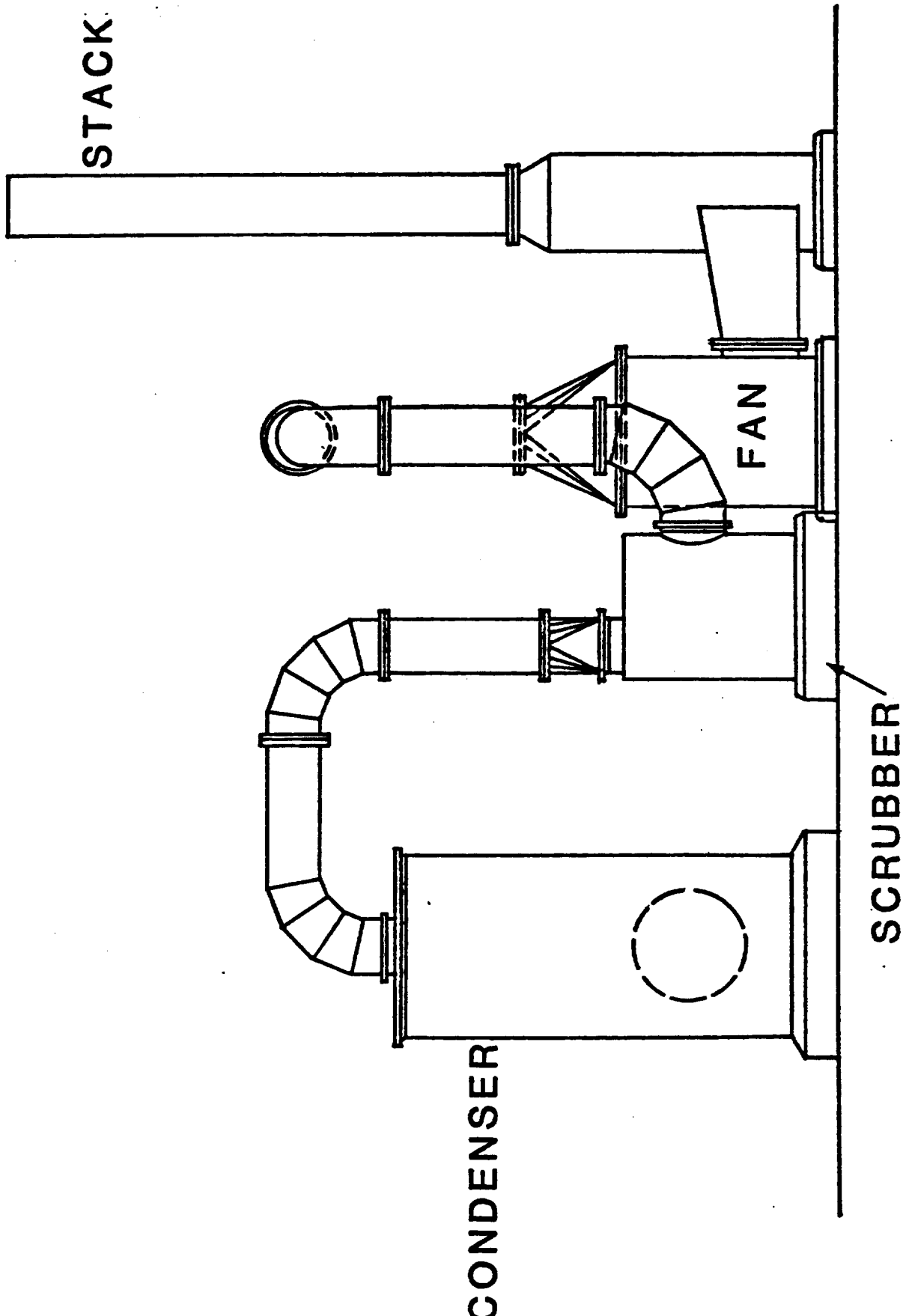


Figure 4-2. F/C Demonstration plant flow diagram forced draft

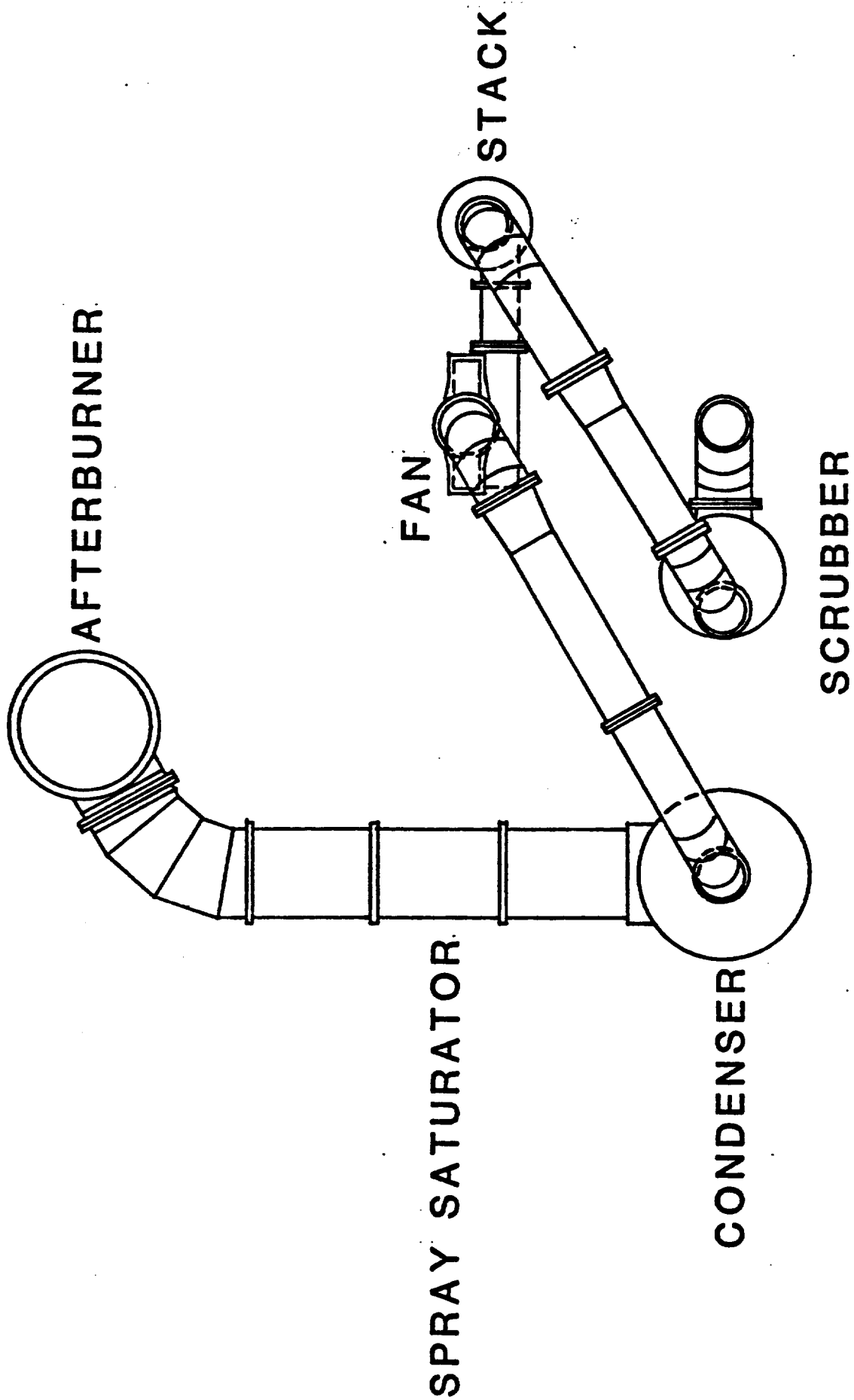


INDUCED DRAFT SYSTEM (PLAN VIEW)

Figure 4-3

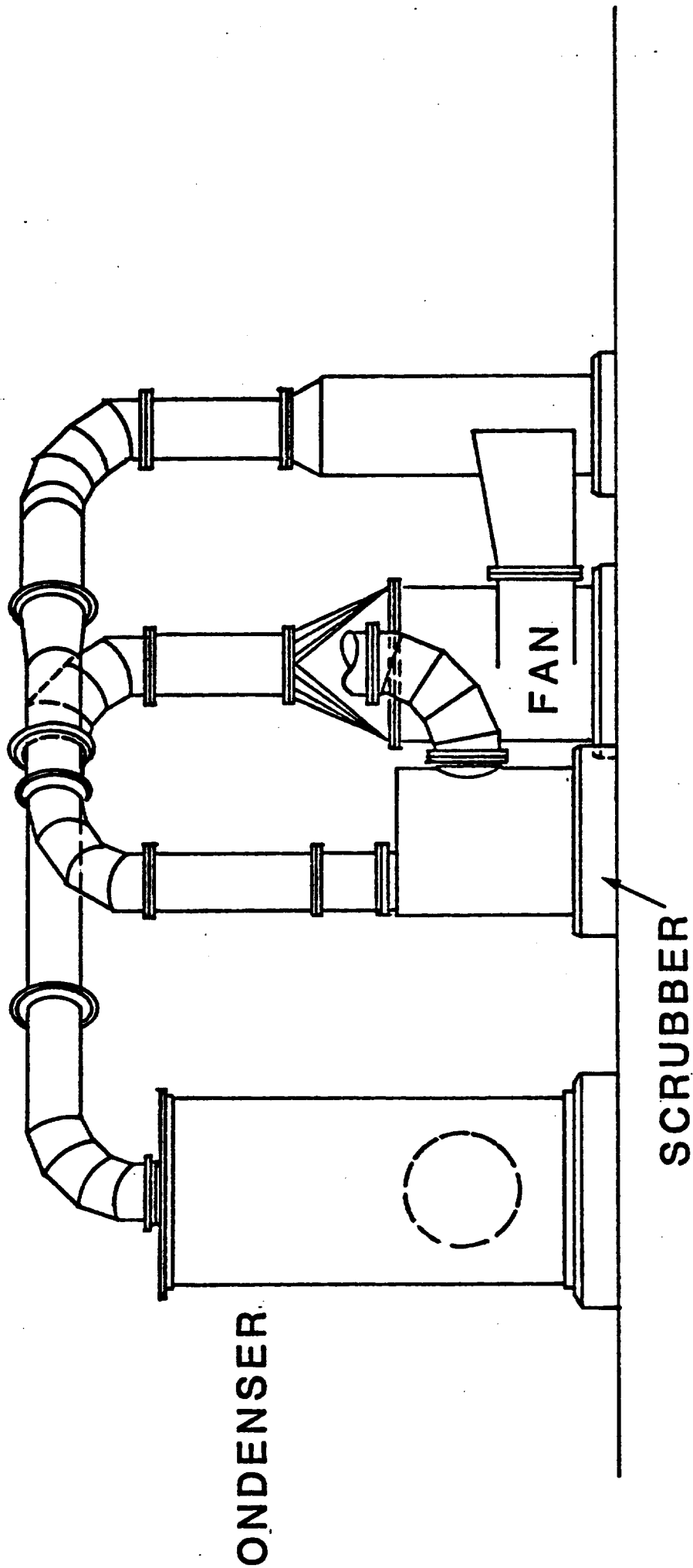


INDUCED DRAFT SYSTEM (ELEVATION VIEW)



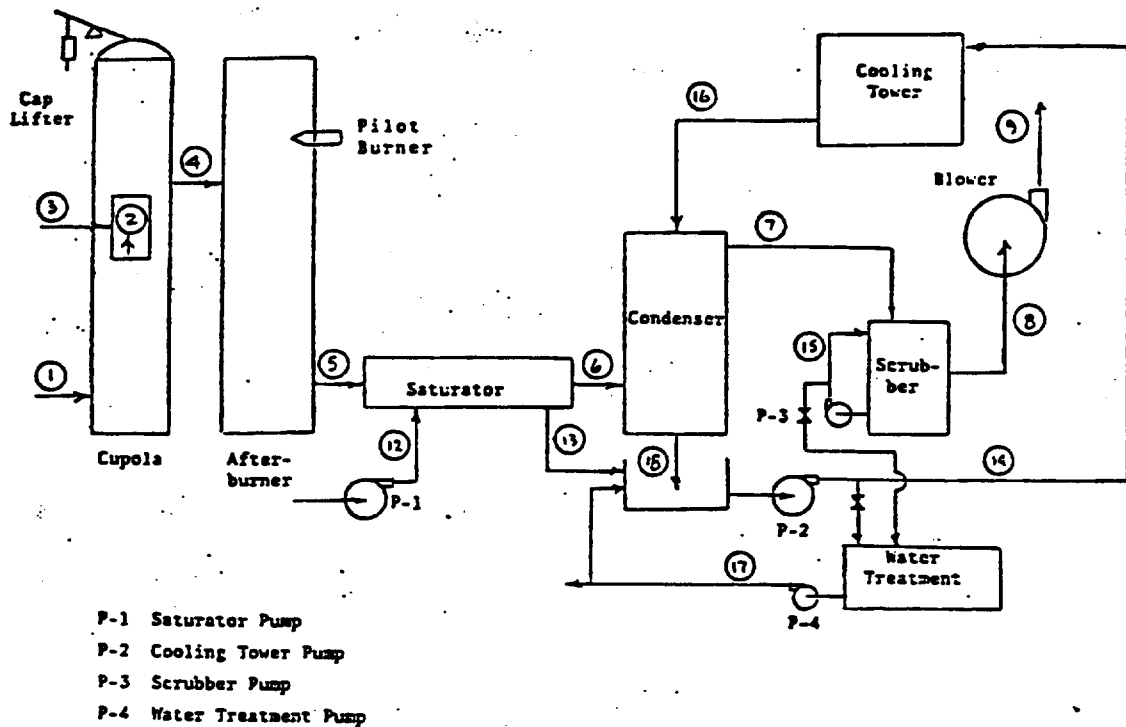
FORCED DRAFT F/C SYSTEM (PLAN VIEW)

Figure 4-5



FORCED DRAFT F/C SYSTEM (ELEVATION VIEW)

Figure 4-6

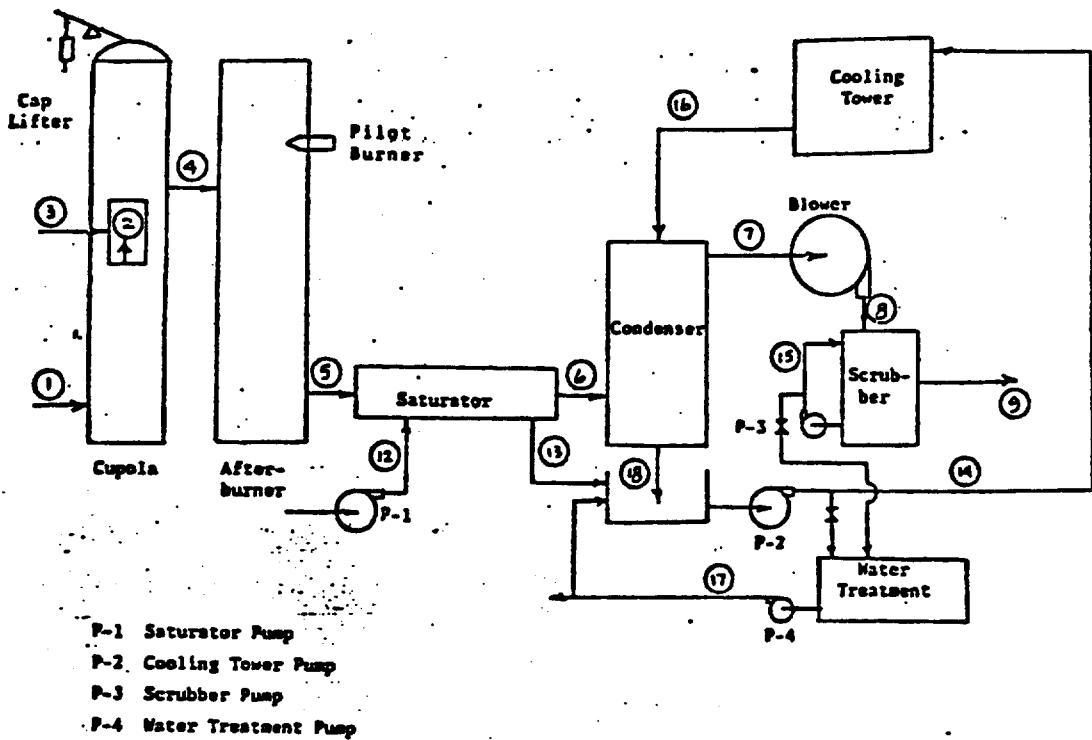


PROCESS FLOWS

	<u>GAS</u>									
	1	2	3	4	5	6	7	8	9	10
Mass Flow Rate (Dry) lb/min	700	792	325	1,120	1,120	1,120	1,120	1,120	1,120	1,120
Mass Flow Rate (Wet) lb/min	710	792	333		1,135	1,605	1,245	1,245	1,245	1,245
Composition										
O ₂ lb/min (lb mol/min)	163(5.09)	-	76(2.38)		15(.47)	15(.47)	15(.47)	15(.47)	15(.47)	15(.47)
N ₂ lb/min (lb mol/min)	537(19.2)	537(19.2)	252(8.97)		789(28.2)	789(28.2)	789(28.2)	789(28.2)	789(28.2)	789(28.2)
CO lb/min (lb mol/min)	-	107(3.82)	-		-	-	-	-	-	-
CO ₂ lb/min (lb mol/min)	-	148(3.36)	-		316(7.18)	316(7.18)	316(7.18)	316(7.18)	316(7.18)	316(7.18)
H ₂ O lb/min (lb mol/min)	10(0.56)	1.6(0.56)	5(.28)		15(.84)	485(26.9)	125(6.94)	125(6.94)	125(6.94)	125(6.94)
		H ₂								
Total (lb mol/min)	(24.85)	(26.94)	(12.77)		(36.7)	(62.8)	(42.8)	(42.8)	(42.8)	(42.8)
Temp °F	90		90		1,800	170	130	130	130	130
Pressure, in. Hg	33	29.88	29.92		29.85	29.77	29.41	27.57	29.99	29.99
GA Pressure, in. W.C.	+42	-0.5	0		-1	-2	-7	-32	+1	+1
ACFM	9,315		5,130		60,700	30,200	20,000	21,300	19,600	19,600
SCFM (Wet)	10,275		4,940		14,200					
DSCFM	9,340		4,830		13,900	13,900	13,900	13,900	13,900	13,900

	<u>LIQUID</u>							
	11	12	13	14	15	16	17	18
Mass Flow Rate, lb/hr		620	150	9,110	2,990	8,960	75-150	9,430
GPM		75	18	1,100	360	1,080	10-20	1,136
Temperature °F		80	170	150	130	100	90	150
Pressure, psig		200	0	20-30	0	0	0	0

Figure 4-7. Process Flow Sheet Induced Draft System



PROCESS FLOWS

	GAS									
	1	2	3	4	5	6	7	8	9	10
Mass Flow Rate (Dry) lb/min	700	792	328	1,120	1,120	1,120	1,120	1,120	1,120	1,120
Mass Flow Rate (Wet) lb/min	710	792	333		1,135	1,605	1,245	1,245	1,245	
Composition										
O ₂ lb/min (lb mol/min)	163(5.09)	-	76(2.38)		15(.47)	15(.47)	15(.47)	15(.47)	15(.47)	15(.47)
N ₂ lb/min (lb mol/min)	537(19.2)	537(19.2)	252(8.97)		789(28.2)	789(28.2)	789(28.2)	789(28.2)	789(28.2)	789(28.2)
CO lb/min (lb mol/min)	-	107(3.82)	-		-	-	-	-	-	-
CO ₂ lb/min (lb mol/min)	-	148(3.36)	-		316(7.18)	316(7.18)	316(7.18)	316(7.18)	316(7.18)	316(7.18)
H ₂ O lb/min (lb mol/min)	10(0.56)	1.6(0.56)	5(.28)		15(.84)	485(26.9)	125(6.94)	125(6.94)	125(6.94)	125(6.94)
Total (lb mol/min)	(24.85)	(26.94)	(12.77)		(36.7)	(62.8)	(42.8)	(42.8)	(42.8)	
Temp °F	90		90		1,800	170	130	130	130	
Pressure, in. Hg	33	29.88	29.92		29.85	29.77	29.41	31.24	29.99	
GA Pressure, in. W.C.	+42	-0.5	0		-1	-2	-7	+18	+1	
ACFM	9,315		5,130		60,700	30,200	20,000	18,800	19,600	
SCFM (Wet)	10,275		4,940		14,200					
DSCFM	9,340		4,830		13,900	13,900	13,900	13,900	13,900	

	LIQUID							
	11	12	13	14	15	16	17	18
Mass Flow Rate, lb/min		620	150	9,110	2,990	8,960	75-150	9,430
GPM		75	18	1,100	360	1,080	10-20	1,136
Temperature °F		80	170	150	130	100	90	150
Pressure, psig		200	0	20-30	0	0	0	

Figure 4-8. Process Flow Sheet Forced Draft System

The scrap and coke are charged together in 1,800 kg charges (2 tons) with an iron to coke mass ratio of 6. Small amounts of limestone, 20-30 kg, are also charged to act as a fluxing agent in the formation of slag. The nominal melting rate is 12,500 kg/hr. The tuyere air flow rate can be varied by means of a damper on the blower. The normal tuyere air flow rate is 3.5 DNm³/s.

The exhaust gases from the bed of material in the cupola are composed of carbon monoxide, carbon dioxide and nitrogen. The gas analysis is typically 14% CO, 13% CO₂, and 73% N₂. Additional combustion air at a rate of 2.3 DNm³/s enters the charging door to allow for complete conversion of carbon monoxide to carbon dioxide. An ignition burner is installed to ensure that a flame source is available for combustion of the CO to CO₂.

Combustion is completed in a brick-lined afterburner tank. The exhaust gases leave the afterburner tank at a temperature ranging from 800 - 1,000°C. The exhaust gas flow rate at this point is about 6.6 DNm³/s.

The hot gases leave the afterburner and are cooled in the saturator by means of water sprays. The gas is cooled and the temperature approaches the adiabatic saturation temperature which depends upon the hot gas temperature. Typically, the saturation temperature achieved ranges from 71°C to 77°C. The maximum water spray rate in the saturator is 4.7 l/s (75 gpm).

The saturated gases next enter the condenser which further cools the gases causing condensation of water vapor. The cooling capacity of the condenser depends upon the rate of cooling water flow and the cold water temperature which depends upon the cooling tower performance. The condenser and cooling tower system has a design heat rejection rate of 9.6×10^6 J/s (33×10^6 BTU/hr). The water flow rate can be varied up to 69 L/S (1,100 gpm). The cold gas temperature leaving the condenser is about 55°C at design flow rates. The condenser is a counter current packed bed.

Particle collection occurs in the condenser by the mechanisms of inertial impaction, diffusion, thermophoresis and diffusio-phoresis.

The condensation of water vapor on the particles results in substantial growth of the submicron particles. This growth phenomenon is a primary aspect of F/C scrubbing which differentiates this process from other scrubbing applications.

The exhaust gases leave the condenser and enter either the exhaust fan or the scrubber, depending on the ducting configuration. The system is designed to allow testing with the scrubber either in the induced draft or forced draft mode. The scrubber is the primary particle collection device in the system. The design is a gas atomized scrubber with variable area throat. The design incorporates an integral water sump and entrainment separator.

The exhaust fan provides the draft for the system. The fan was designed and built to A.P.T. specifications and is a straight radial blade design. The flow rate of the fan is approximately 14 Am³/s (30,000 cfm) at - 96 cm W.C. (- 38 in. W.C.).

The cooling tower cools the water to be pumped into the condenser. It is designed to cool 69 l/s (1,100 gpm) of water from 66°C to 38°C using ambient air. This is accomplished by evaporative cooling.

The settler is designed to remove particles collected by the scrubbing liquid. A 1.3 l/s (20 gpm) stream of sump water is clarified by the settler. The thickened sludge (10-30% by wt.) is disposed of as land fill. The clarified water (100 ppm solids) is returned to the sump.

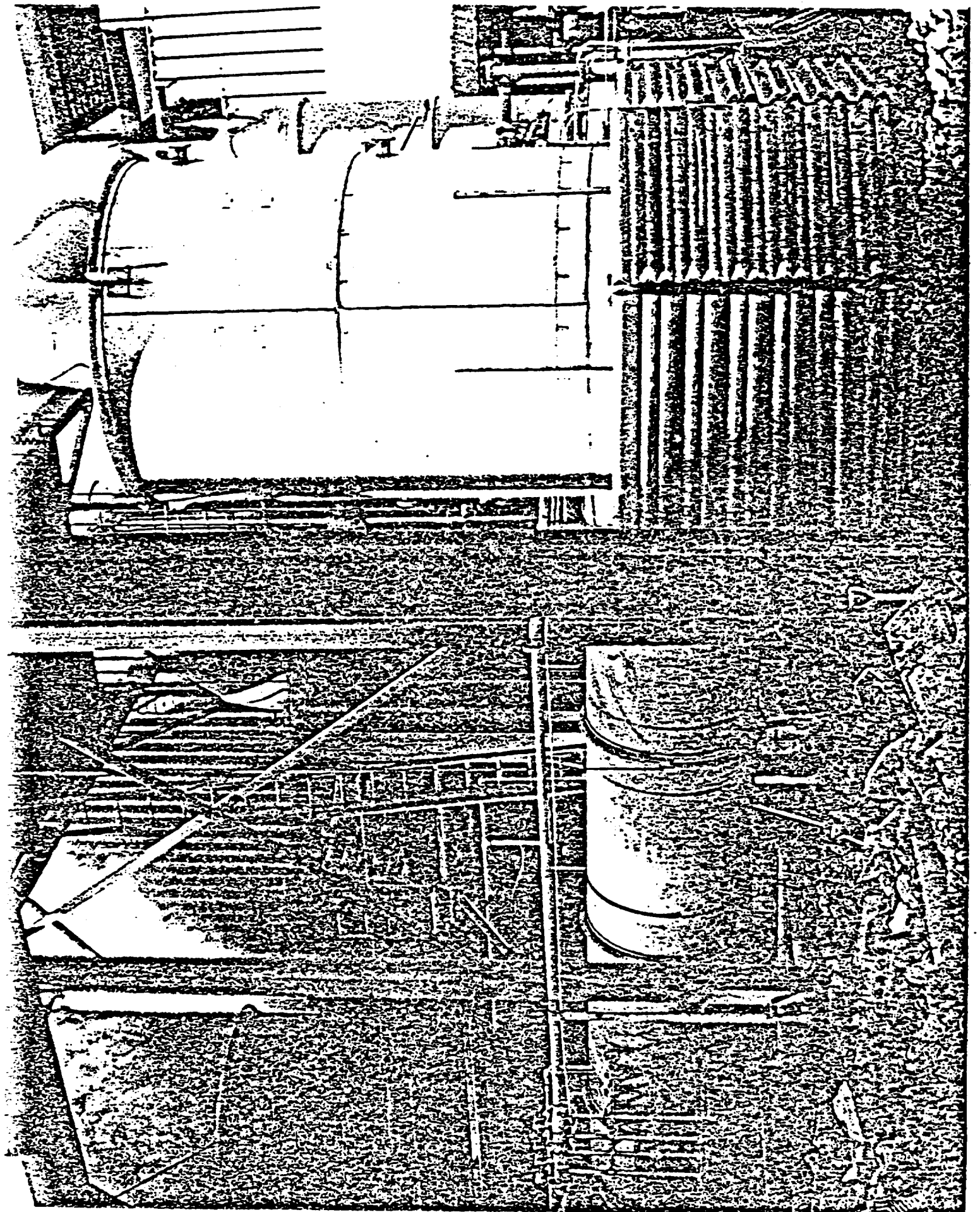
MECHANICAL DESIGN

The major F/C scrubber system components which are listed below will be described in detail:

- | | | |
|------------------|---------------------|----------------------------|
| 1. Afterburner | 5. Venturi scrubber | 9. Piping & ducting |
| 2. Saturator | 6. Settler | 10. Instrumentation |
| 3. Condenser | 7. Fan | 11. Structure & foundation |
| 4. Cooling tower | 8. Pumps | |

Photographs of the system and its components are shown in Figures 4-9 through 4-12.

Why diff. from other



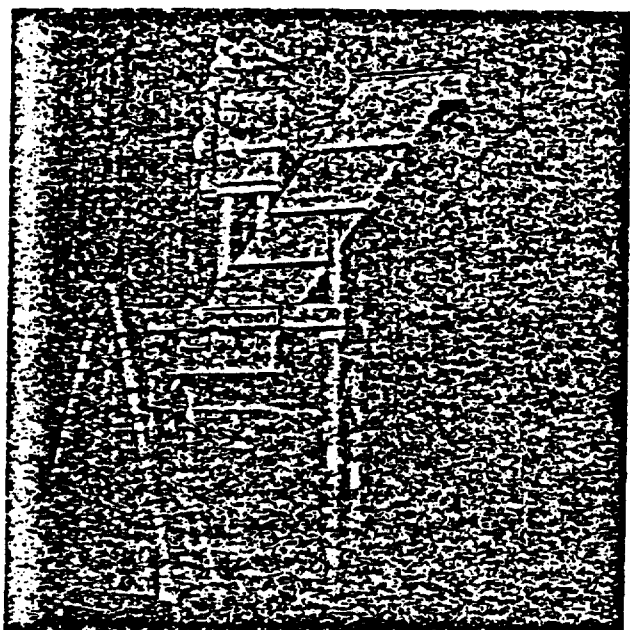


Figure 4-10 Settler

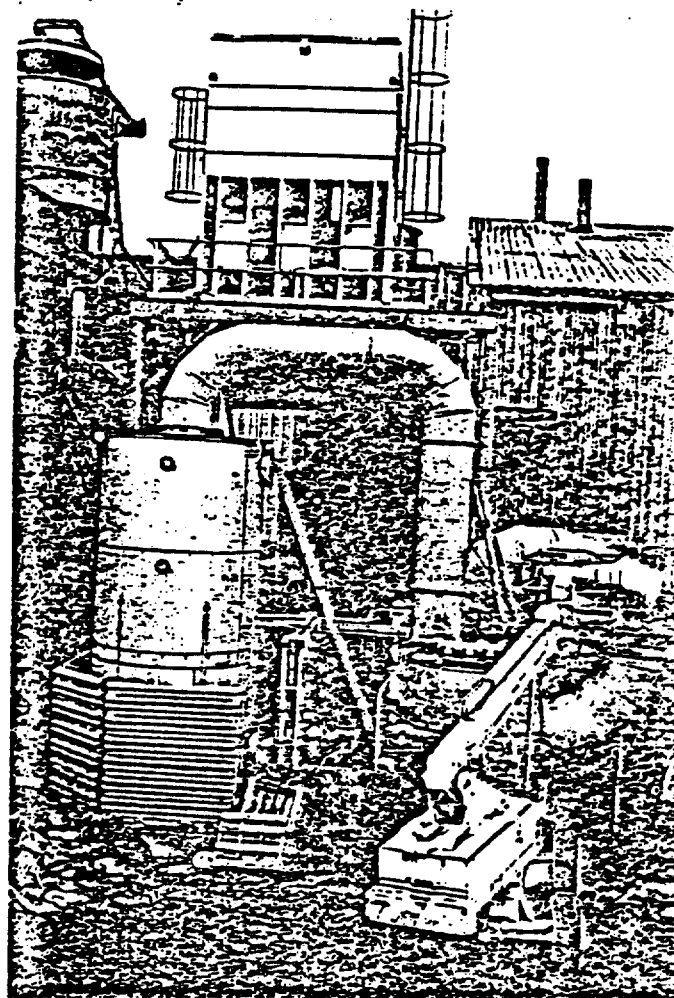


Figure 4-11 Condenser
Scrubber and Cooling Tower

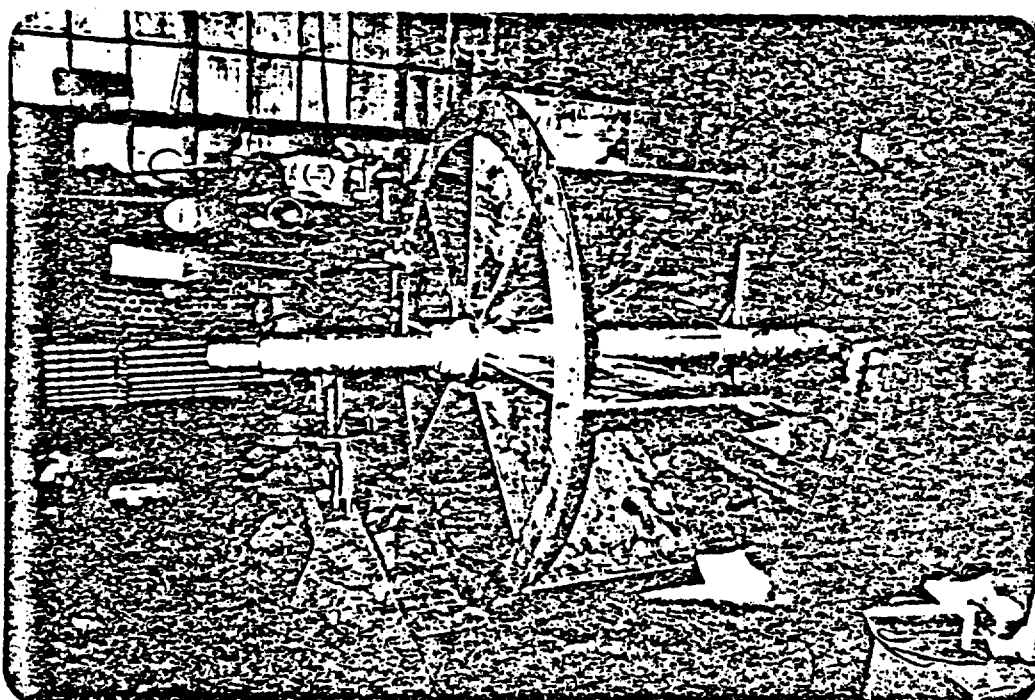


Figure 4-12 Exhaust Fan Wheel as revised by A.P.T.

Afterburner

The afterburner vessel is a cylindrical steel shell 7.3 m high with a diameter of 2.4 m. The top third of the afterburner which was added in a plant expansion is made of stainless steel while the lower portion is carbon steel. The shell is lined with 7.6 cm of castable insulation. Gas from the cupola enters the top portion and flows out the bottom into the saturator. The ignition burner is located in the duct coming out of the cupola before the afterburner vessel. The ignition burner is a Hauck gas pilot size #3 and operates on 0.057 m³/min (2 cfm) of natural gas at a pressure of 15.24 cm W.C. (6 in. W.C.). A 2.54 cm pipe tapped off a foundry gas line is used. The burner unit also requires a flow of air of about 0.7 m³/min (25 cfm) which was tapped off the tuyere air fan with a 3.8 cm pipe.

Saturator

The saturator is a horizontal cylinder rolled from 3.5 mm (10 gauge) 316 stainless steel sheet. The saturator has a straight section and an elbow section which connects to the afterburner tank. The cylinder is 9.1 m long and has a diameter of 1.5 m. The vessel is built in three sections and connected by flanges. The elbow section of the vessel is welded to the afterburners while the other end forms an expansion joint at the condenser inlet. The section of the saturator leaving the afterburner is insulated with firebrick because of the high temperatures at that location.

The spray pattern in the saturator is obtained by the arrangement of spray nozzles. The spray banks are designed to provide easy access to the nozzles. Three nozzles with radial sprays are located in the first (elbow) section of the saturator. A spray header with 4 nozzles transverses the duct. Forty nozzles are located on 12 header pipes in the straight section of the saturator. Three or four nozzles are mounted on 2.54 cm diameter stainless steel pipes. These pipes can be removed from outside for maintenance. A flow switch has also been installed on the main water supply line to the nozzles. When the flow to the

saturator nozzles decreases below 75.8 l/min (20 gpm), the switch activates an alarm system and shuts off the main exhaust blower. This is to prevent high saturator temperatures from damaging the spray bank and saturator gaskets.

The mechanical design of the saturator was based on two constraints. First, the vessel has to have enough volume so the residence time is sufficient for evaporation of the water drops. The second constraint involves the available space for construction of the F/C system. The primary equipment area was to be located north of the existing sump, hence, a long horizontal spray chamber was designed to connect the afterburner with the condenser.

Condenser

The condenser vessel is a 316 stainless steel cylindrical shell, which is 2.75 m in diameter and 6.1 m high. The wall thickness is 3.5 mm (10 gauge). The gas enters the bottom of the condenser from the saturator and is distributed by turning vanes. Counter current contact is made with cold water in a packed bed having a packing depth of 1.2 m. Intalox rings of 3.8 cm nominal diameter are used as packing. This packed bed is irrigated by water falling from a trough type distribution plate. Some of the water droplets are entrained in the rising gas and a second packed bed, 0.3 m deep, is used as an entrainment separator. The gas flows out the top of the condenser through a 0.8 m diameter duct to the scrubber. The water drains down to the condenser reservoir at the bottom of the condenser and is drained through a 0.3 m diameter pipe back into the sump.

Scrubber

The scrubber consists of a cylindrical shell 2.1 m in diameter and 2.7 m high. The scrubber shell was rolled from 3.5 mm (10 gauge) stainless steel sheet. The shell houses both a gas atomized scrubber section and the entrainment separators.

The inlet ducting is bolted to the gas atomized scrubber section which in turn is bolted to the scrubber shell. The scrubber

section has a variable area throat with hydraulic or manual control which allows the area to be varied from 0.08 m² to 0.22 m². Scrubber water is pumped to six distribution headers located just upstream of the converging section of the scrubber. The gas is directed downward through the scrubber. Scrubber water is collected in the bottom of the scrubber shell and recirculated to the scrubber throat.

Drops of water generated in the scrubber throat are entrained in the gas stream. To remove these drops entrainment separators are required at the outlet to the scrubber shell. A tube bank entrainment separator is used in this application. The entrainment separators consist of six rows of 4.1 cm stainless steel tubes spaced 4.1 cm from center to center. These rows are offset to force the gas stream to wave its way through the tubes before leaving the scrubber housing. The entrained drops impact on the tubes and drain to the scrubber reservoir. The entrainment separator cross-sectional area is 5.1 m² and is made of 1,080 tubes 76.2 cm long.

Cooling Tower

The cooling tower consists of a 3.7 m x 2.7 m x 5.2 m epoxy coated steel shell. The tower is a standard Commercial design. Ambient air is forced through the packed tower by a fan. Hot water is distributed across the top of the tower packing by means of multiple headers and spray nozzles. Cold water temperature is controlled by an automatic adjustment of the air flow by means of a fan damper.

The cooling tower is designed to cool 69 l/s of water from 66°C to 33°C. The cooling tower incorporates a baffle type entrainment separator to remove entrained drops from the exhaust air.

Settler

Solids are removed from the circulating water system by means of a gravity settler. The settler which was used had a settling area of 11 m². The design incorporates parallel

plates inclined at a 55° angle to minimize the required area for the unit.

The cleaned liquid (overflow) flows upward along the plates and overflows through flow distribution orifices. The solids collect on the plates and slide downward into a sludge hopper. The sludge is discharged periodically through a sludge valve and disposed of as landfill.

A flocculant aid is used to increase the settling rate of the solids. A chemical feed system involving a mix tank and metering pump supplies the flocculant at a dose rate of 5-10 ppm. The settler design incorporates a flash mix tank and a floc growth tank as well as agitators with speed controllers. The nominal flow rate through the settler is 1.3 l/s. The settler reduces the solids content of the circulating water from several thousand ppm to a few hundred ppm.

Blower

During the initial phase of the project the blower from the existing scrubber system was used to provide flow for the F/C system. The fan then had a straight radial blade design and was driven by a directly coupled 400 HP electrical motor at 1,800 rpm. The current demand was excessive; requiring 480-500 amps at 480 volts. The performance of the fan was poor and several modifications were made to obtain the required flow.

Early testing indicated that significant leakage of ambient air was occurring through the fan housing resulting in reduced flow through the F/C scrubber system. The entire inlet section of the fan housing was rebuilt which solved the air leakage problem allowing design flow through the F/C system. The fan still had poor efficiency and the developed head was excessive for the requirements of the F/C system.

Finally, a new fan wheel was designed in order to obtain more flow and a lower head. The new fan wheel also had straight radial blades, but the wheel diameter was reduced to 1.47 m from 1.60 m and a new blade profile was designed to conform closer to the fan housing. Figure 4-13 shows a new wheel design. The

new fan wheel was installed and successfully operated. The desired flow rate was attained at a lower head and the motor power requirement dropped to 360-380 amps at 480 v.

Pumps

Table 4.1 shows the pump specifications for each of the pumps used on the demonstration plant. All of the pumps are of a proven commercial design and presented no unusual operating problems.

The saturator pump supplies city water to the spray nozzles in the saturator. A two stage centrifugal pump is used to provide the high pressure required to give fine atomization for effective evaporation.

The sump pump causes the circulation of water from the sump to the cooling tower. A vertical turbine pump with the suction submerged in the sump was used for this purpose.

The scrubber pump circulates the water from the bottom of the scrubber to the scrubber throat. A single stage centrifugal pump is used for this purpose.

Two diaphragm pumps are used in the system. The smaller pump is used to transport sump water to the settler. The larger pump is used for maintenance purposes such as cleaning condenser and scrubber, etc. These pumps are portable, driven from compressed air available at the plant and are capable of pumping liquids as well as sludges with a high solids content.

TABLE 4.1 PUMP SPECIFICATIONS

<u>Pump</u>	<u>Type</u>	<u>Capacity</u>	<u>Driver</u>
P-1 Saturator Pump	2-stage centrifugal	54 l/s @ 15 atm	20 Hp, 240 V, 3Ø motor
P-2 Sump Pump	Vertical turbine	750 l/s @ 2 atm	30 Hp, 240 V, 3Ø motor
P-3 Scrubber Pump	Centrifugal	250 l/s @ 1 atm	5 Hp, 240 V, 3Ø motor
P-4 Water Treatment Pump	Diaphragm	1.3 l/s @ 1 atm	Compressed Air
P-5 Sludge Pump	Diaphragm	2.6 l/s @ 1 atm	Compressed Air

Piping, Ducting, and Valves

The piping system is composed of four separate subsystems: (1) saturator piping, (2) cooling water piping, (3) scrubber piping and (4) water treatment system piping.

Saturator piping

City water is used in the saturator to cool the exhaust gas. The water is piped to the saturator pump (P-1) and then passes through one of two parallel strainers which remove solids which might plug the spray nozzles. Galvanized pipe having a diameter of 6.4 cm (2 1/2 in.) is used up to the individual spray headers. Flexible copper hoses (2.5 cm diameter) are used to connect to the saturator.

Cooling Water Piping

The cooling water piping runs from the sump pump (P-2) to the cooling tower, from the cooling tower to the condenser and from the condenser to the sump. A bypass line around the cooling tower is also included. The material used for the cooling water system is schedule 40 fiberglass pipe 20 cm diameter (8 in.).

Scrubber Piping

The scrubber piping runs from the scrubber internal sump to the gas atomized scrubber throat. Fiberglass pipe having a diameter of 10 cm (4 in.) is used. At the scrubber throat 6 header pipes each 5 cm (2 in.) in diameter distribute the scrubber liquor. A bypass line allows the scrubber water to be pumped to the settler.

Water Treatment Piping

The settler system is connected to the circulating water system by 5 cm diameter PVC piping.

Valves

The valves used in the system were generally for two purposes (1) flow control and (2) shut-off. The scrubber liquid flow was controlled using a rubber lined diaphragm pump. Ball valves were used on the saturator spray lines for on-off control. Butterfly valves were used in other locations for control or shut-off.

Ducting

The ducting used on the project was Fiberglass reinforced polyester (FRP) ducting. The ducting sections between the condenser and scrubber are 0.81 m diameter. The exhaust gas ducting is 0.91 m diameter. The nominal wall thickness is 0.5 cm. The ducting system was designed to allow operation in both the forced draft and induced draft mode.

Foundations and Structural Design

A reinforced concrete foundation was required to support the condenser and scrubber vessels. The saturator and scrubber pumps are also installed on this foundation. The condenser foundation is a concrete block 3.5 m square by 1.8 m deep. The adjacent scrubber and pump foundation is a rectangular pad 3.5 m wide by 4.7 m long and 0.5 m deep.

A structural steel platform was required to support the cooling tower. The platform also included a sampling area just above the scrubber where particulate sampling could be performed both at the scrubber inlet ducting and at the scrubber outlet ducting.

INSTRUMENTATION AND CONTROL SYSTEM

Instrumentation

The process instrument diagram is shown in Figure 14-14. Temperatures were measured by means of chromel-alumel thermocouples (K type). The temperatures were recorded on a strip chart recorder and observable on a digital indicator with a 20 point selector switch.

The liquid flow rates are measured with venturi meters, transducers, and indicators as shown in Table 4-2. Liquid pressures are measured with standard pressure gauges, both locally at the pumps and remotely in the instrument trailer.

The gas pressures and differential pressures across the condenser and scrubber were measured by means of Minihelic and Magnihelic gauges. Pressure tubing was used between the equipment and the instrument trailer where the gauges were located.

Saturator Process Measurements

- a. Gas inlet temperature (TR-5)
- b. Gas outlet temperature (TR-6)
- c. Liquid flow rate (FM-12, FI-12)
- d. Liquid temperature (TR-12)
- e. Pump suction pressure (PI-12.1)
- f. Pump discharge pressure (PI-12.2)
- g. Strainer discharge pressure (PI-12.3)

Condenser Process Measurements

- a. Gas inlet temperature (TR-6)
- b. Gas outlet temperature (TR-7)
- c. Gas inlet pressure (PI-6)
- d. Gas outlet pressure (PI-7)
- e. Condenser total pressure drop (PI-7/8)
- f. Entrainment separator pressure drop
- g. Liquid flow rate (FM-14, FI-14)

- h. Liquid inlet temperature (TR-16)
- i. Liquid outlet temperature (TR-18)

Cooling Tower Process Measurements

- a. Liquid flow rate (FM-14)
- b. Liquid inlet temperature (TI-14)
- c. Liquid outlet temperature (TI-16)

Scrubber Process Measurements

- a. Gas inlet temperature (TI-8)
- b. Gas outlet temperature (TI-9)
- c. Liquid flow rate (FM-15)
- d. Liquid temperature (TI-15)
- e. Pump discharge pressure (PI-15)
- f. Scrubber total pressure drop (PI-8/9)
- g. Entrainment separator pressure drop
- h. Scrubber liquid level

Water Treatment System Process Flows

- a. Liquid flow rate (FM-25)

Control System

Saturator Water System

The saturator water flow rate is controlled by manually opening or closing the shutoff valves located on the spray bar headers. The saturator water system also contains two liquid "Y" strainers piped in parallel to remove particulate which could clog the spray nozzles. Pressure gauges located upstream and downstream of the strainers monitored pressure loss across the strainer.

Cooling Water Flow

The cooling water low rate is controlled by means of the bypass valve V-14.1. The cooling tower can be bypassed by opening the cooling tower bypass valve V-28 and closing the cooling tower valve V-14.2. This allows water to be pumped directly to the condenser from the sump.

Scrubber Liquid Flow

The scrubber liquid flow is controlled by means of the flow control valve V-15. In addition the scrubber bypass valve V-23 allows scrubber liquid to be pumped to the sump or to the sewer.

Scrubber Liquid Level

The scrubber liquid level is controlled by means of a level controller which actuated valve V-21.1 on signal of low level.

Scrubber Flow Area

The scrubber flow area can be controlled by a hydraulic system which opens and closes the scrubber throat area. In addition, manual adjustment is possible using extension levers located outside the scrubber.

Gas Flow Rate

The gas flow rate is controlled by a combination of fan inlet damper and scrubber throat area.

Water Treatment Flow Rate

The flow rate to the water treatment system is controlled by the air regulator used on the diaphragm pump.

Circulating Water pH

The pH of the circulating water system is measured using a pH meter and controlled between the range of 6-9 using additions of sodia ash.

Safety System

The safety system protects the equipment from excessive temperature in the event that the saturator sprays or pump fails to provide enough cooling water. The saturator water flow rate is

74 1000000
monitored by flow switch (FI-12). If the flow rate decreases below 25 gpm the flow switch will shut down the exhaust fan and initiate automatic opening of the cupola cup.

A backup safety system involves a temperature switch (TC-7) located in the ducting section coming out of the condenser. In the event gas temperature at this point exceeds the setpoint of 80°C (175°F) the exhaust fan will be shut down and the cupola cap raised.

Both of these safety switches provide an alarm and indicator light to alert operators of the malfunction.

TABLE 4.2 FLOW MEASUREMENT SPECIFICATIONS

<u>Identification</u>	<u>Type</u>	<u>Indicator</u>
FM-12	Venturi meter 6.25 cm cast iron, flanged	Ammeter 0-20 mA
FM-14	Venturi meter 20 cm cast iron, flanged	Ammeter 0-20 mA
FM-15	Venturi meter 10 cm cast iron, flanged	Voltmeter 0-5
FM-25	Venturi meter 5 cm brass, threaded	Magnehelic 0-60 in W.C.

SECTION 5
PERFORMANCE TESTING

After the installation of the scrubber equipment, instrumentation, piping and electrical were completed the F/C system was started up and performance test data obtained. Start up presented no problems with equipment supplied for the project. The original exhaust fan did cause excessive power consumption and electrical overload ~~trips~~. This condition continued until the new fan, which A.P.T. designed, was installed. The system performance was quite good during the test period. No lost production time was experienced by the foundry due to problems associated with the operation of the F/C scrubber system.

Operating Modes

The F/C system was tested in two basic configurations, induced draft and forced draft mode. In the more traditional induced draft system the exhaust gas flows through the afterburner, saturator, condenser, scrubber, and then the exhaust fan to the stack. By using ducting modifications the F/C system was tested in the forced draft mode, wherein the exhaust gas flows through the afterburner, saturator, condenser, then through the exhaust fan, and finally through the scrubber and stack. This operating mode has the advantage of reducing the fan power requirement.

The major operating parameters which were varied during the test program were the condenser liquid flow rate and scrubber pressure drop. The condenser liquid flow rate affected the amount of cooling in the condenser and hence the condensation ratio. The scrubber pressure drop could be varied by changing the scrubber

throat flow area and the scrubber liquid to gas ratio. The scrubber pressure drop determines the collection efficiency in the scrubber.

Test Locations

Sampling was performed at three locations in the F/C system. At each of these locations two sampling ports located 90° apart were available. The sampling ports were made of 10 cm (4 in) pipe couplings.

The sampling location was at the cold end of the saturator just before the condenser vessel. The sampling ports at this location were easily accessible from the ground. The remaining two sampling locations were in the scrubber inlet and outlet ducting. These sampling ports were accessible from a sampling platform which was constructed as part of the cooling tower platform.

Testing Methods

This section describes the test procedures that were used to determine the F/C system performance. Sampling was usually performed at the inlet to the condenser and at the scrubber outlet. For some runs sampling was also performed at the scrubber inlet. Testing at three locations allowed the condenser performance and scrubber performance to be evaluated separately.

Impactor Runs

The particle size distribution and mass concentration was obtained using University of Washington Cascade Impactors. Pre-cutters were used on the impactors to remove large particles and entrainment. Fiberglass and greased aluminum substrates were used in the impactors.

Modified EPA Method 5

Several modified EPA Method 5 total filter runs were made to determine total mass concentration. These tests were done for compliance tests and to confirm impactor mass loadings.

Sampling Equipment

The sampling equipment used involves four sampling trains as shown in Figure 5-1. The cascade impactor runs were made in stack. The precutters used had cut points in the range of 6 to 9 μm , depending upon sampling flow rate. Nozzle sizes were chosen to maintain isokinetic sampling. The filter tests were made with heated filters out-of-stack and heated sampling probes. The probes were made from 0.95 cm (3/8") stainless steel and incorporated S-type Pitot tubes. Cyclones were not used in the method 5 testing.

Data Analysis

Cascade Impactors

The cascade impactor tests provide data on the cumulative mass concentration at specific particle sizes or cut points. From this data penetrations as a function of particle size could be determined. The data analysis utilized was a computer program developed by Dr. Leslie Sparks. The program calculated impactor cut points and cumulative mass loading based on weight gain per stage, impactor flow rate and impactor calibration data.

The overall penetration was calculated from the total mass concentrations as follows.

$$\overline{P_t} = \overline{P_{t_C}} \times \overline{P_{t_S}} \quad (5-1)$$

$$= \frac{C_{SI}}{C_{CI}} \times \frac{C_{SO}}{C_{SI}} \quad (5-2)$$

$$\overline{P_t} = \frac{C_{SO}}{C_{CI}} \quad (5-3)$$

where $\overline{P_t}$ = overall penetration condenser and scrubber

$\overline{P_{t_C}}$ = overall penetration condenser

$\overline{P_{t_S}}$ = overall penetration scrubber

C_{CI} = particle mass concentration condenser inlet, g/Dnm^3

C_{SI} = particle mass concentration scrubber inlet, g/Dnm^3

C_{SO} = particle mass concentration scrubber outlet, g/Dnm³

The penetration as a function of particle size was evaluated in two ways, each of which is based on the following equation:

$$Pt (d_{pa}) = \frac{\left[\frac{dC}{d(d_{pa})} \right]_{\text{outlet}}}{\left[\frac{dC}{d(d_{pa})} \right]_{\text{inlet}}} \quad (5-4)$$

where $\frac{dC}{d(d_{pa})}$ is the slope of the cumulative mass concentration curve at a specific particle aerodynamic diameter.

The graphical method involves plotting the cumulative mass loading versus particle diameter curves for both the inlet and outlet and determining the slopes of these curves at various points. The fractional penetration curve is then plotted on the size range of interest by performing the division shown in equation (5-4) at each specific diameter required.

The second method used, known as the discrete or finite difference method, involves approximating the slope of the cumulative mass concentration curve by use of the individual impactor stage weight gain and cut points, i.e.

$$Pt = \frac{\left(\frac{\Delta C}{\Delta \ln d_p} \right)_{\text{inlet}}}{\left(\frac{\Delta C}{\Delta \ln d_p} \right)_{\text{outlet}}} \quad (5-5)$$

This method is described by McCain et al. (1978) and has the advantage of being easily adapted to computer calculations. It is not subject to errors due to determining the slope of the cumulative mass concentration curve.

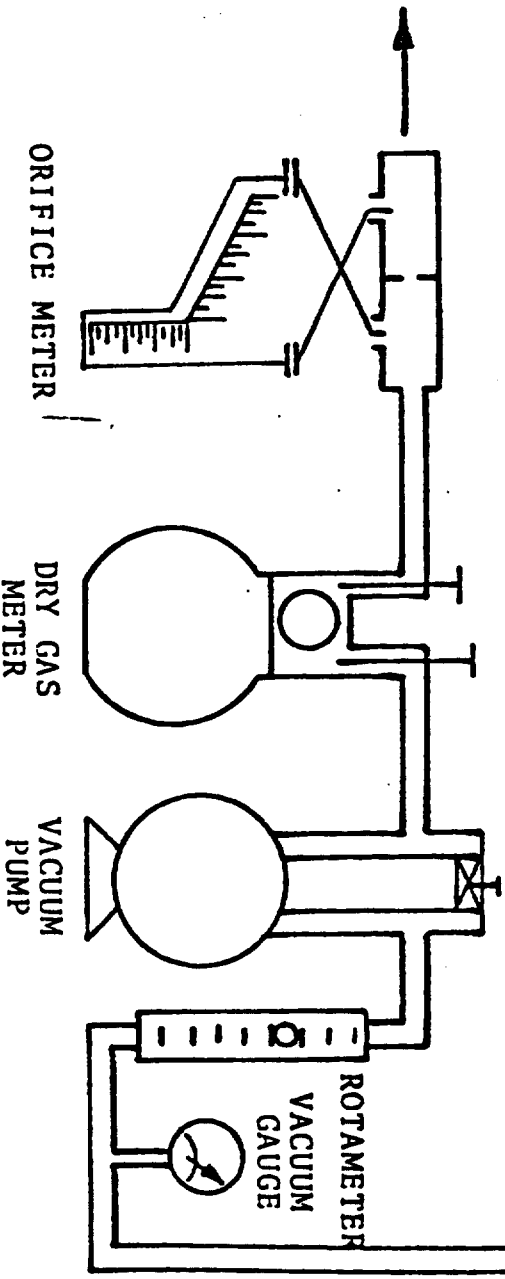
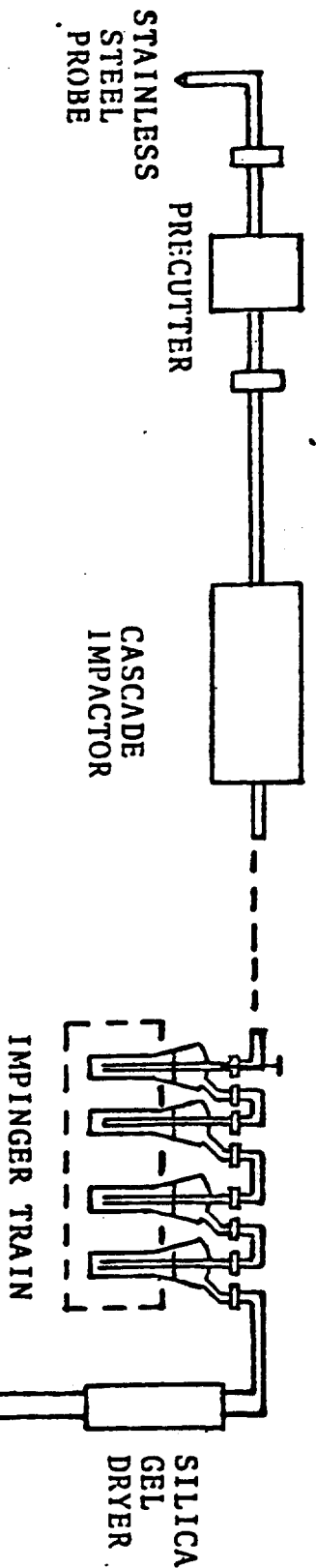


Figure 5-1. Modified E.P.A. sampling train with in stack cascade impactor.

SECTION 6

SYSTEM PERFORMANCE MODEL

INTRODUCTION

The system performance model predicts the particle removal efficiency in the flux force/condensation scrubber system. The model can be used to predict the emission from a F/C scrubber system installed on a pollutant source with a known particle concentration and size distribution. The model allows one to vary independently the two primary variables which influence the performance of the F/C system. These two variables are the condensation ratio and scrubber pressure drop.

Under previous EPA contracts, Air Pollution Technology, Inc. conducted detailed studies on the technical and economic feasibilities of F/C scrubbing (Calvert et al., 1973, '75, '77). These studies included theoretical development of design equations for F/C scrubbing as well as experimental verification of on both pilot plants and demonstration plant equipment. The model used in this project also uses scrubber performance methods developed in the scrubber system study (Calvert, 1972) and recent revisions for gas atomized scrubbers (Yung, 1978).

BASIC CONCEPTS

Before proceeding to the details of the mathematical model, the basic concepts and outline of the approach will be discussed. If we consider a typical F/C scrubbing system, it might have the features shown in Figure 6-1. The gas leaving the source is hot and has a water vapor content which depends on the source process. The first step is to saturate the gas by quenching it with water. This will cause no condensation if the particles are insoluble, but will if they are soluble. There will be a diffusiphoretic force directed away from the liquid surface.

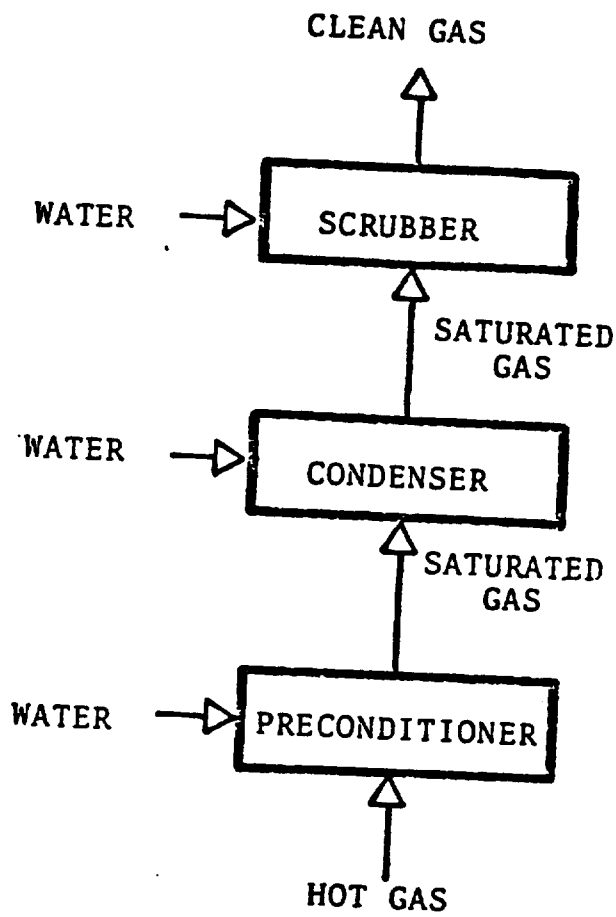


Figure 6-1. Simplified F/C scrubber system.

Condensation is required in order to have diffusiphoretic deposition, any growth on insoluble particles, and extensive growth on soluble particles. Contacting with cold water or a cold surface is employed to cause condensation. While condensation occurs there will be diffusiphoretic and thermophoretic deposition as well as some inertial impaction (and, perhaps, Brownian diffusion). The particles in the gas leaving the condenser will have grown in mass due to the layer of water they carry.

Subsequent scrubbing of the gas will result in more particle collection by inertial impaction. This will be more efficient than impaction before particle growth because of the greater inertia of the particles. There may be additional condensation, depending on water and gas temperatures, and its effects can be accounted for as discussed above.

The mathematical model for the F/C demonstration plant is outlined below:

Saturator

- a. Gas is humidified and cooled to adiabatic saturation temperature.
- b. No condensation occurs (particles are assumed insoluble).
- c. Particle collection is assumed to be negligible in the saturator.

Condenser

- a. Particles are collected by impaction in packed column.
- b. Condensation occurs causing growth of particles.
- c. Collection occurs in condenser due to diffusiphoresis.

Scrubber

- a. Grown particles are collected by impaction in scrubber.
- b. Negligible condensation occurs.

PREDICTION OF PENETRATION

Collection by Impaction in Condenser

The particulate collection in the condenser is primarily due to inertial impaction. The inlet (dry) particle size distribution

is used for these calculations (no credit is taken for growth for collection within the condenser). The penetration is calculated with the following equation for collection in a packed bed.

$$Pt_{CI} = \exp \left[\frac{\pi}{2(j+j^2) (\epsilon-H_d)} \frac{Z}{d_C} K_p \right] \quad (6-1)$$

where $K_p = \text{impaction parameter} = \frac{u_G d_{pa}^2}{9\mu_G d_C}$

u_G = superficial gas velocity, cm/s

μ_G = gas viscosity, g/cm-s

d_C = packing diameter, cm

Z = packing depth, cm

j = channel width fraction, dimensionless

ϵ = void fraction, dimensionless

H_d = liquid holdup fraction, dimensionless

d_{pa} = particle aerodynamic diameter, cm $(g/cm^3)^{1/2}$

For the F/C demonstration plant the condenser was packed with 5.0 cm intalox packing to a depth of 122 cm. The void fraction was 0.97 and the channel width fraction was estimated to be 0.15.

Condensation and Growth

The growth of the particulate, due to condensation of water vapor is predicted based on the humidity entering and leaving the condenser. The grown particle size is calculated from equation (6-2).

$$d_{p2} = \left[\frac{6 f_p q^1}{772 \pi n_p} + d_p^3 \right]^{1/3} \quad (6-2)$$

where d_{p_1} = initial particle (physical) diameter, cm
 d_{p_2} = grown particle (physical) diameter, cm
 f_p = particle condensation fraction
 q^1 = condensation ratio, g H₂O/g Dry Gas
 n_p = particle number concentration, particles/cm³

The grown particle density is then calculated by the following equation:

$$\rho_{p_2} = \left(\frac{d_{p_1}}{d_{p_2}} \right)^3 \left(\rho_{p_1}^{-1} \right) + 1.0 \quad (6-3)$$

where ρ_{p_1} = initial (dry) particle density, g/cm³

The grown particle density allows one to calculate the final grown particle aerodynamic diameter with the following equation:

$$d_{pa} = d_p (C^1 \rho_p)^{1/2} \quad (6-4)$$

where

d_p = particle physical diameter, cm

C^1 = Cunningham slip correction factor, dimensionless

ρ_p = particle density, g/cm³

Collection by Diffusiophoresis

Collection by diffusiophoresis in the condenser can be calculated by means of the following equation:

$$Pt_{CD} = 1 - 0.85(f_v) (1-f_p) \quad (6-5)$$

where f_v = mole fraction of gas condensing

The total penetration in the condenser is then calculated from the product of equation (6-1) and (6-5).

$$Pt_C = Pt_{CI} \times Pt_{CD} \quad (6-6)$$

Collection by Impaction in Scrubber

The collection of the grown particulate in the scrubber is by inertial impaction. The scrubber penetration is calculated according to the method developed by Yung et al (1978) for collection in a venturi throat. The penetration equation used is as follows:

$$\frac{\ln Pt_s}{B} = \frac{1}{K_{po} U^* = 0.7} \times \left[4K_{po} U^{*1.5} + 4.2 U^{*0.5} - 5.02 K_{po}^{0.5} \right. \\ \left. \times \left(U^* + \frac{0.7}{K_{po}} \right) \tan^{-1} \left(\frac{U^* K_{po}}{0.7} \right)^{0.5} \right] - \frac{1}{K_{po} + 0.7} \quad (6-7)$$

$$\times \left[4 K_{po} + 4.2 - 5.02 K_{po}^{0.5} \left(1 + \frac{0.7}{K_{po}} \right) \tan^{-1} \left(\frac{K_{po}}{0.7} \right)^{0.5} \right]$$

where $B = \frac{Q_L \rho_L}{Q_G \rho_G C_{Do}}$

$$K_{po} = \frac{d_{pa}^2 (U_G - U_d)}{9\mu_G d_d}$$

$$U^* = 1.0 - 2 \left[1 - x^2 + (x^4 - x^2)^{0.5} \right]$$

and $x = \frac{3l C_{Do} \rho_G}{16 d_d \rho_L} + 1$

Q_L/Q_G = liquid to gas volumetric ratio, dimensionless

C_{Do} = drop drag coefficient at throat entrance, dimensionless

d_d = drop diameter, cm

U_d = drop velocity at throat entrance, cm/s

l = throat length, cm

The penetration in the F/C system can then be obtained from the product of the condenser and scrubber penetrations:

$$Pt = Pt_C \times Pt_S \quad (6-8)$$

$$Pt = Pt_{CI} \times Pt_{CD} \times Pt_S \quad (6-9)$$

A computer program has been written to perform these calculations. The program allows prediction of the scrubber performance as a function of particle size. The input required for the program is listed in Table 6-1 along with numbers for a sample calculation.

Figure 6-2 shows the initial and grown size distributions for the sample case. Figure 6-3 shows the penetration as a function of particle size for the condenser, gas atomized scrubber and the combined system. The penetrations are plotted vs dry particle size. The actual scrubber penetration is based on the grown particle size distribution as shown in Table 6-2.

TABLE 6-1. INPUT VARIABLES FOR PREDICTION
OF SCRUBBER PERFORMANCE

gas velocity through condenser	180 cm/s
void fraction of packing	0.97
liquid hold up fraction	0.0
packing depth	122 cm
packing diameter	5 cm
particle condensation fraction	0.15
particle number concentration	1×10^8 particles/cm ³
particle density	3.0 g/cm ³
condensation ratio	0.15 g H ₂ O/g D.G.
scrubber throat length	13 cm
scrubber liquid to gas ratio	0.002
scrubber throat velocity	5,000 cm/s

TABLE 6-2. EXAMPLE CALCULATIONS

Initial Particle Aerodynamic Diameter μm	Grown Particle Aerodynamic Diameter μm	Penetration, fraction		
		Condenser Ptc	Scrubber Pts	Total Pt
0.40	0.93	0.88	0.18	0.16
0.50	0.93	0.81	0.18	0.16
0.60	0.95	0.86	0.18	0.15
0.80	1.02	0.85	0.14	0.12
1.00	1.10	0.83	0.12	0.10
1.25	1.25	0.81	0.07	0.06
1.50	1.50	0.78	0.04	0.03
2.00	2.00	0.72	0.02	0.01
3.00	3.00	0.56	0.01	0.005
5.00	5.00	0.25	0.01	~0
10.00	10.00	0.01	0.01	~0

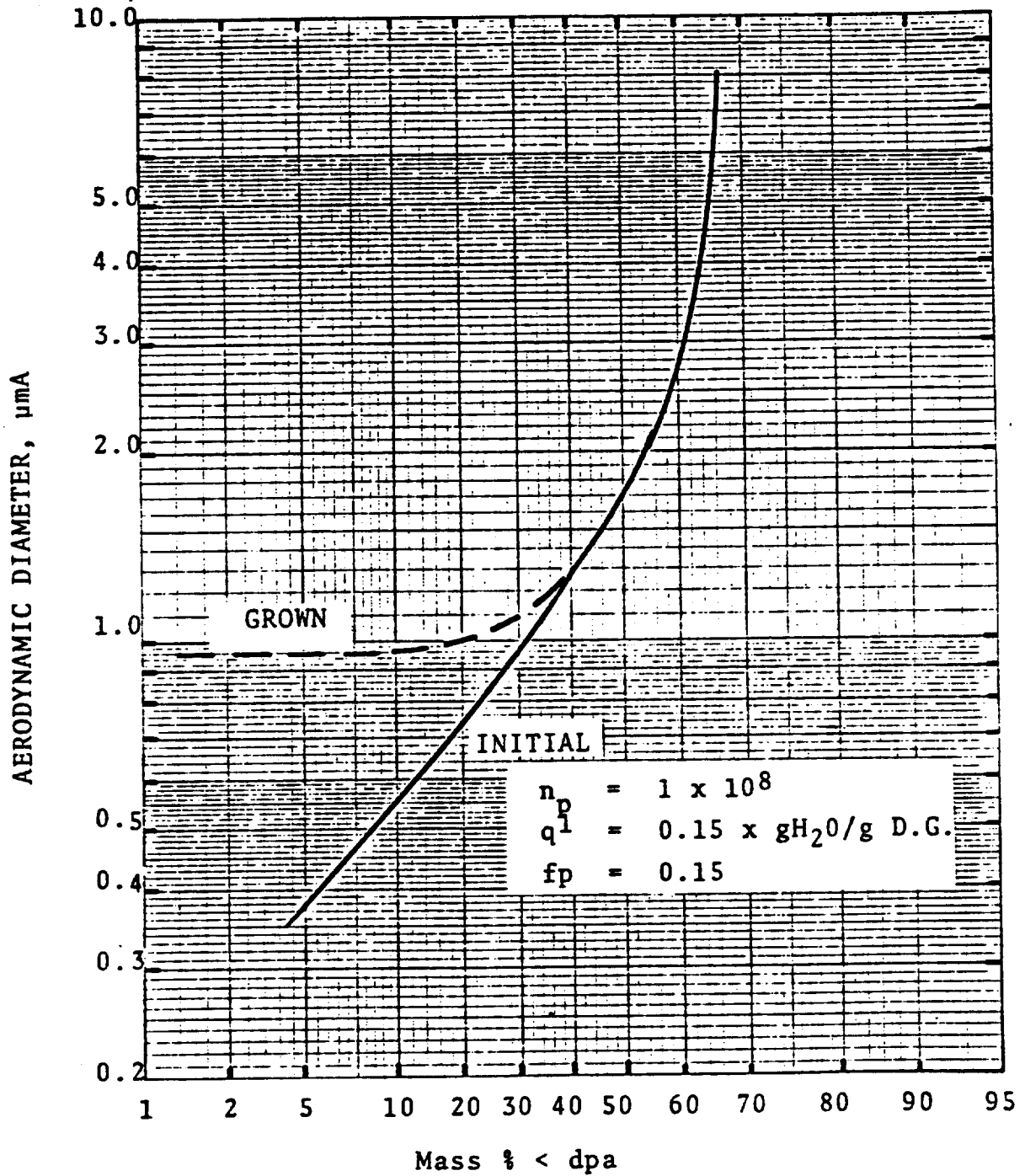


Figure 6-2. Example of initial and grown size distributions.

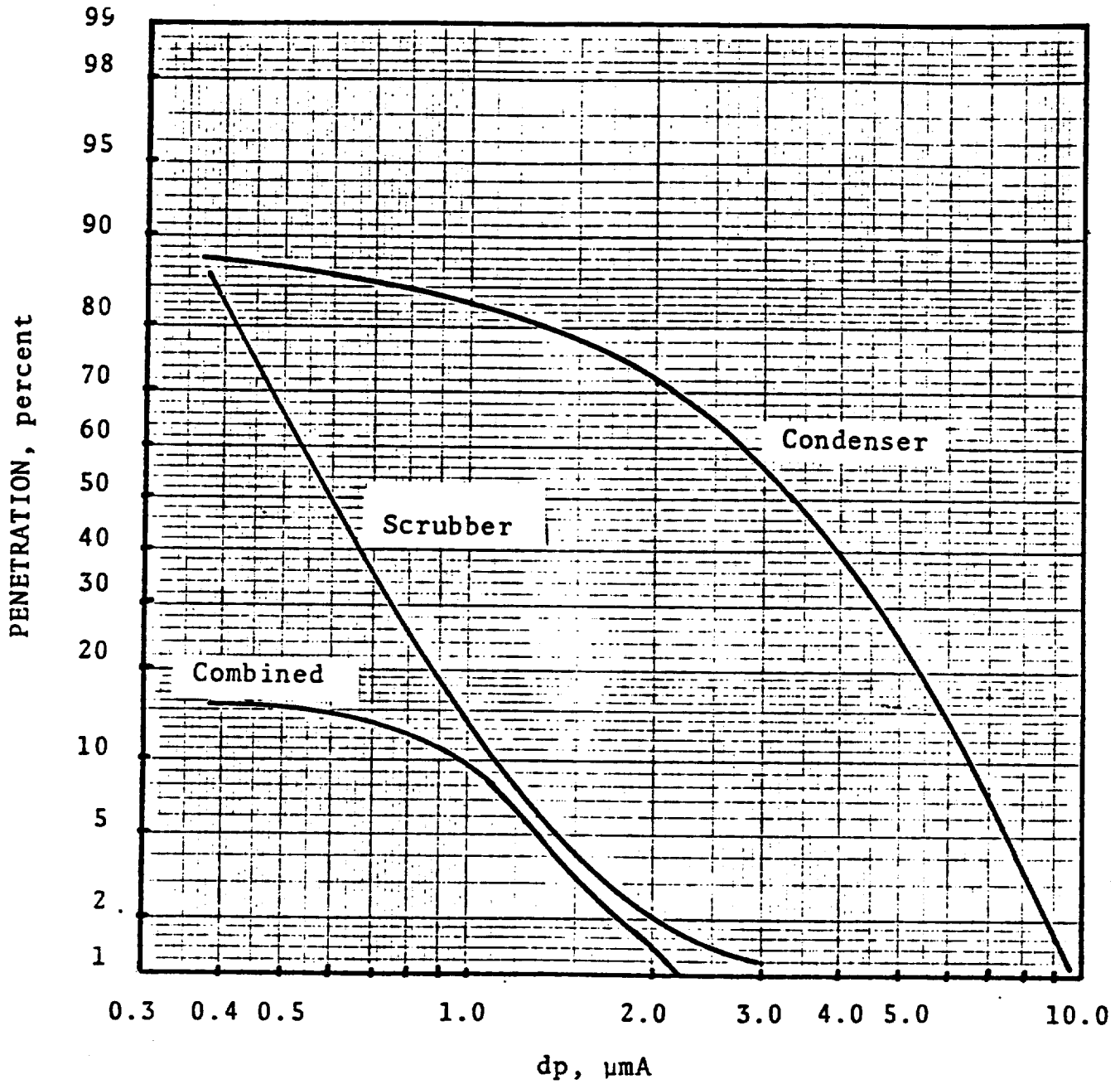


Figure 6-3 Example of Condenser, Scrubber, And Combined Penetration

Calculation of Particle Number Concentrations

The particle number concentrations were calculated from the size distribution and mass concentration assuming a log normal fit to the lowest three impactor cut points. The particle size distribution at the condenser inlet was bimodal probably due to a very small condensation aerosol and somewhat larger particles of ash, sand and soot carried with the exhaust gas to the scrubber system. If the smallest three cut points are used to construct a log normal size distribution the proper mass median particle diameter is generally obtained.]?

The particle number concentration is related to the mass concentration and mass mean diameter by the following equation:

$$n_p = \frac{6C}{\pi \rho_p d_m^3} \quad (6-10)$$

where

C = particle mass concentration, g/cm³
d_m = mass mean diameter, cm

The mass mean diameter is related to the mass median diameter by the following equation:

$$\ln d_m = \ln d_{pg} - 1.5 \ln \sigma_g^2 \quad (6-11)$$

where

d_{pg} = mass median diameter, cm
σ_g = geometric standard deviation

For several runs the number concentration calculated in this manner was found to be excessively high. For example aerosol systems with number concentration in excess of 10⁹ particles/cm³ can not exist ever for short periods of time before agglomeration of individual particles begins to reduce the particle number

concentration. Coagulation theory describes the rate of particle agglomeration as:

$$\frac{dn_p}{dt} = -Kn_p^2 \quad (6-12)$$

where

K = coagulation constant

For iron oxide which is the major constituent of the cupola particulate, K can be estimated to be $1 \times 10^{-9} \text{ cm}^3/\text{s}$ at the after burner temperature of 1200°K (Green and Lane, 1964).

Integration of equation (6-12) for various initial particle concentrations shows that a steady state particle concentration is reached after a few seconds independent of the initial particle concentration. The residence time of the exhaust gas to the saturator is about two seconds.

An upper limit particle number concentration can then be estimated at 5×10^8 particles/cms. This limit was applied to the previously calculated number concentrations when the initial number concentration was found to exceed 5×10^8 particle/cm³.

SECTION 7

COMPARISON OF EXPERIMENTAL RESULTS AND PERFORMANCE MODEL

TEST OPERATING CONDITIONS

The primary F/C scrubber system operating parameters of condenser liquid flow, scrubber pressure drop and condensation ratio are shown in Tables 7-1 and 7-2 for the two months of optimum performance. The "36 series" of tests was made in the induced draft configuration while the "37 series" was run in the forced draft mode.

The gas temperatures, flow rate and the measured condensation ratio are shown in Tables 7-3 and 7-4 for these runs. The hot gas temperature leaving the afterburner was for most of the runs significantly lower than anticipated. The design-basis hot gas temperature was 1,000°C. The maximum temperature measured was about 850°C. The reasons for the low gas temperature was (1) excessive air leakage through the cupola charging door and (2) the pilot burner was not available for installation until after testing was completed.

The lower than expected hot gas temperature resulted in lower gas humidity and a consequent reduction in the condensation ratio which could be achieved. The maximum condensation ratio obtained was about 0.20 gH₂O/gD.G. It had been anticipated that a condensation ratio of 0.30 g H₂O/gD.G. could be achieved with the higher gas temperature. The higher condensation ratio would further improve particulate collection due to condensation effects.

PARTICULATE MASS CONCENTRATIONS AND SIZE DISTRIBUTIONS

The particulate mass concentrations were measured both with total filters and cascade impacters. Tables 7-5 and 7-6 show the measured particulate mass concentrations. The average particulate

TABLE 7-1. F/C SCRUBBER SYSTEM OPERATING PARAMETERS FOR 36 SERIES

<u>Run No.</u>	<u>Condenser Flow l/s</u>	<u>Condensation Ratio g H₂O/g Dry Gas</u>	<u>Scrubber Δp cm W.C.</u>
36/1	47.3	0.13	43
36/2	47.3	0.21	48
36/3	47.3	0.18	51
36/4	47.3	0.06	66
36/5	47.3	0.23	64
36/6	47.3	0.19	76
36/7	47.3	0.14	76
36/8	25.2	0.03	76
36/9	25.2	0.12	74
36/10	25.2	0.08	53
36/11	25.2	0.10	53
36/12	25.2	0.10	64
36/13	25.2	0.16	61
36/14	47.3	0.17	38
36/15	47.3	0.17	38
36/16	25.2	0.13	41
36/17	44.2	0.15	58
36/18	47.3	0.03	66
36/19	47.3	0.12	66
36/20	47.3	0.05	51
36/21	47.3	0.18	53
36/22	25.2	0.11	53

TABLE 7-2. F/C SCRUBBER SYSTEM OPERATING PARAMETERS FOR 37 SERIES

<u>Run No.</u>	<u>Condenser Flow l/s</u>	<u>Condensation Ratio g H₂O/g Dry Gas</u>	<u>Scrubber Δp cm W.C.</u>
37/1	68	0.15	79
37/2	66	0.11	51
37/3	67	0.17	53
37/4	67	0.06	41
37/5	47	0.09	64
37/6	47	0.05	38
37/7	47	0.02	38
37/8	47	0.16	76
37/9	47	0.09	76
37/10	25	0.14	61
37/11	25	0.10	61
37/12	25	0.04	38
37/13	25	0.04	38
37/14	47	0.10	51
37/15	25	0.03	69
37/16	25	0.03	71
37/17	38	0.02	66
37/18	38	0.00	64
37/19	47	0.11	51
37/20	25	0.05	64
37/21	47	0.01	76
37/22	25	0.11	76
37/23	25	0.16	76
37/24	47	0.19	64
37/25	73	0.12	64
37/26	82	0.02	51

TABLE 7-3. GAS FLOW RATES, TEMPERATURES AND MEASURED CONDENSATION RATIO FOR 36 SERIES

Run No.	Gas Flow Rate DNm ³ /s	Sat. Inlet Temp °C	Cond. Inlet Temp °C	Cond. Outlet Temp °C	Cond. Ratio g H ₂ O/g D.G.
36/1	7.88	566	66	41	0.13
36/2	7.13	855	70	48	0.21
36/3	7.13	741	73	43	0.18
36/4	7.13	700	71	41	0.06
36/5	7.13	766	74	42	0.23
36/6	6.80	713	72	45	0.19
36/7	6.80	733	67	43	0.14
36/8	6.80	585	66	52	0.03
36/9	6.56	780	75	59	0.12
36/10	6.56	766	74	61	0.08
36/11	6.56	627	70	59	0.10
36/12	6.42	858	74	61	0.10
36/13	6.42	749	71	59	0.16
36/14	6.18	583	66	38	0.17
36/15	6.18	619	69	38	0.17
36/16	7.97	649	71	58	0.13
36/17	6.00	792	75	59	0.15
36/18	7.00	460	65	59	0.03
36/19	6.60	683	70	56	0.12
36/20	6.08	605	70	59	0.05
36/21	5.90	648	73	57	0.18
36/22	5.94	639	71	56	0.11

6.69 Sout
6.74 Sin
6.67 Sin

TABLE 7-4. GAS FLOW RATES, TEMPERATURES AND MEASURED CONDENSATION RATIO FOR 37 SERIES

Run No.	Gas Flow Rate DNm ³ /s.	Sat. Inlet Temp °C	Cond. Inlet Temp °C	Cond. Outlet Temp °C	Cond. Ratio g H ₂ O/g D.G.
37/1	6.09	645	74	57	0.15
37/2	7.27	649	74	58	0.11
37/3	6.98	705	70	54	0.17
37/4	7.22	574	73	60	0.06
37/5	7.74	719	77	63	0.09
37/6	6.61	500	66	66	0.05
37/7	7.22	452	67	58	0.02
37/8	7.98	836	77	60	0.16
37/9	8.11	498	61	51	0.09
37/10	6.18	802	75	61	0.14
37/11	5.14	816	76	75	0.10
37/12	5.43	840	75	70	0.04
37/13	5.80	714	73	71	0.04
37/14	7.13	662	77	60	0.10
37/15	6.42	649	71	65	0.03
37/16	6.42	621	70	65	0.03
37/17	5.14	671	69	69	0.02
37/18	5.14	688	70	68	0.00
37/19	5.14	496	64	52	0.11
37/20	6.89	483	63	56	0.05
37/21	6.61	219	51	48	0.01
37/22	5.68	796	77	63	0.11
37/23	5.80	740	73	60	0.16
37/24	5.00	752	73	55	0.19
37/25	6.50	690	74	56	0.12
37/26	5.64	610	76	60	0.02

TABLE 7-5. PARTICULATE MASS CONCENTRATIONS

MASS CONCENTRATIONS, g/DNm³

<u>Run No.</u>	<u>Cond. Inlet</u>	<u>Scrubber Inlet</u>	<u>Scrubber Outlet</u>
36/1	1.27	-	0.40
36/2	4.32	-	0.72
36/3	-	-	0.50
36/4	2.50	-	0.52
36/5	2.63	-	0.73
36/6	2.57	1.13	0.47
36/7	-	0.77	0.57
36/8	1.00	0.85	0.41
36/9	1.51	1.33	0.40
36/10	1.07	0.77	0.45
36/11	-	0.73	0.45
36/12	1.58	-	0.51
36/13	1.17	-	0.37
36/14	4.84	-	0.15
36/15	1.56	-	0.71
36/16	2.74	1.19	0.73
36/17	2.77	-	0.77
36/18	2.15	-	0.54
36/19	2.02	0.97	0.34
36/20	5.16	1.29	0.65
36/21	3.23	-	0.31
36/22	1.82	-	0.46
	<i>AVE</i> 2.42	1.00	

TABLE 7-6. PARTICULATE MASS CONCENTRATIONS

Run No.	MASS CONCENTRATIONS, g/DNm ³		
	<u>Cond. Inlet</u>	<u>Scrubber Inlet</u>	<u>Scrubber Outlet</u>
37/1	1.53	-	0.11
37/2	2.13	-	0.49
37/3	2.51	2.03	0.62
37/4	1.22	-	0.45
37/5	1.20	-	0.28
37/6	2.34	0.76	0.50
37/7	1.55	0.62	0.35
37/8	1.75	-	0.51
37/9	3.43	-	0.26
37/10	1.86	-	0.53
37/11	3.84	-	0.57
37/12	0.89	-	0.45
37/13	1.87	-	0.50
37/14	-	-	0.62
37/15	0.82	-	0.25
37/16	1.42	-	0.54
37/17	4.88	-	1.87
37/18	0.56	1.53	0.30
37/19	1.97	-	0.42
37/20	1.62	-	0.42
37/21	3.10	-	0.40
37/22	2.40	-	-
37/23	1.94	-	0.54
37/24	5.62	-	0.70
37/25	7.23	1.72	0.77
37/26	1.74	-	0.60
	2.38	1.33	

mass concentration at the inlet to the condenser was found to be 2.4 g/DNm³. The design basis mass concentration was 1.8 g/DNm³, the average mass concentration was therefore found to be 33% higher than the design basis.

The mass concentration varied significantly from run to run which reflects sampling during various periods in the charging cycle. Figure 7-1 is a histogram showing the variation in the measured mass concentrations at the inlet to the condenser. The results of the first several preliminary tests showed that insignificant mass was caught in the impingers. This is expected because of the nature of the source. As a consequence of these results the impinger catch was not routinely analyzed for mass, only for volume of condensed water.

The measured particle size distributions are shown in Appendix "A" for the runs in the series 36 and 37. These results also show variation from run to run. A statistical analysis was performed to obtain an average condenser inlet size distribution for use in determining the grade penetration curves. The averaging calculations were performed numerically using a computer program developed by Dr. Leslie Sparks of the U.S. Environmental Protection Agency (Sparks 1979). Figure 7-2 shows the resulting average condenser inlet size distribution. Figure 7-3 shows the cumulative particle mass concentration versus particle aerodynamic diameter.

Figure 7-4 through 7-49 show the measured penetration as a function of particle size. The predicted penetration for the runs are also shown in the dashed line. The agreement between predicted and measured penetrations are good.

*Some are -
Some are not*

FREQUENCY, fraction

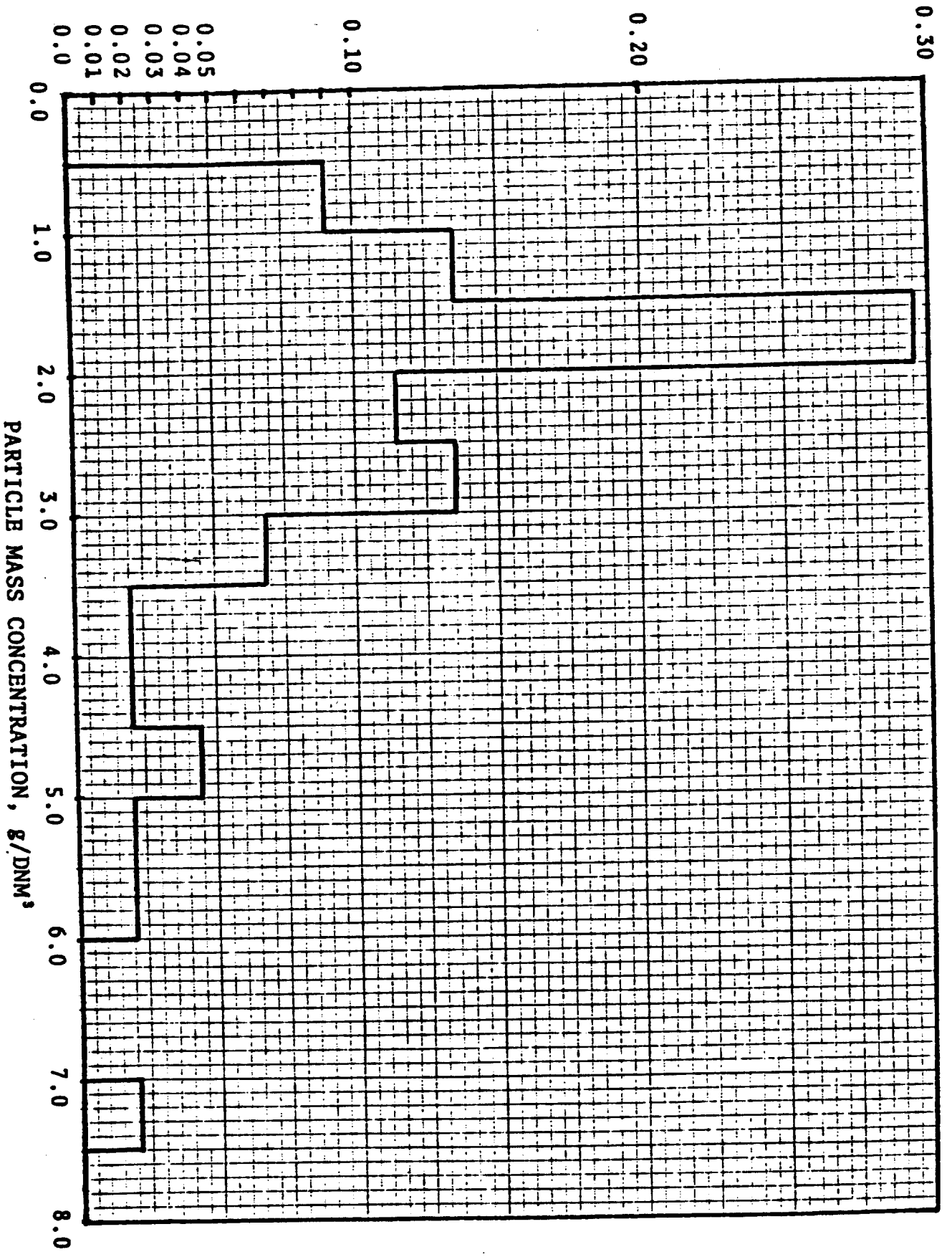


Figure 7-1. Histogram of Condenser Inlet Mass Concentration

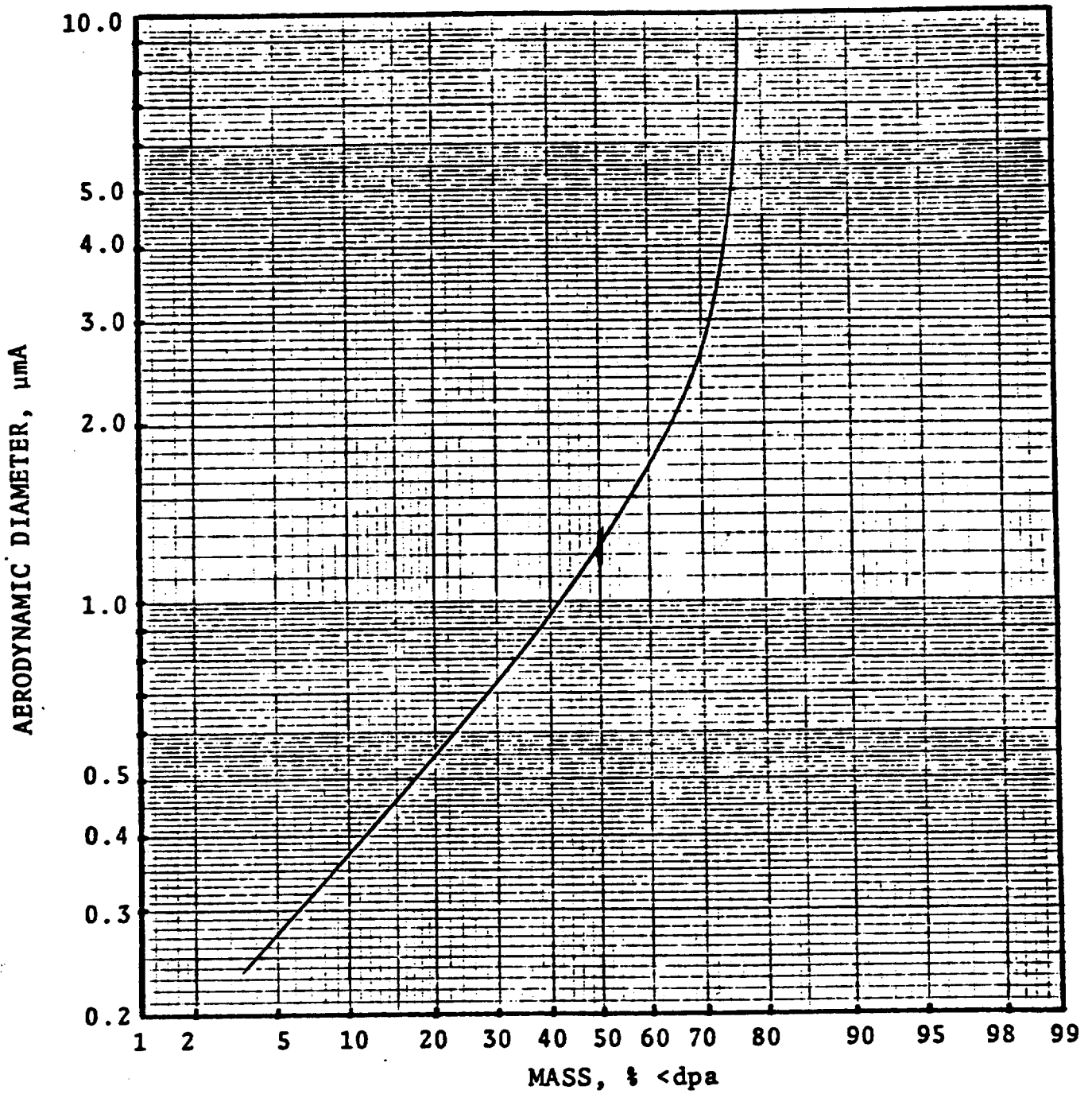


Figure 7-2. Average Condenser Inlet Size Distribution

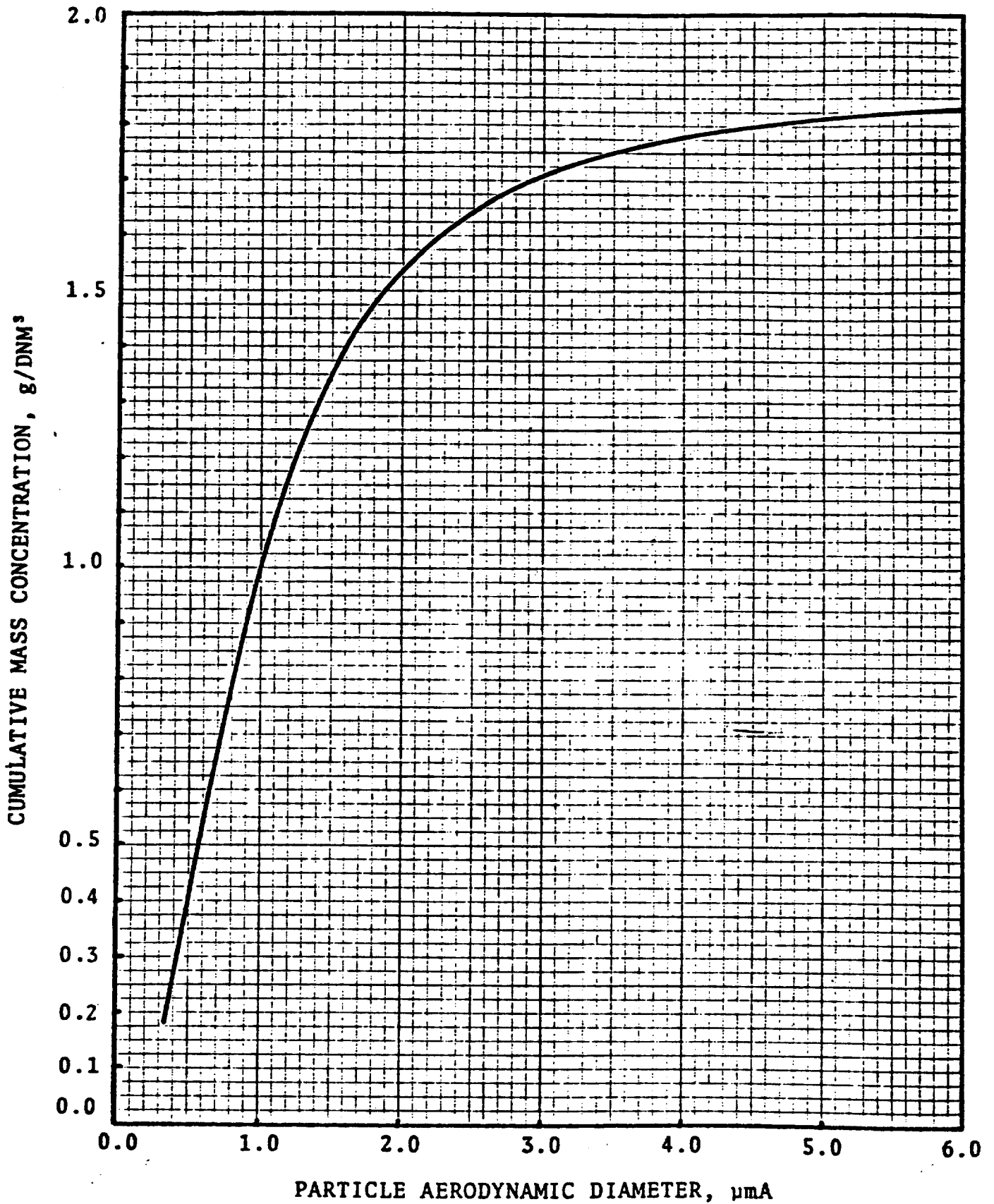


Figure 7-3. Average Condenser Inlet Cumulative Size Distribution

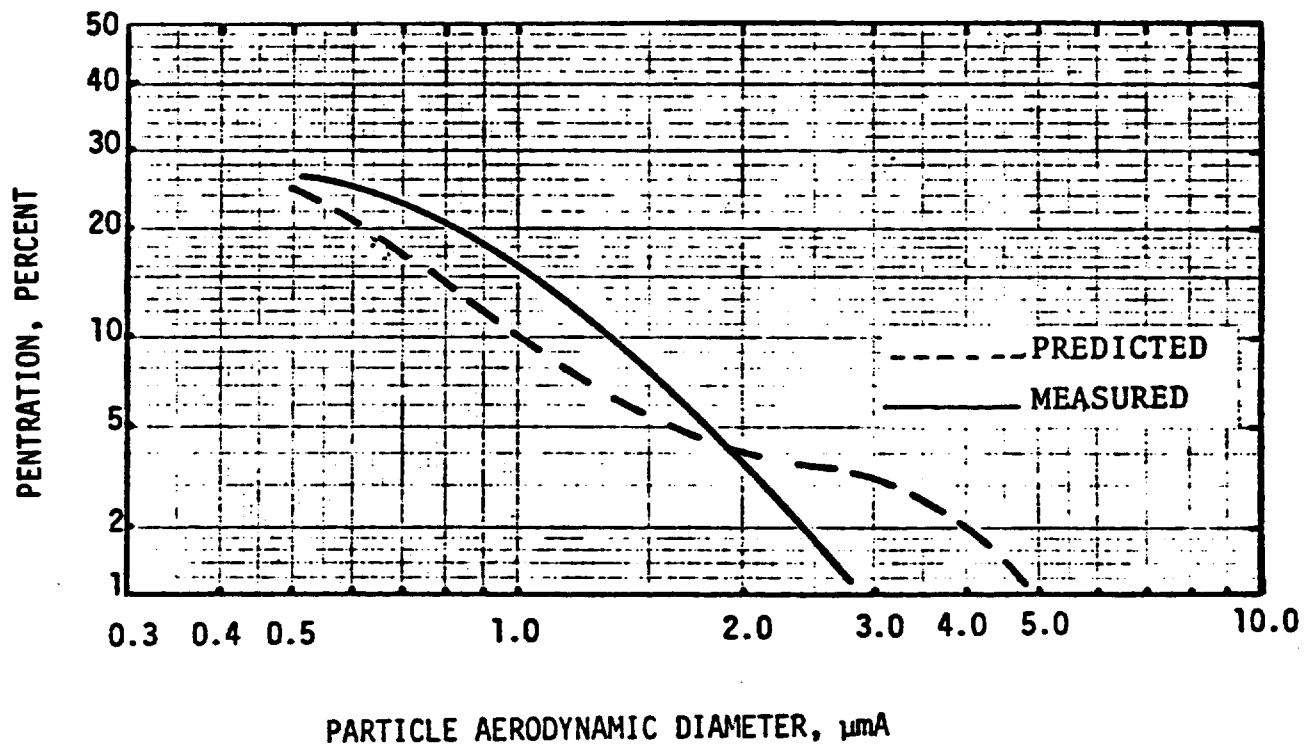


Figure 7-4. Predicted and Experimental Penetration Run 36/1

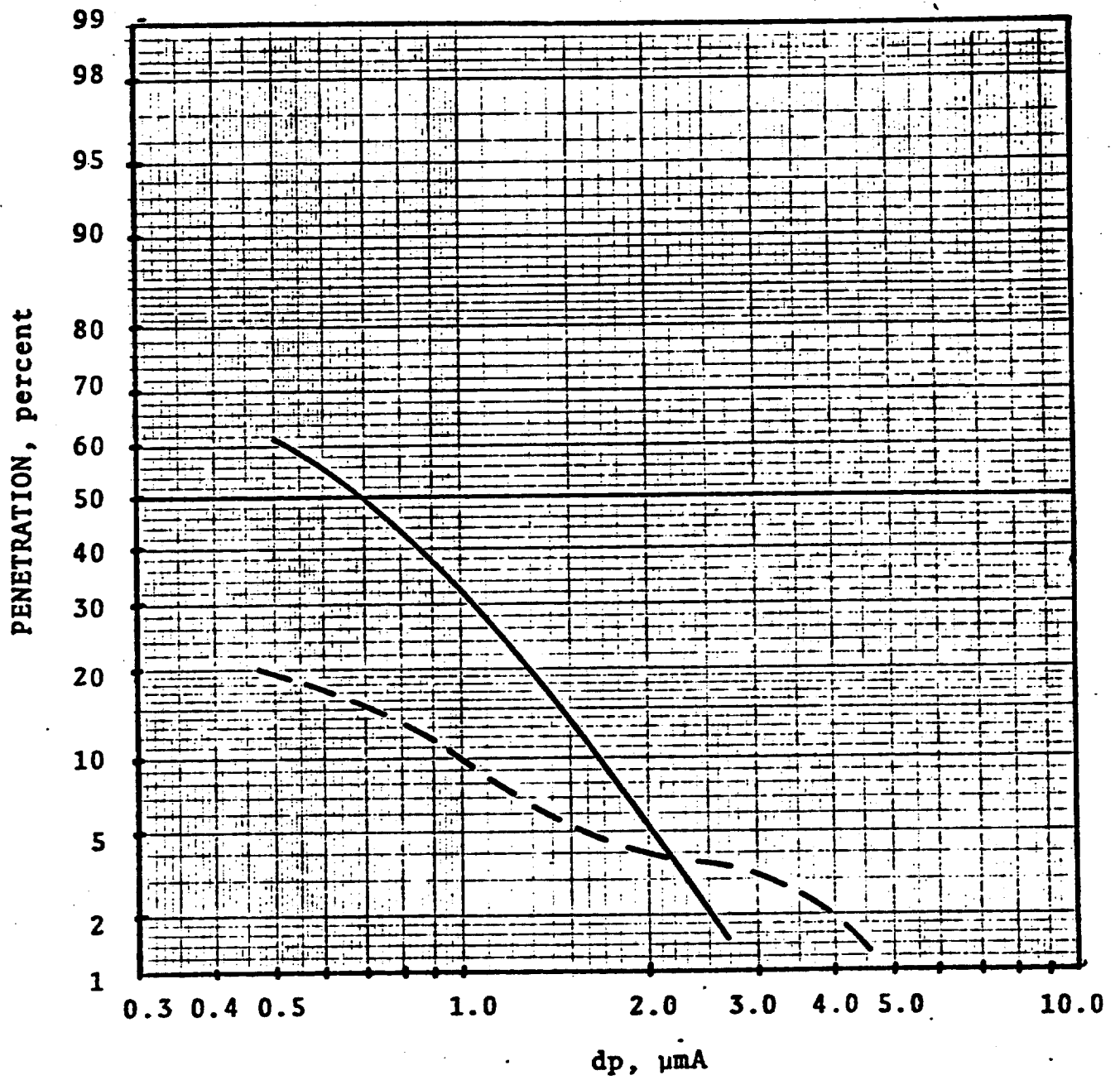


Figure 7-5 Predicted and Experimental Penetration Run 36/2

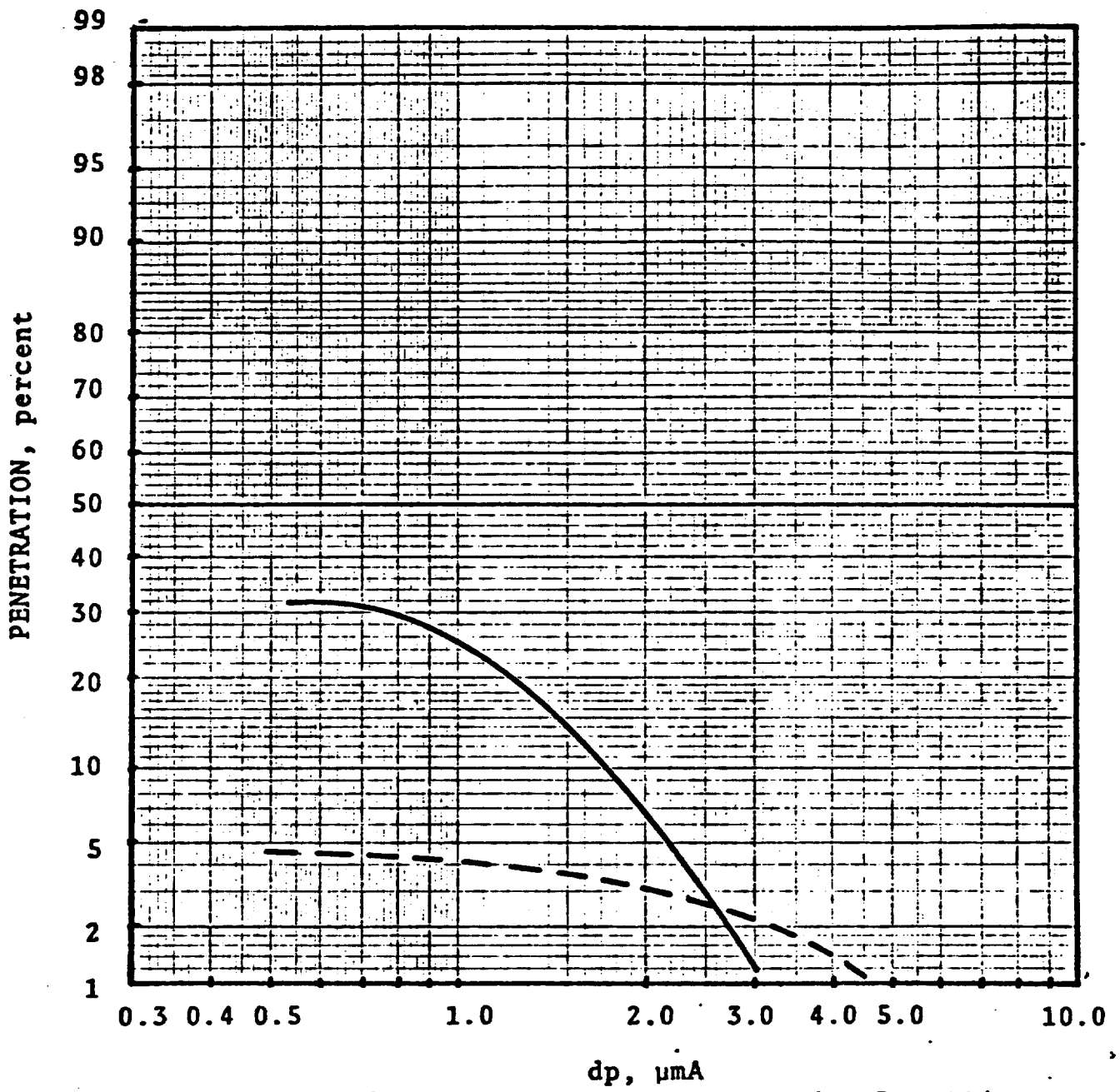


Figure 7-6 Predicted and Experimental Penetration Run 36/3

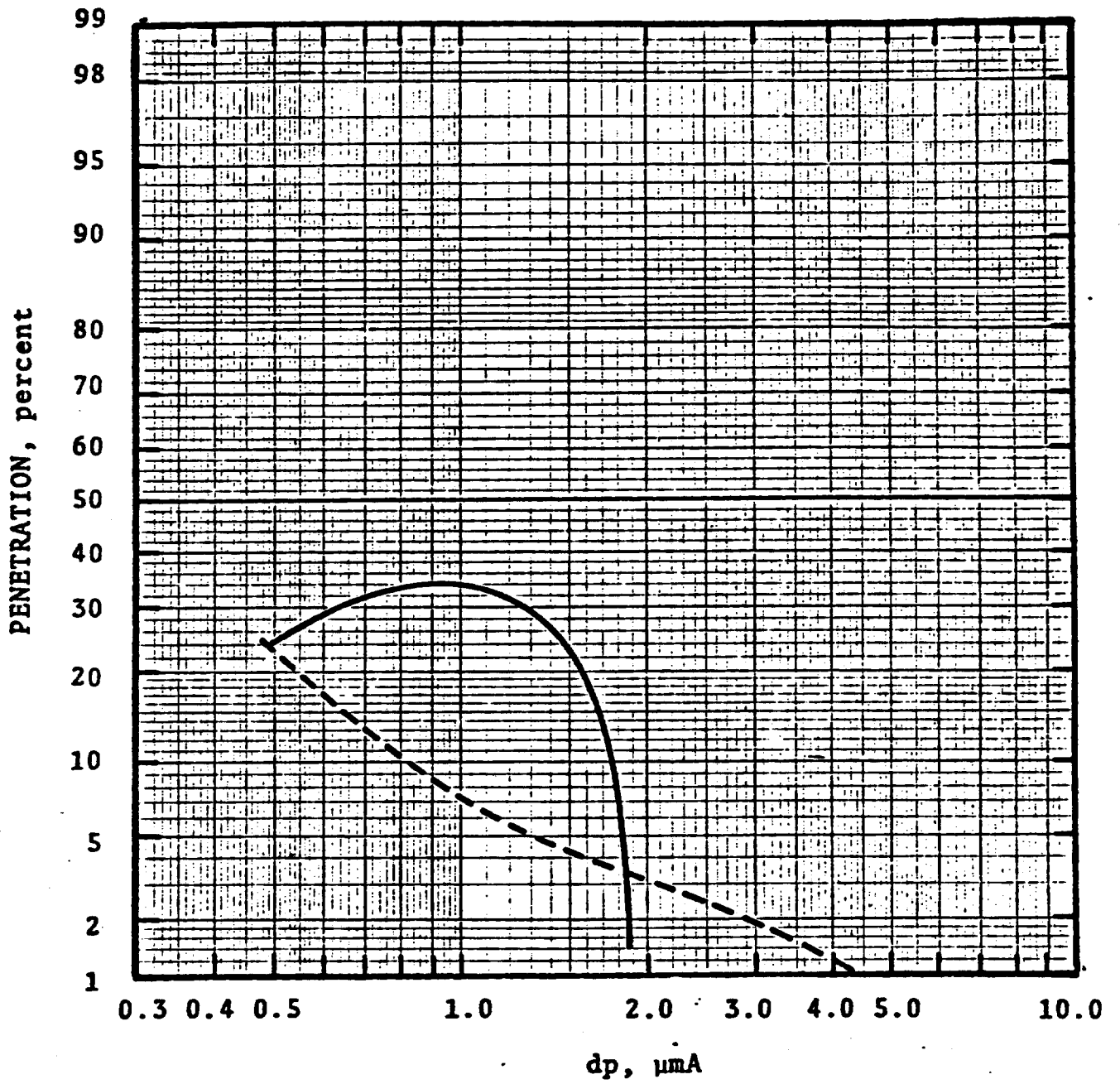


Figure 7-7 Predicted and Experimental Penetration Run 36/4

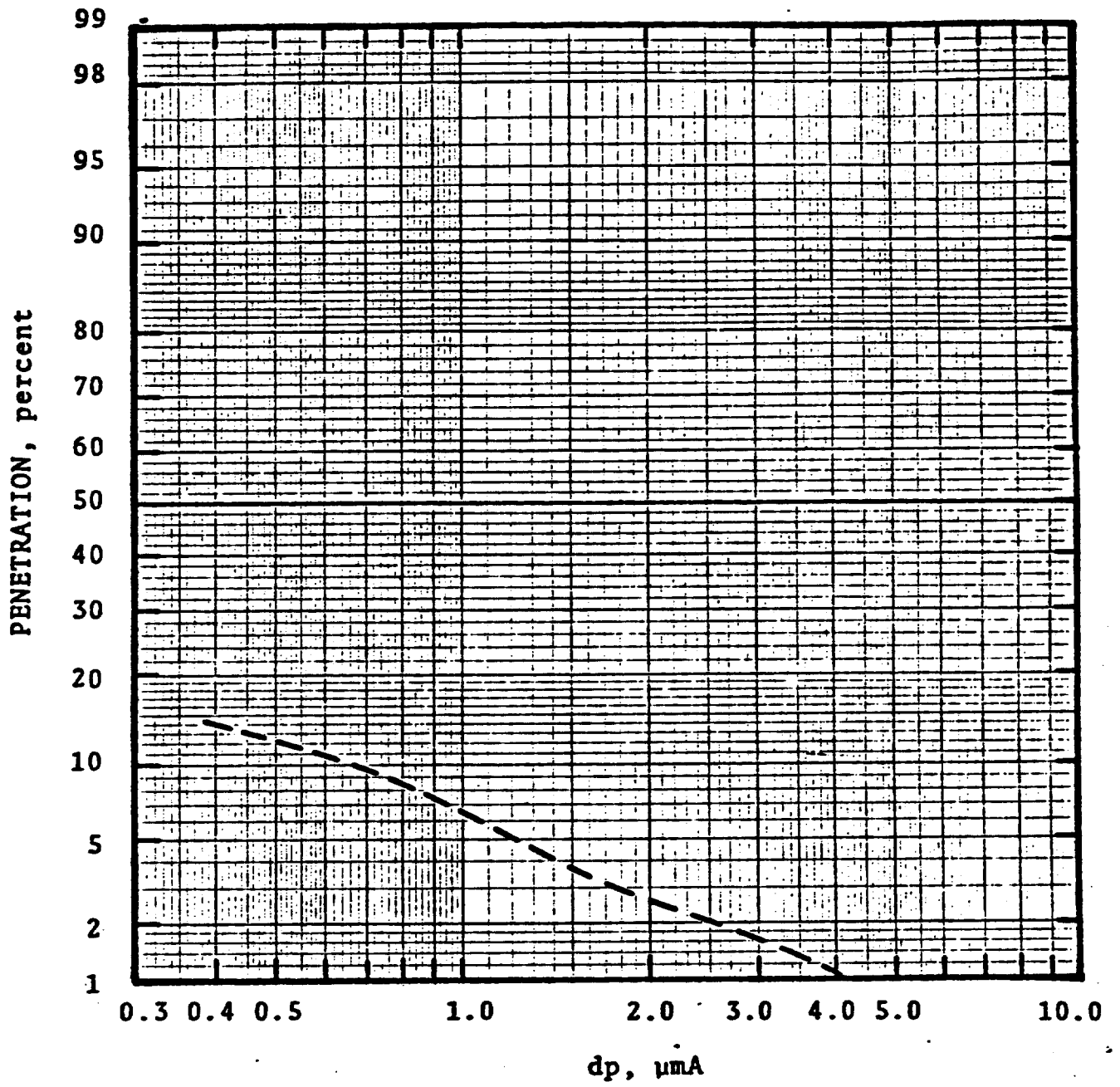


Figure 7-8 Predicted and Experimental Penetration Run 36/5

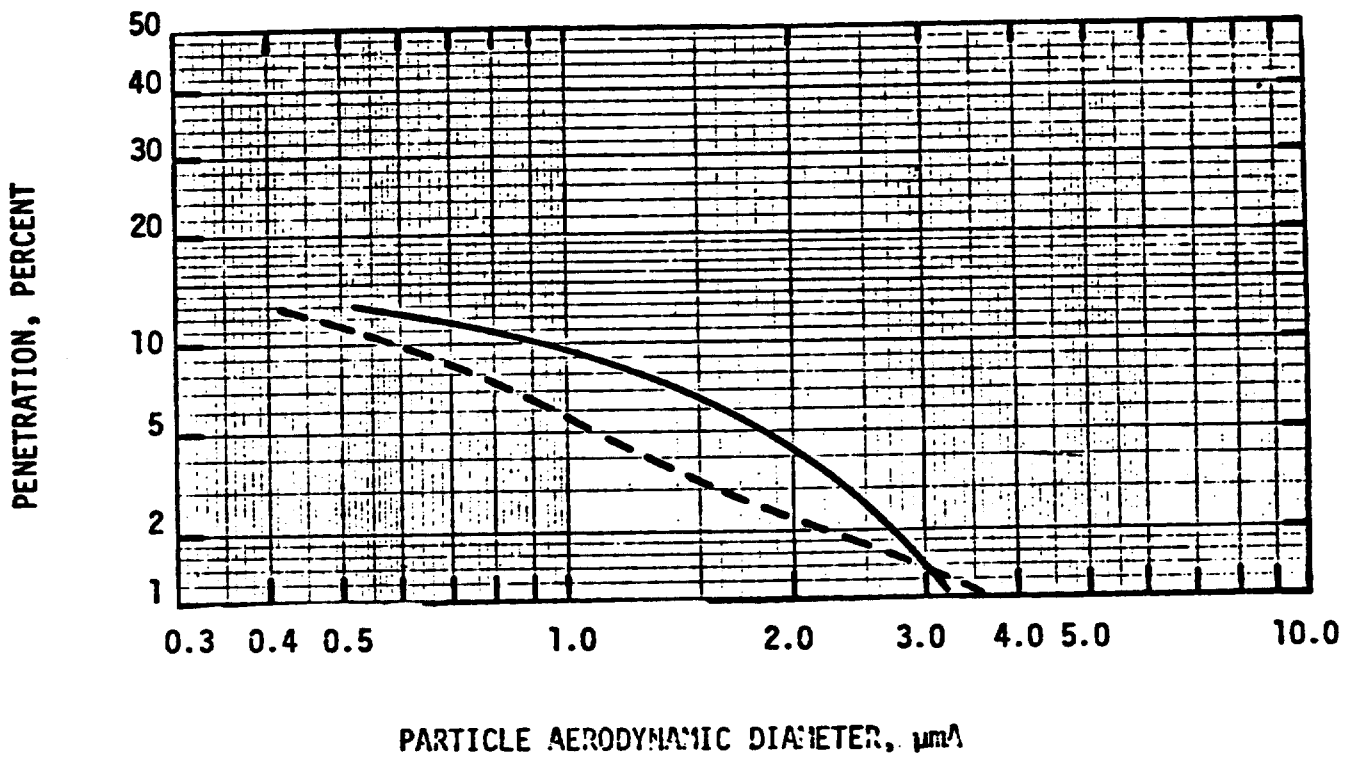


Figure 7-9. Predicted and Experimental Penetration Run 36/6

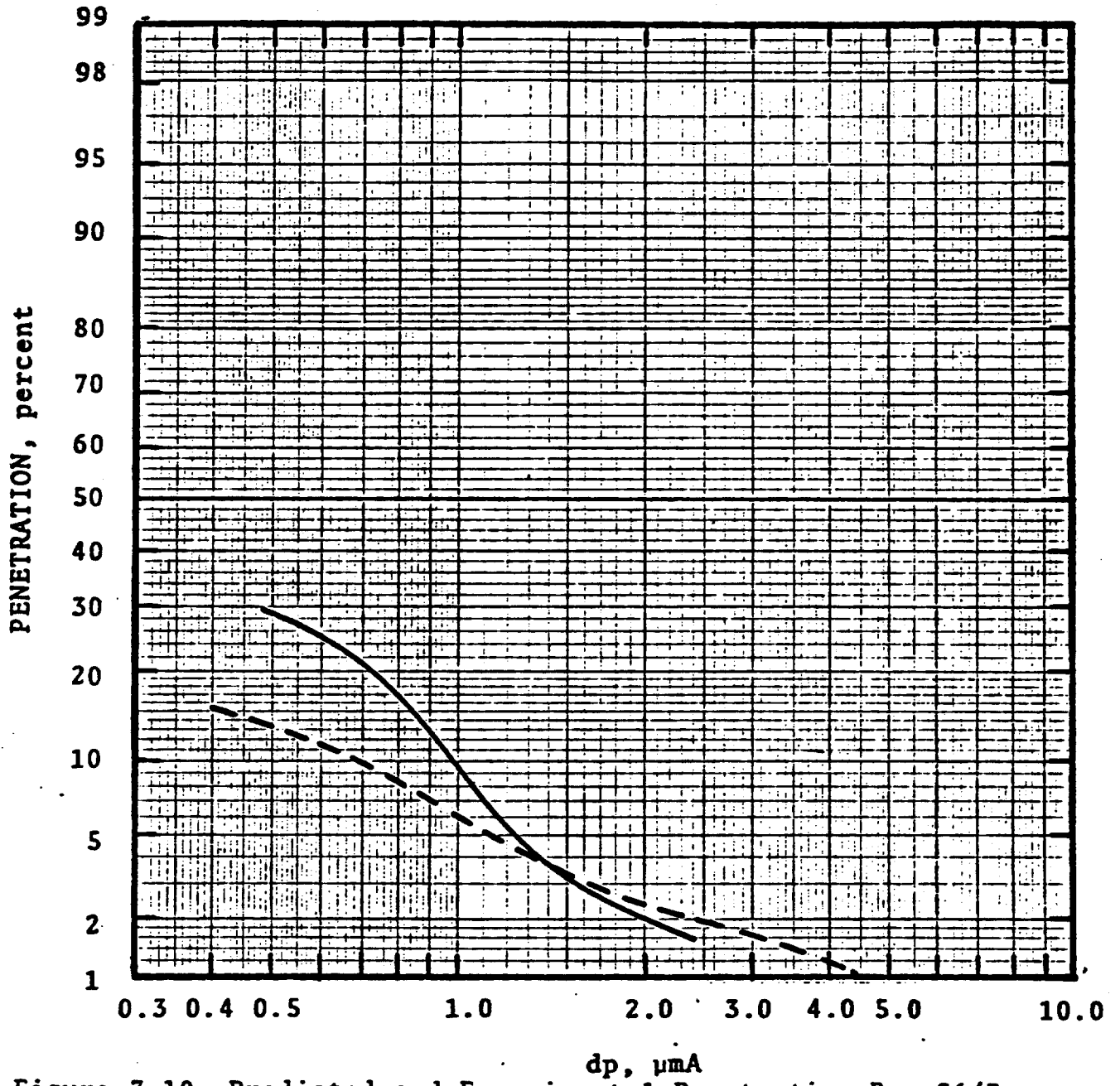


Figure 7-10 Predicted and Experimental Penetration Run 36/7

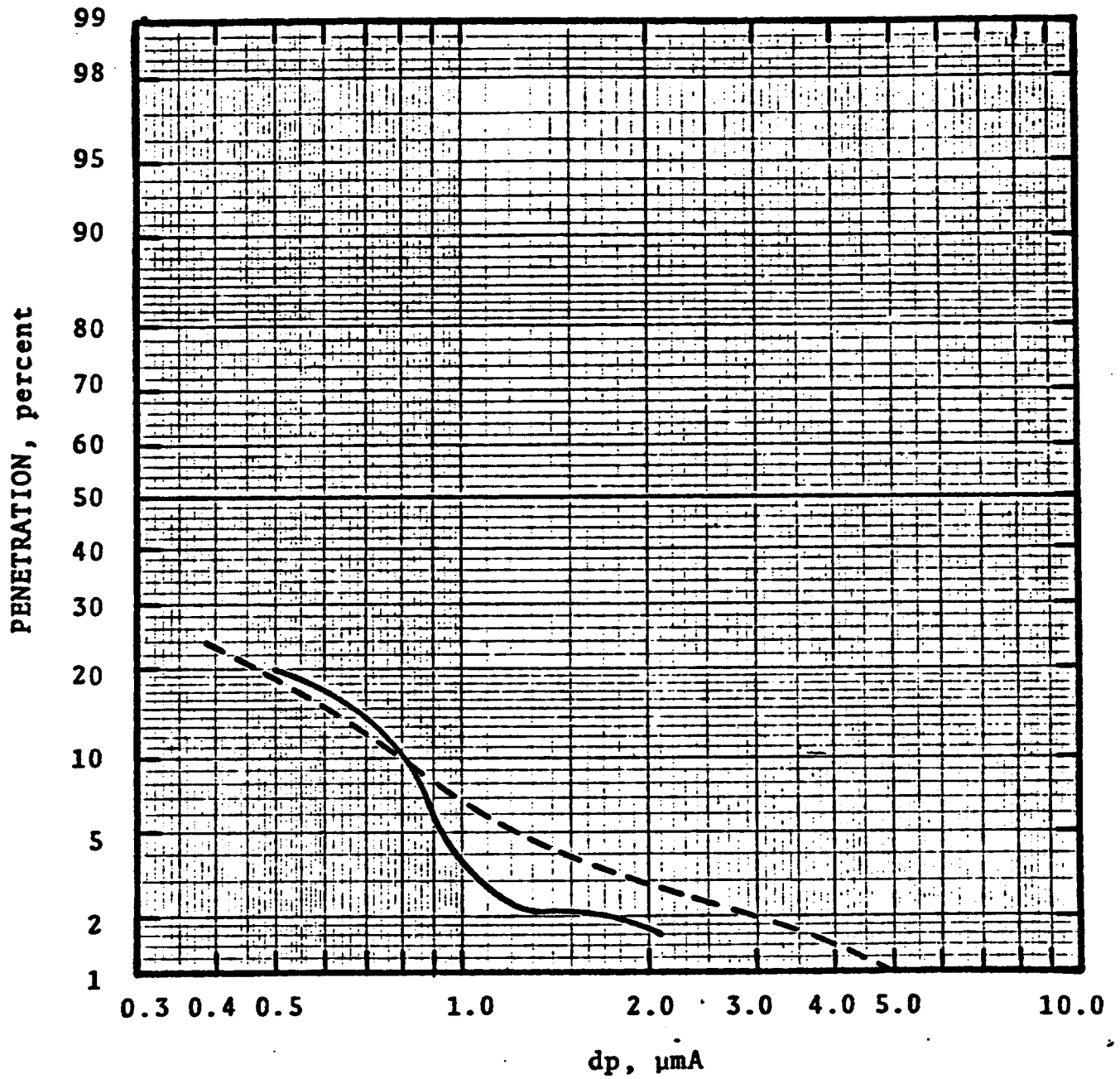


Figure 7-11 Predicted and Experimental Penetration Run 36/8

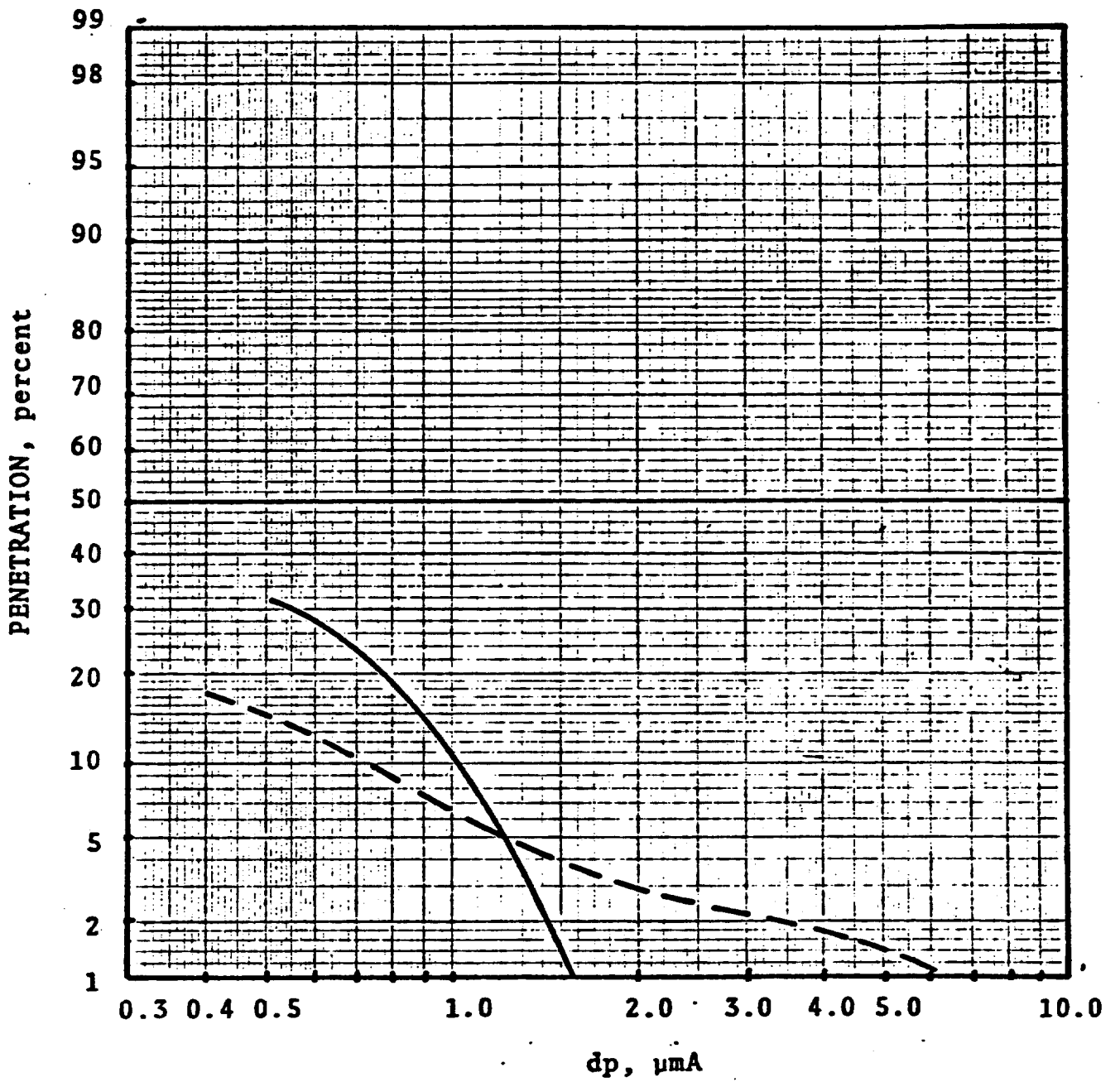


Figure 7-12 Predicted and Experimental Penetration Run 36/9

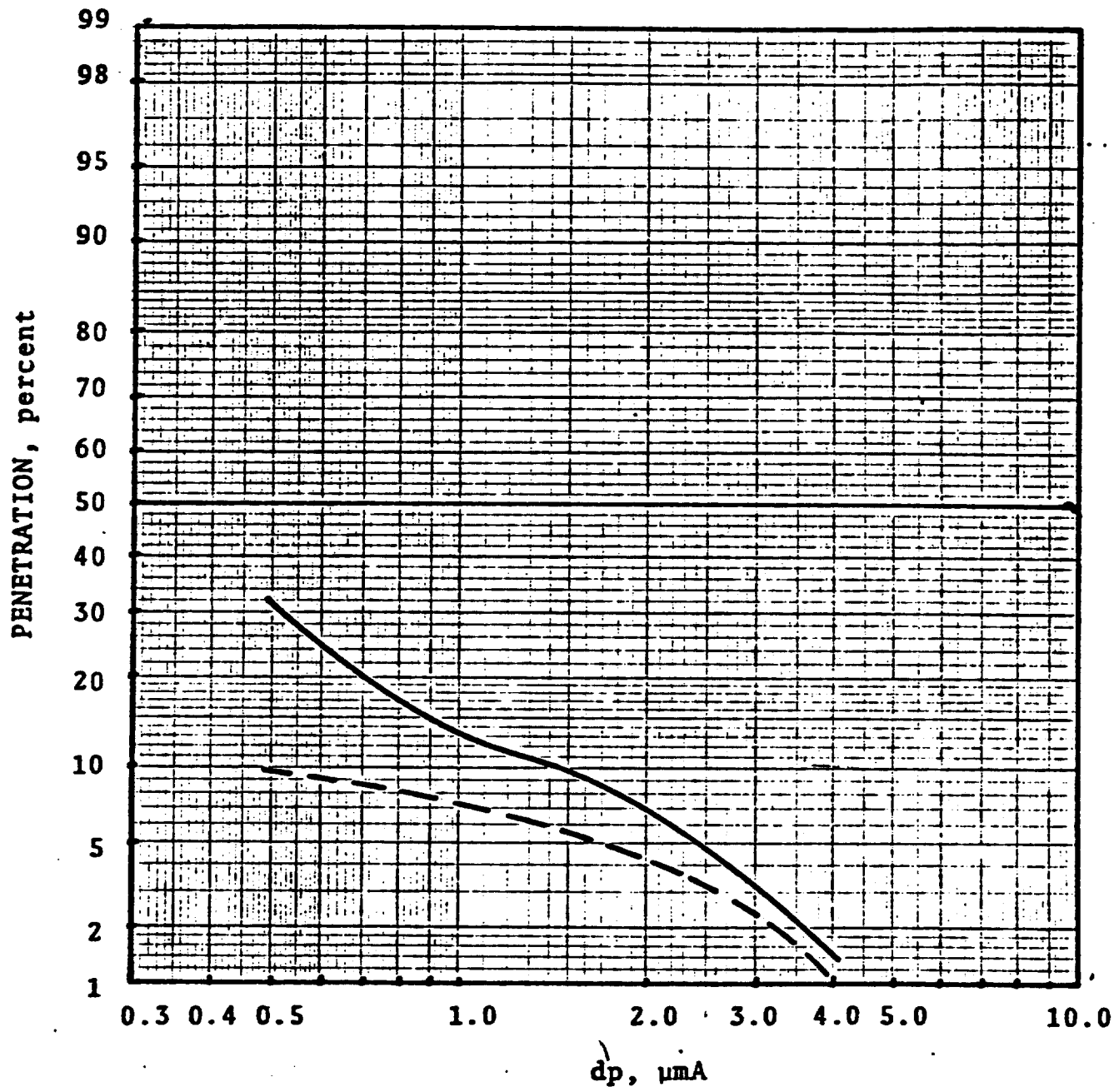


Figure 7-13| Predicted and Experimental Penetration Run 36/10

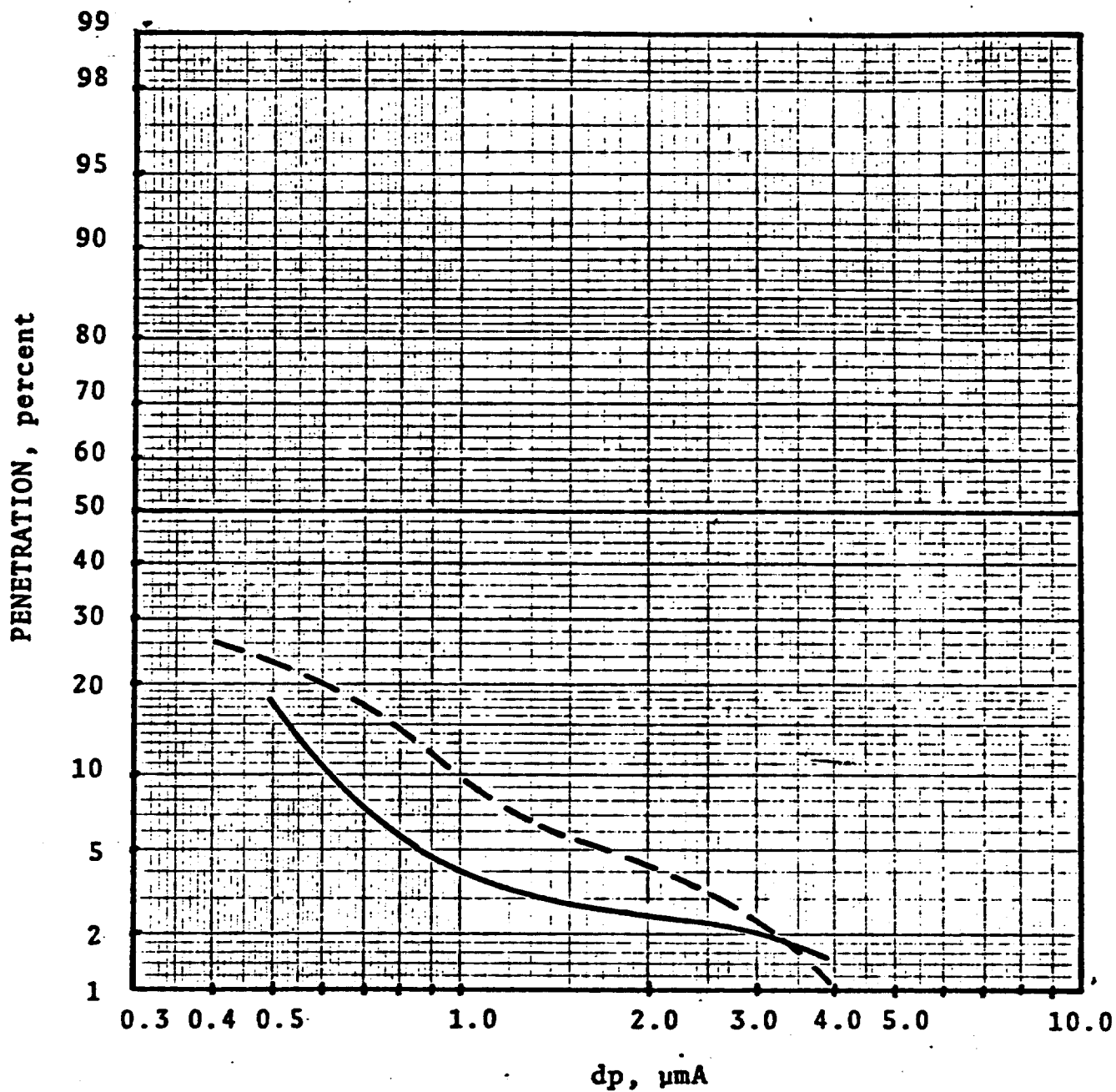


Figure 7-14 Predicted and Experimental Penetration Run 36/11

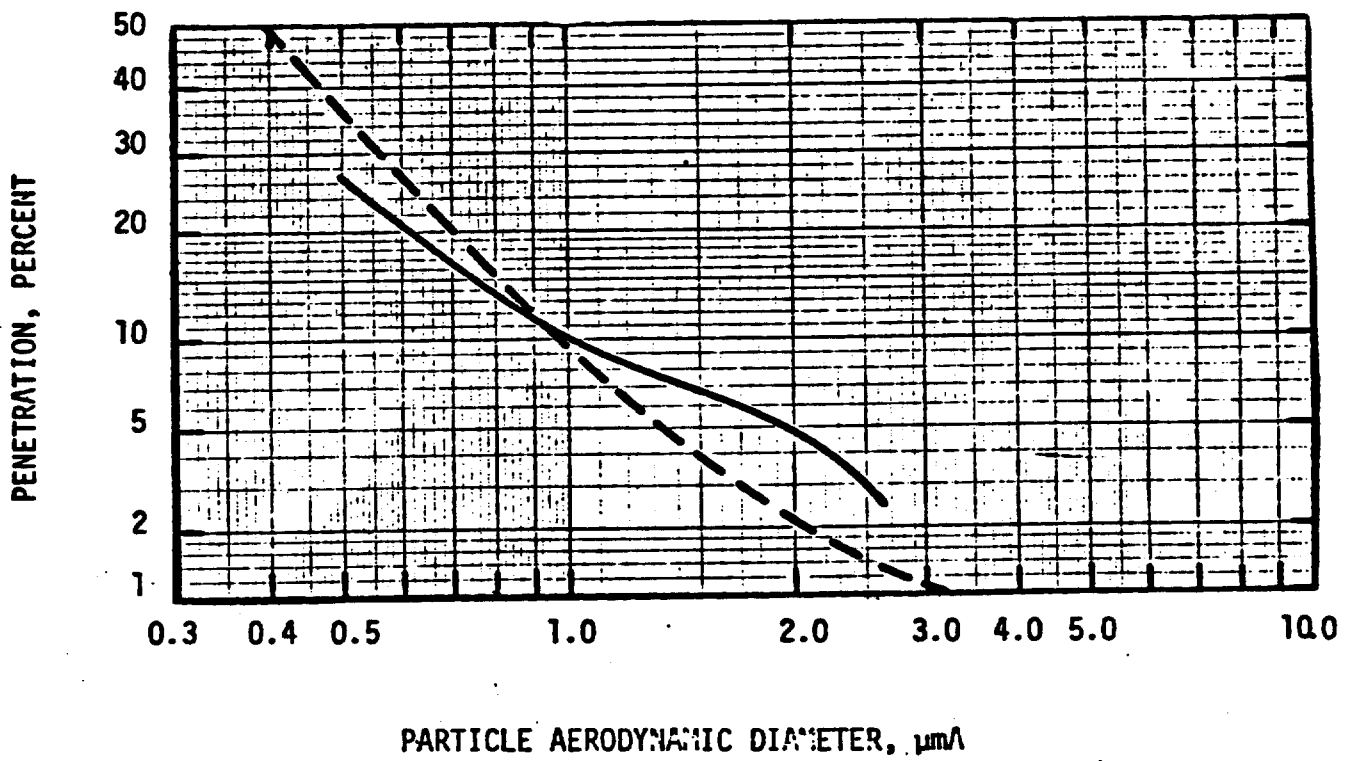


Figure 7-15. Predicted and Experimental Penetration Run 36/12

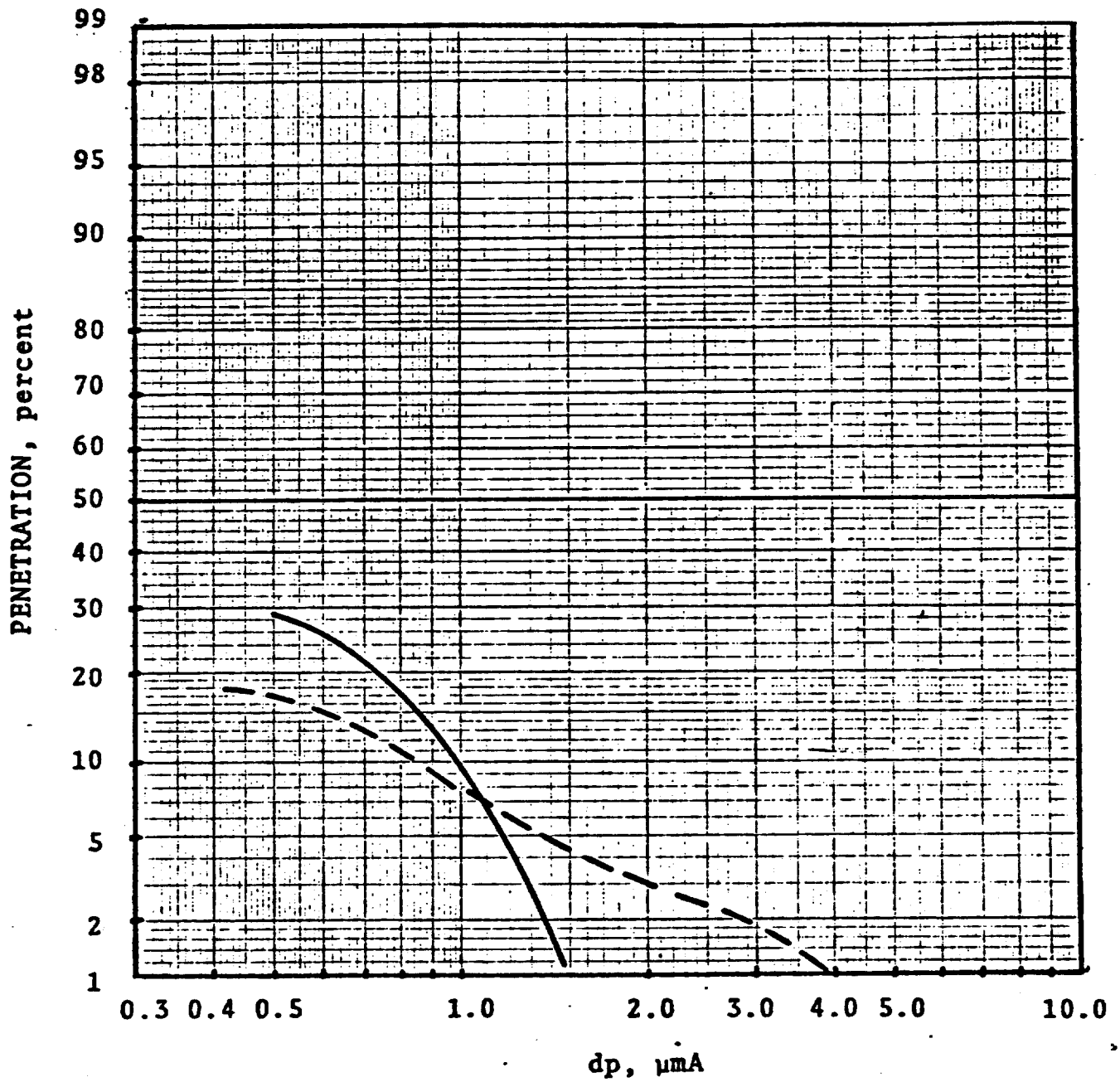


Figure 7-16! Predicted and Experimental Penetration Run 36/13

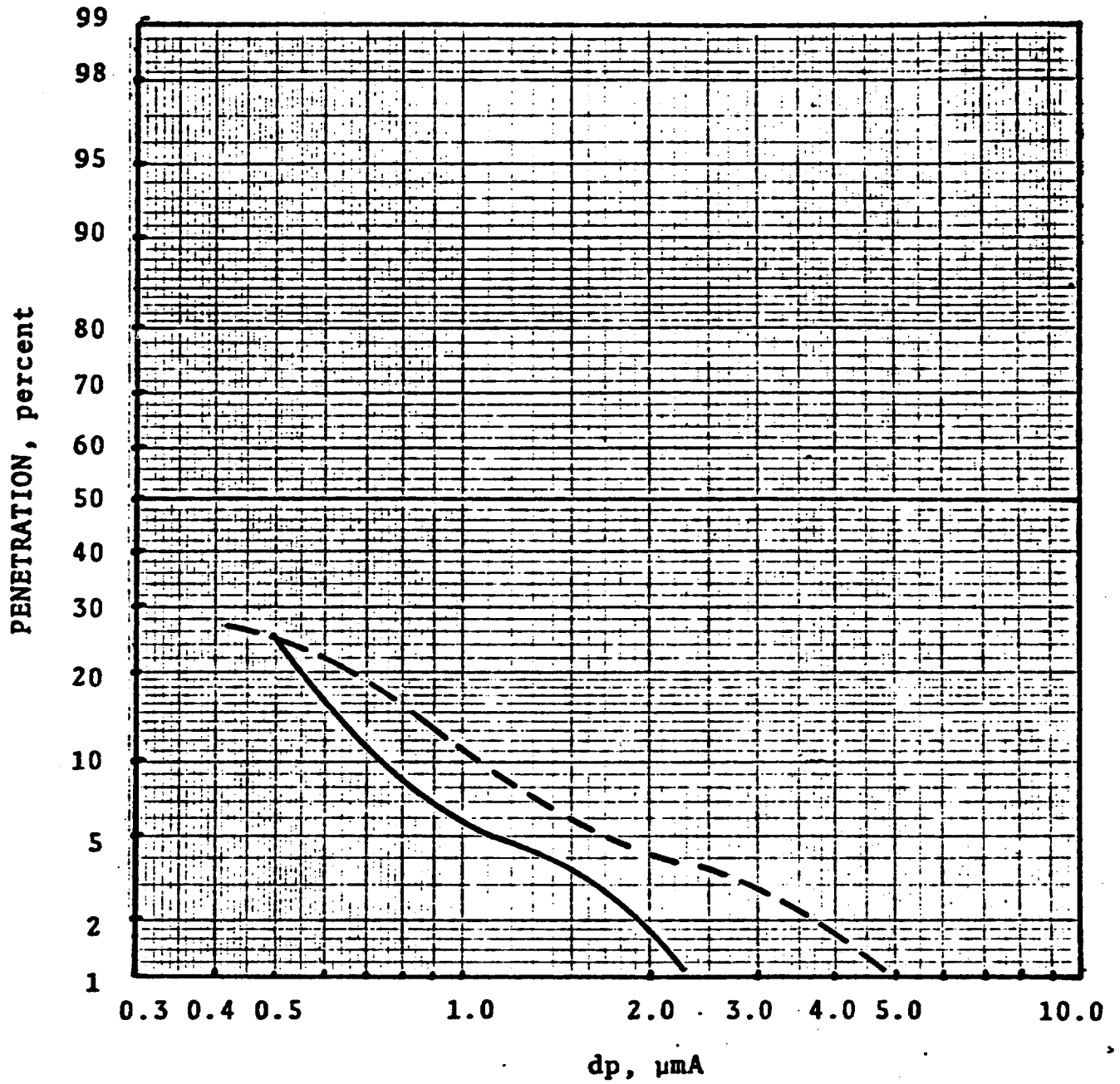


Figure 7-17 | Predicted and Experimental Penetration Run 36/14

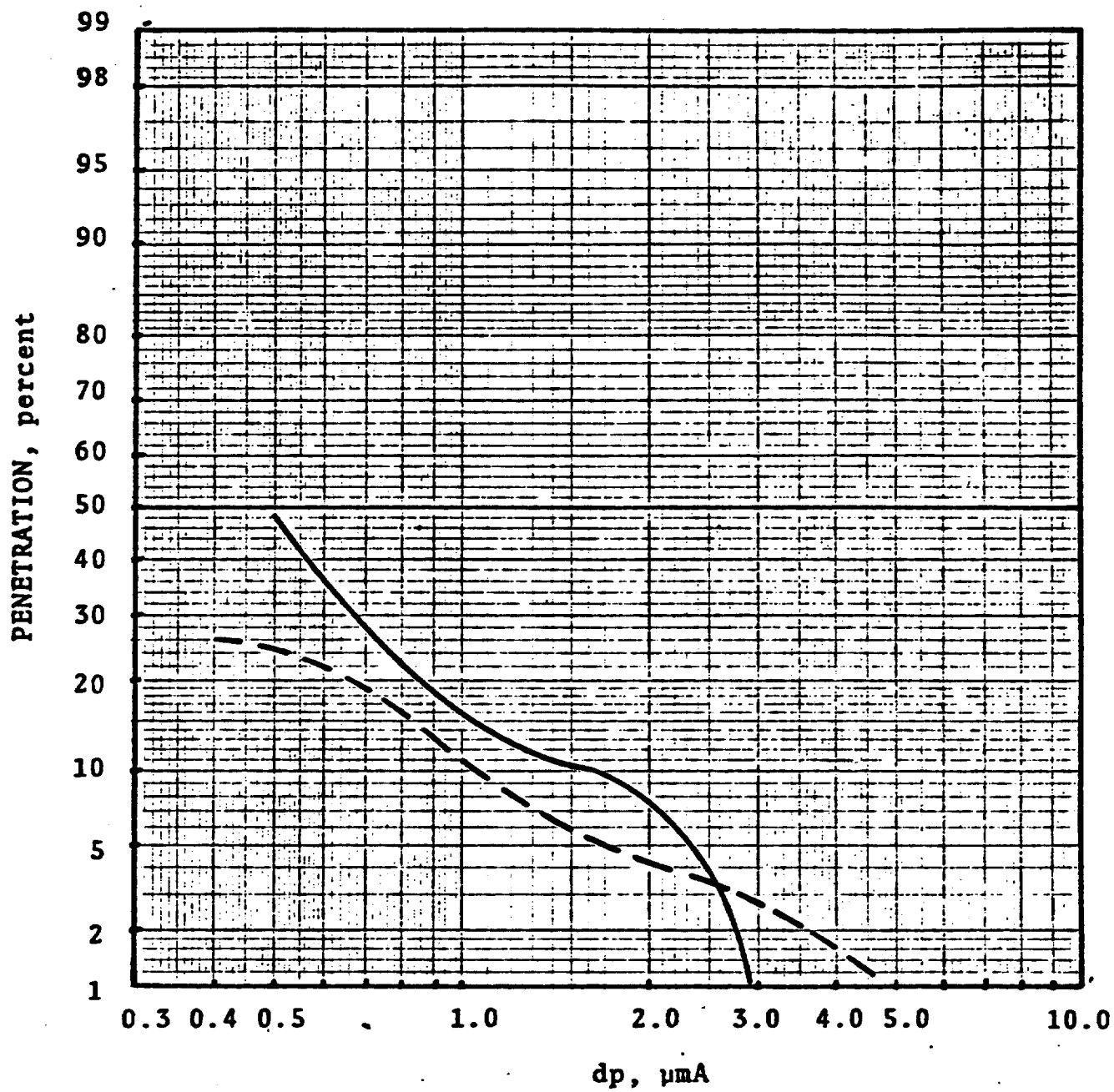


Figure 7-18 | Predicted and Experimental Penetration Run 36/15

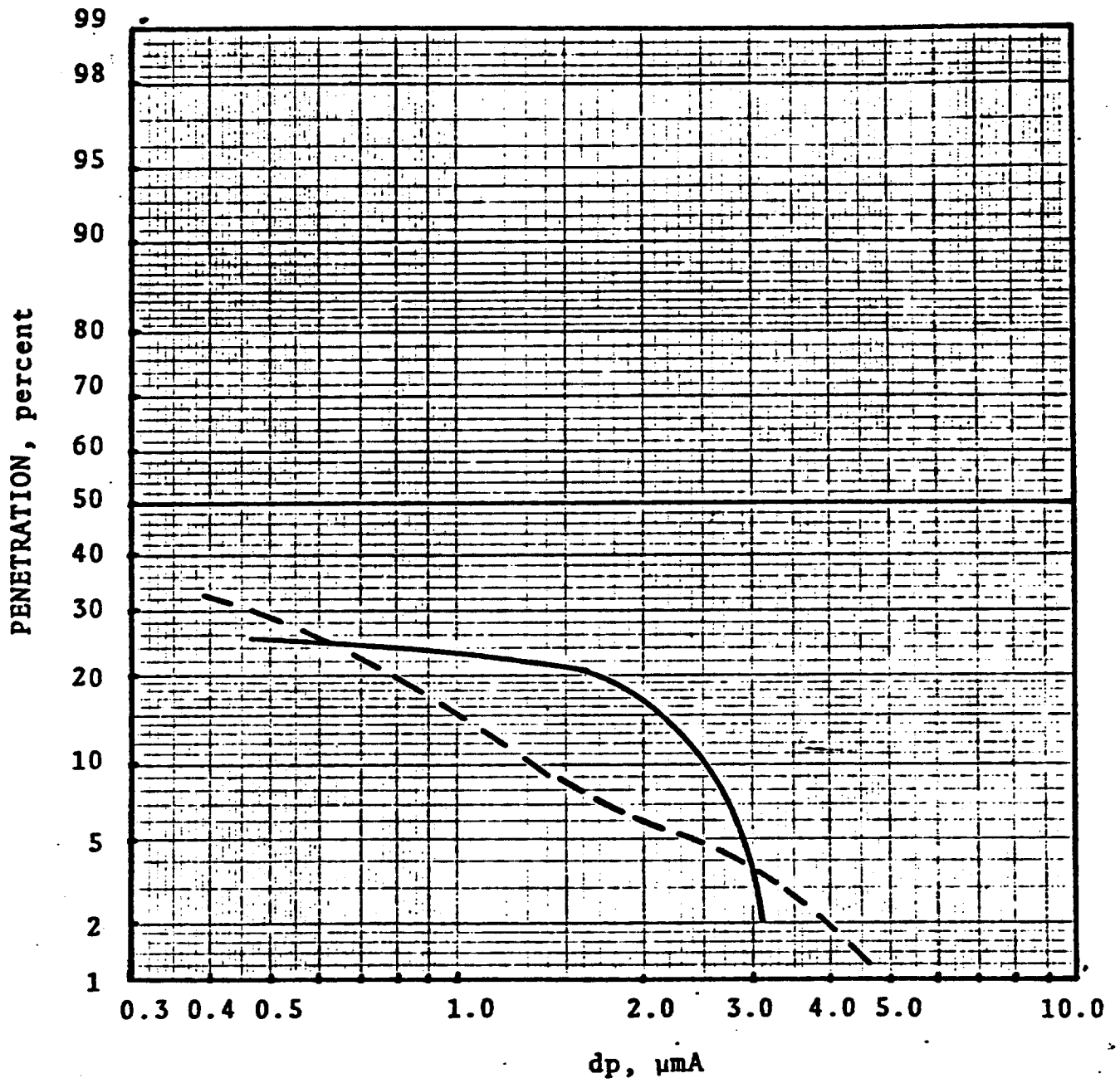


Figure 7-19 Predicted and Experimental Penetration Run 34/16

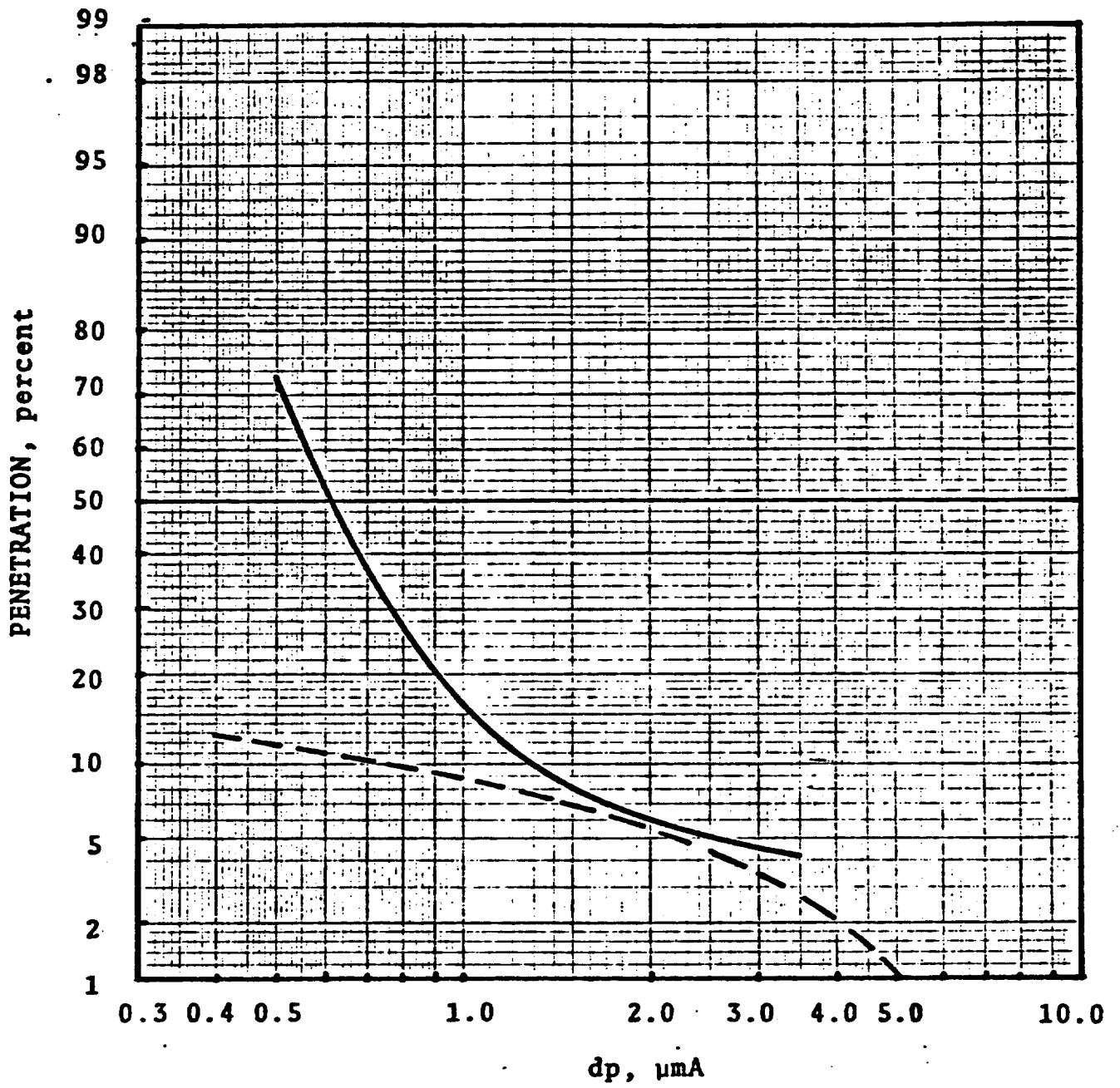


Figure 7-20 Predicted and Experimental Penetration Run 36/17

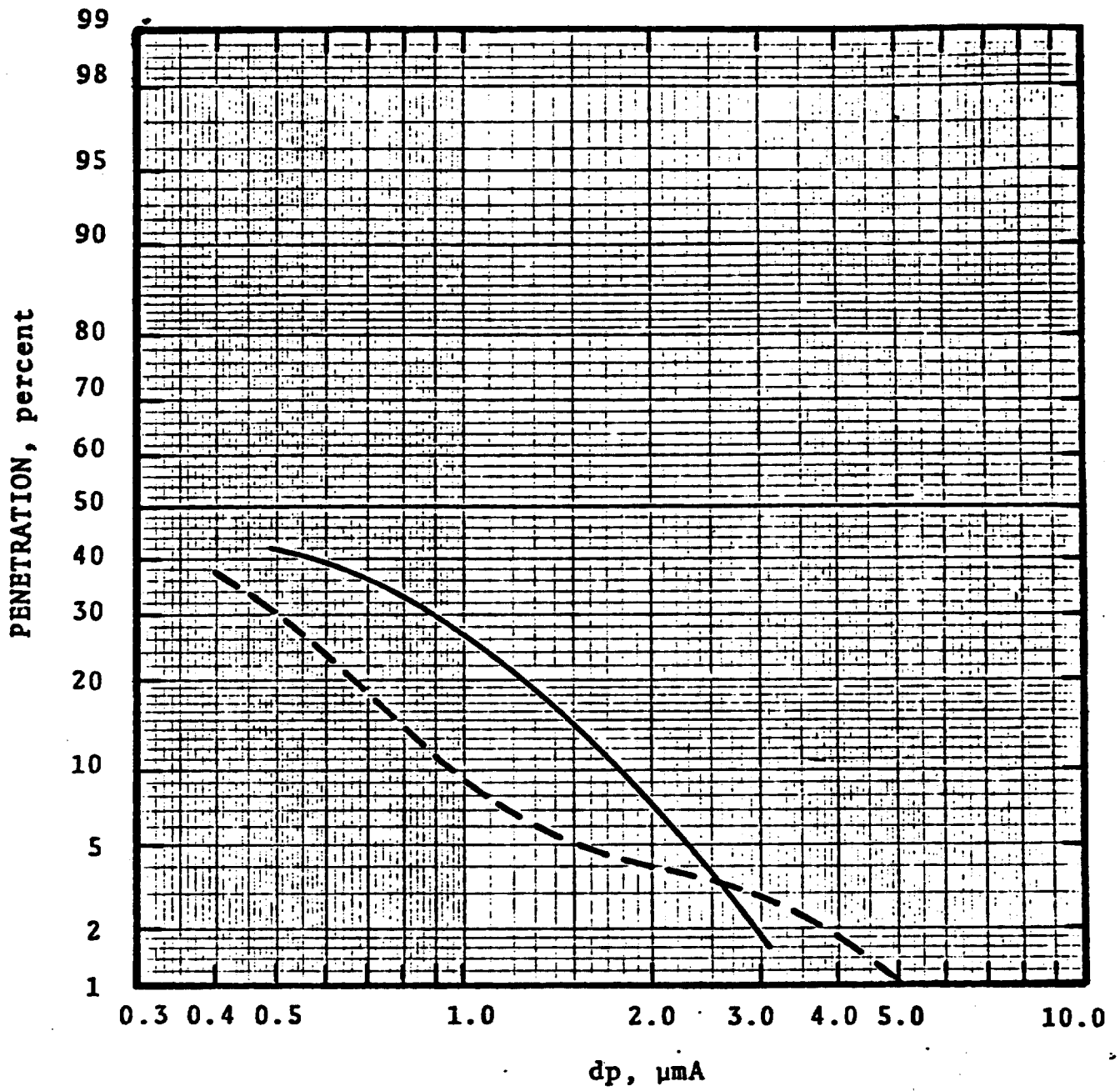


Figure 7-23 | Predicted and Experimental Penetration Run 36/20

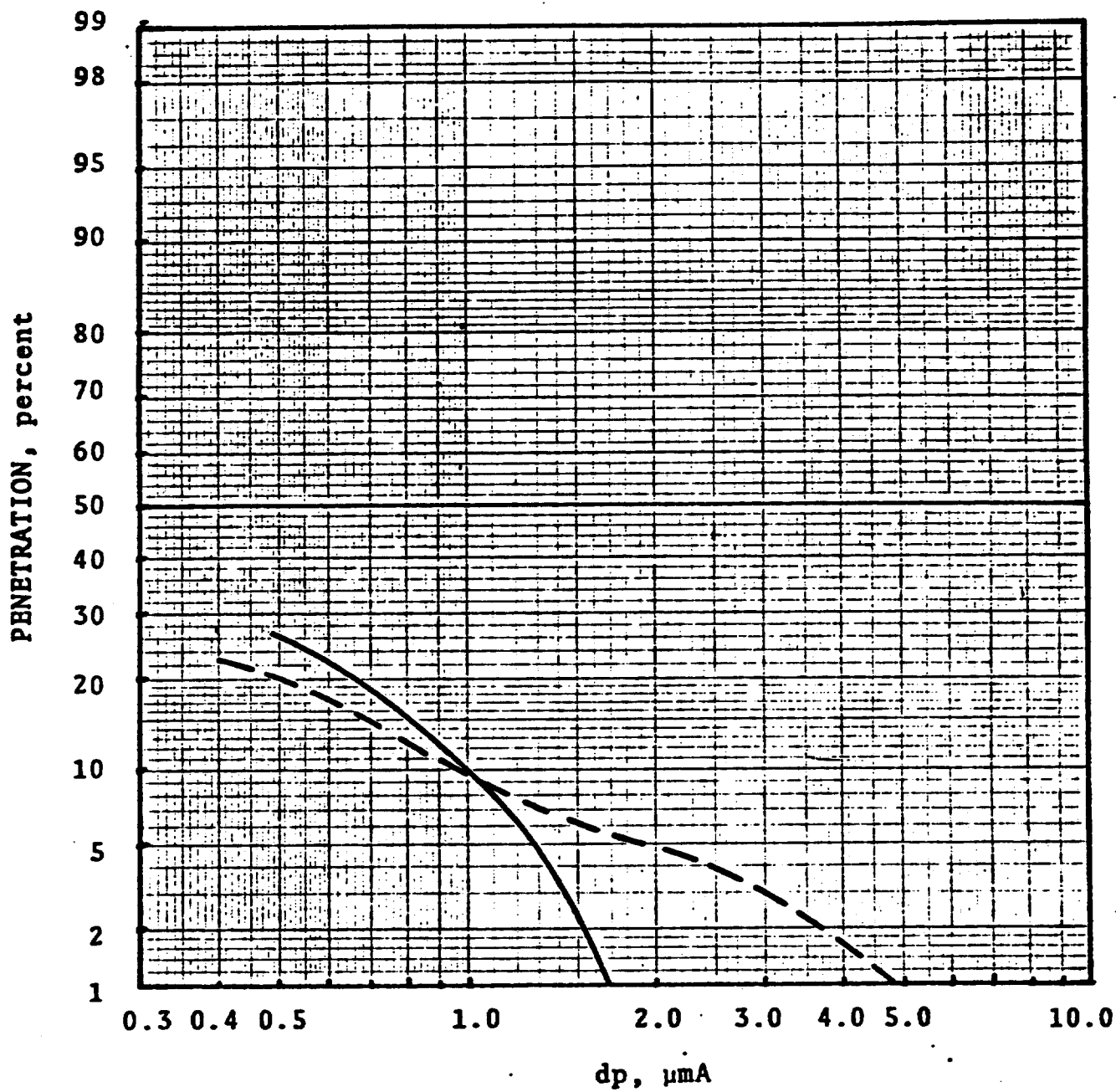


Figure 7-22 | Predicted and Experimental Penetration Run 36/19

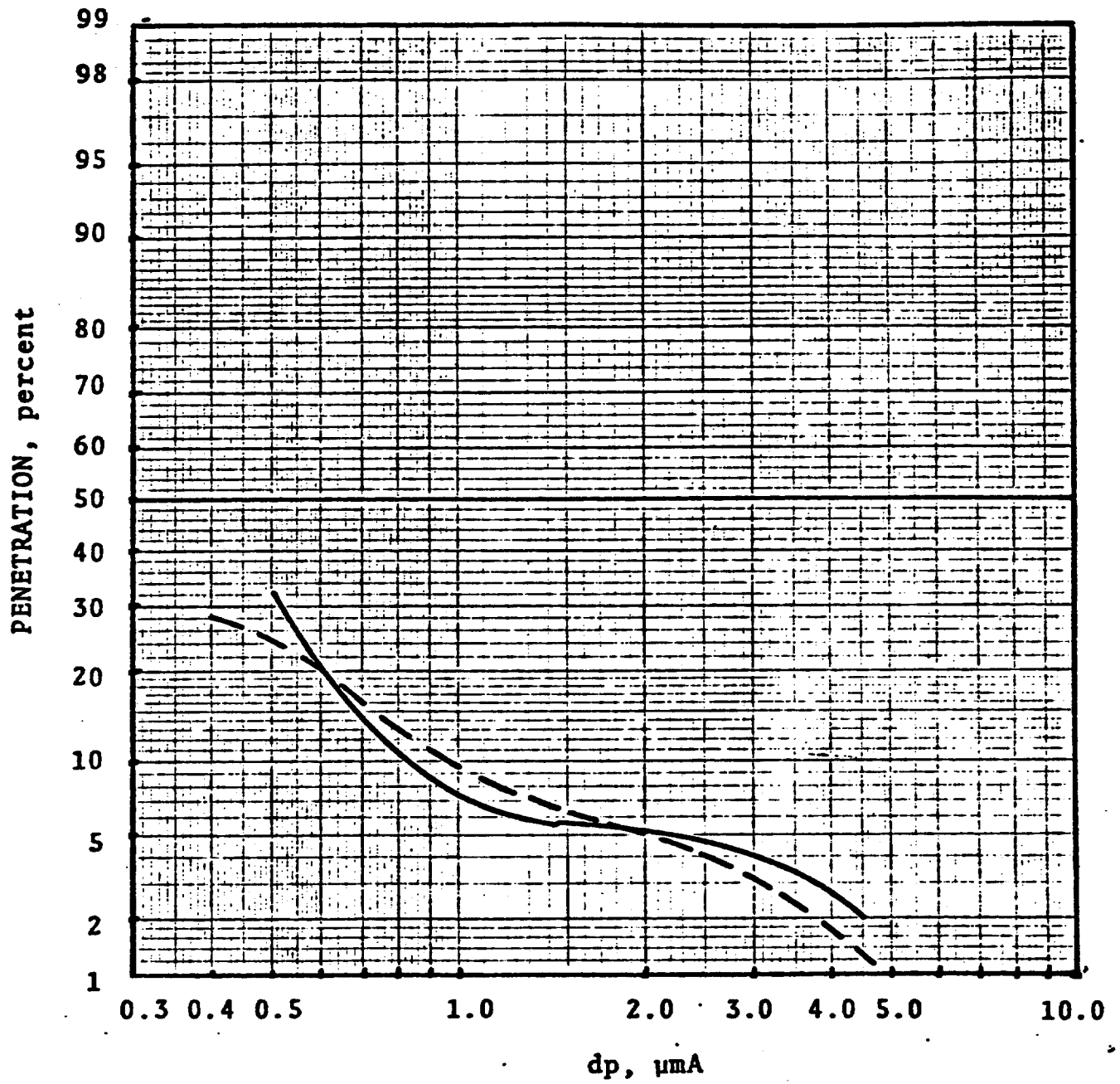


Figure 7-21 Predicted and Experimental Penetration Run 36/18

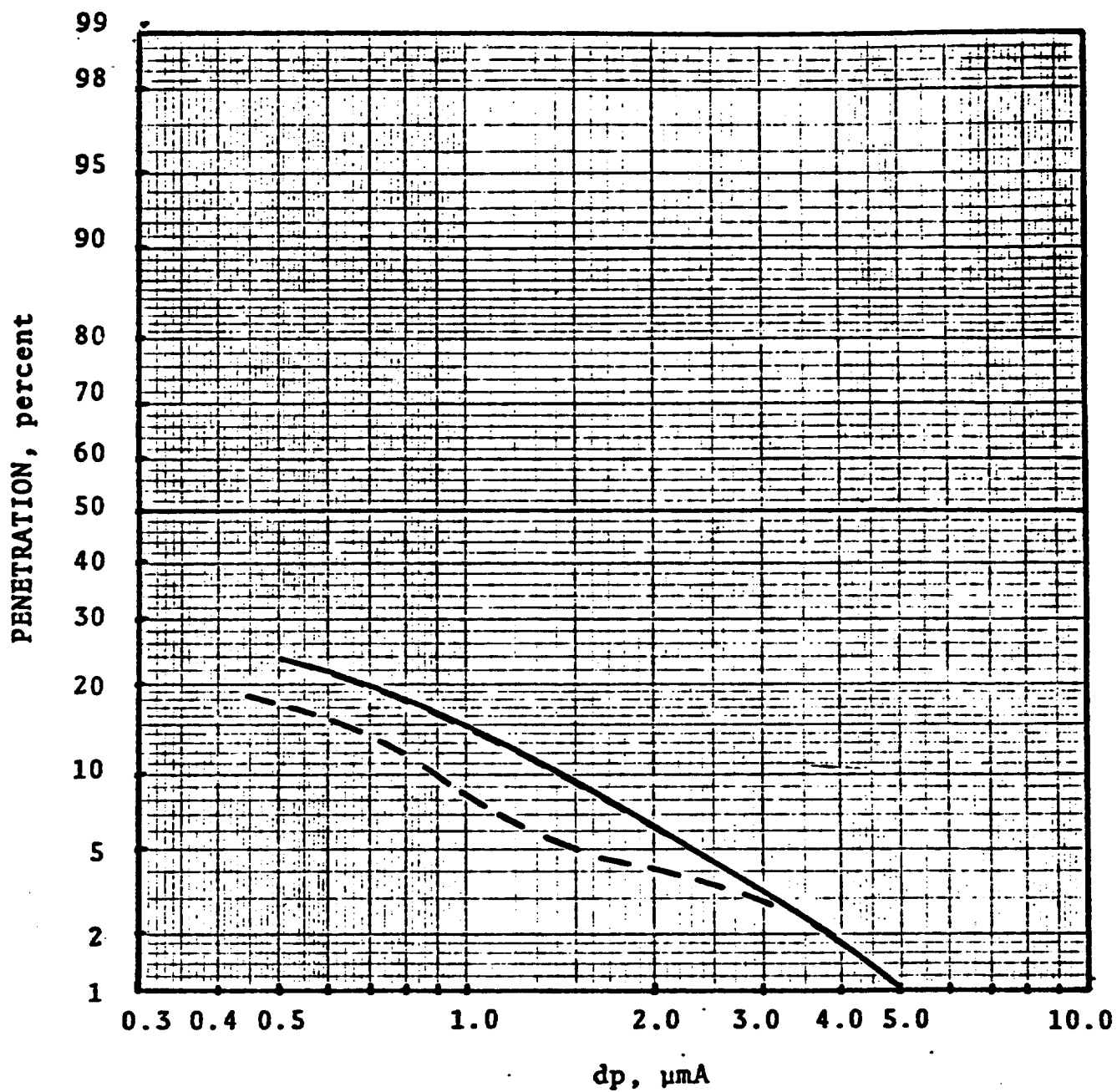


Figure 7-24 | Predicted and Experimental Penetration Run 36/21

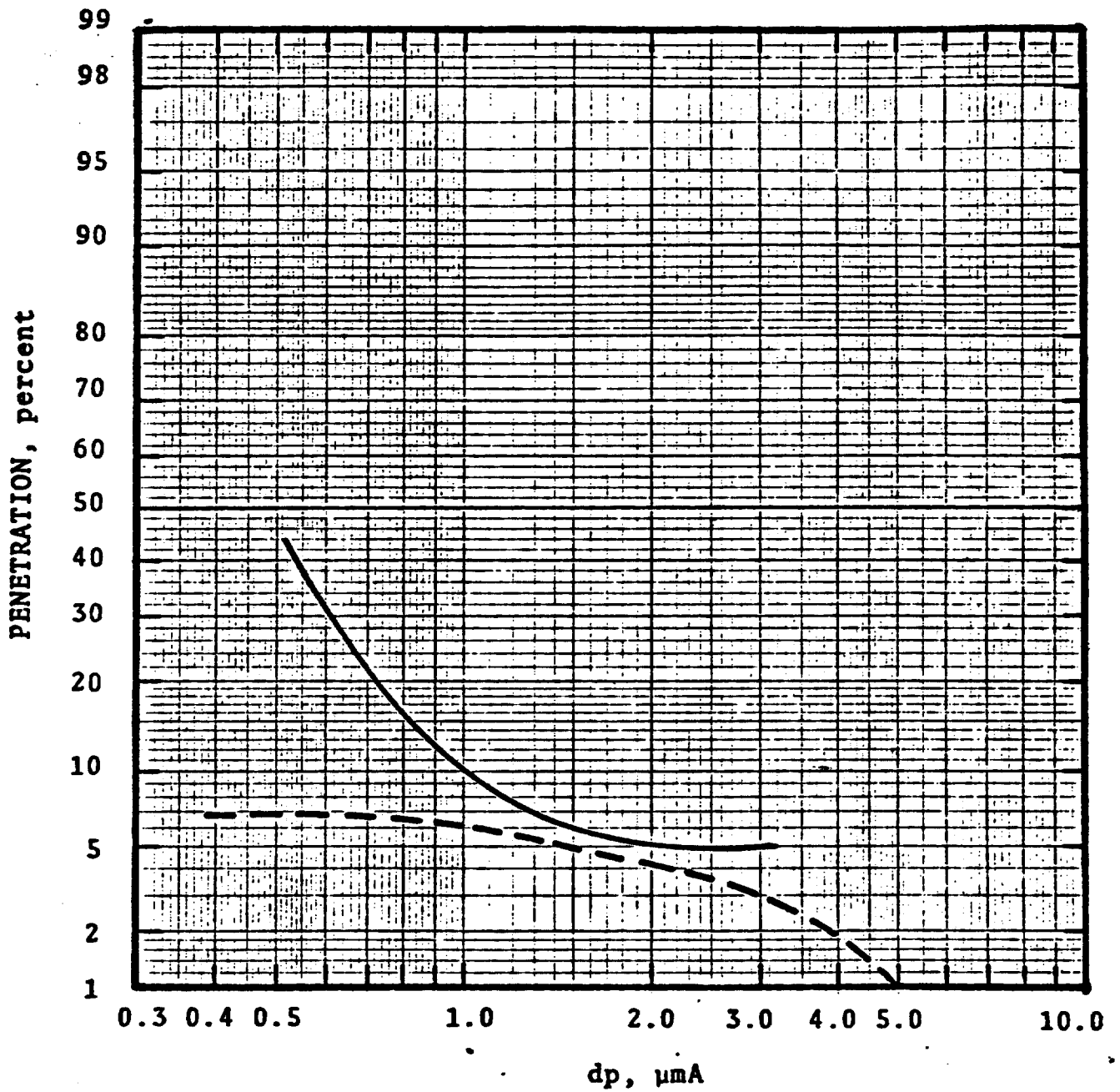


Figure 7-25 | Predicted and Experimental Penetration Run 36/22

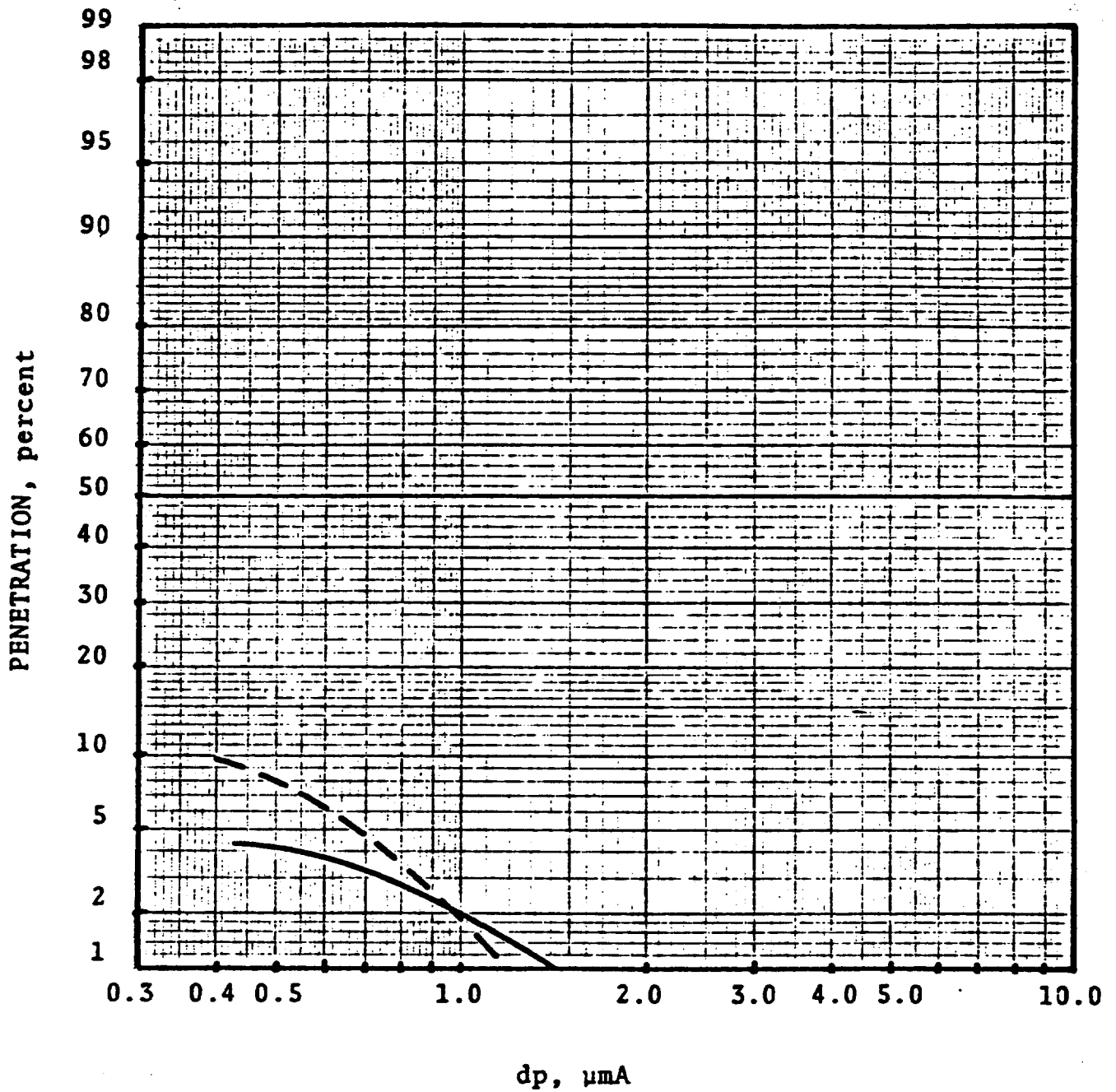


Figure 7-26 Predicted and Experimental Penetration Run 37/1

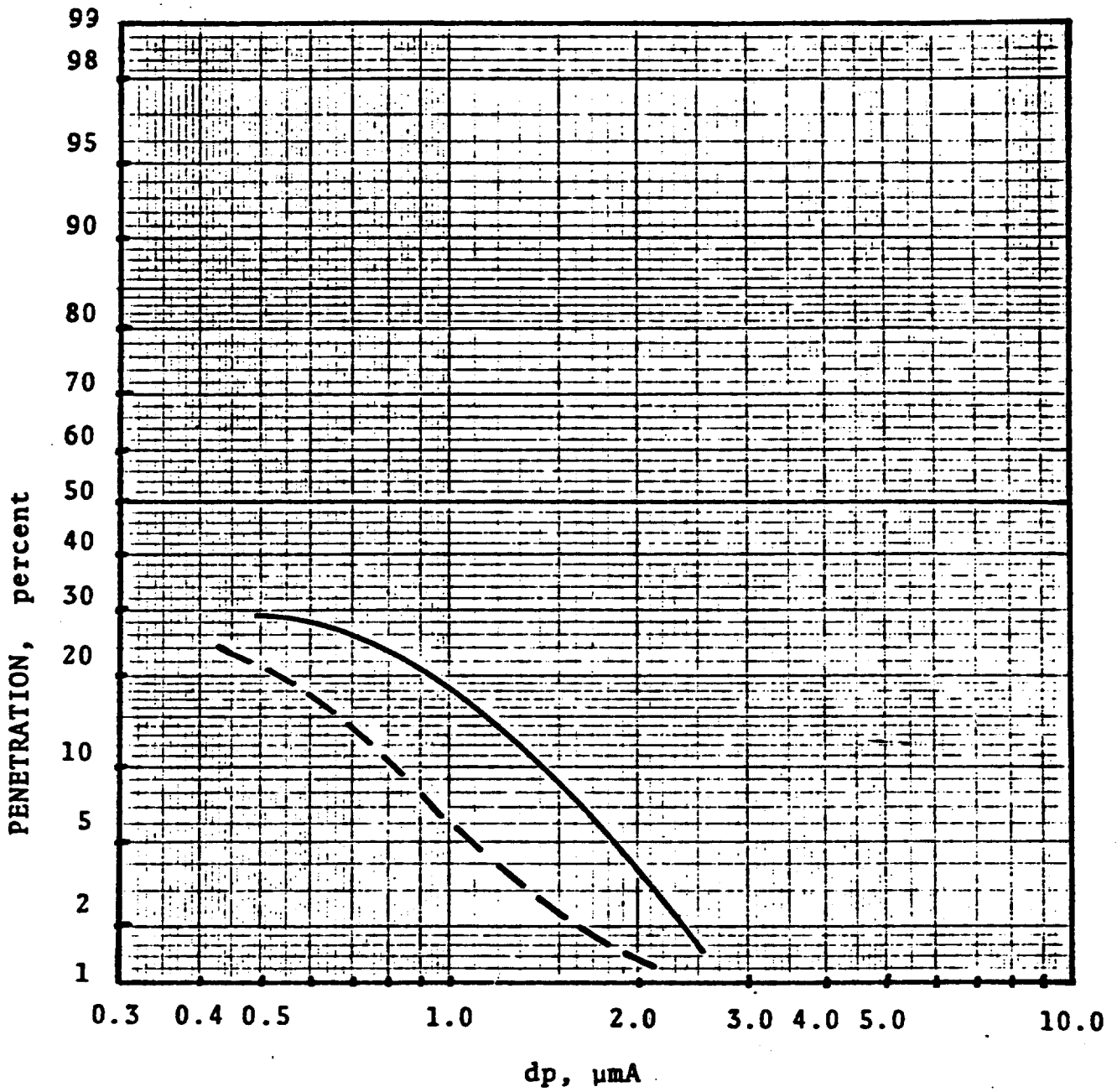


Figure 7-27 Predicted and Experimental Penetration Run 37/2

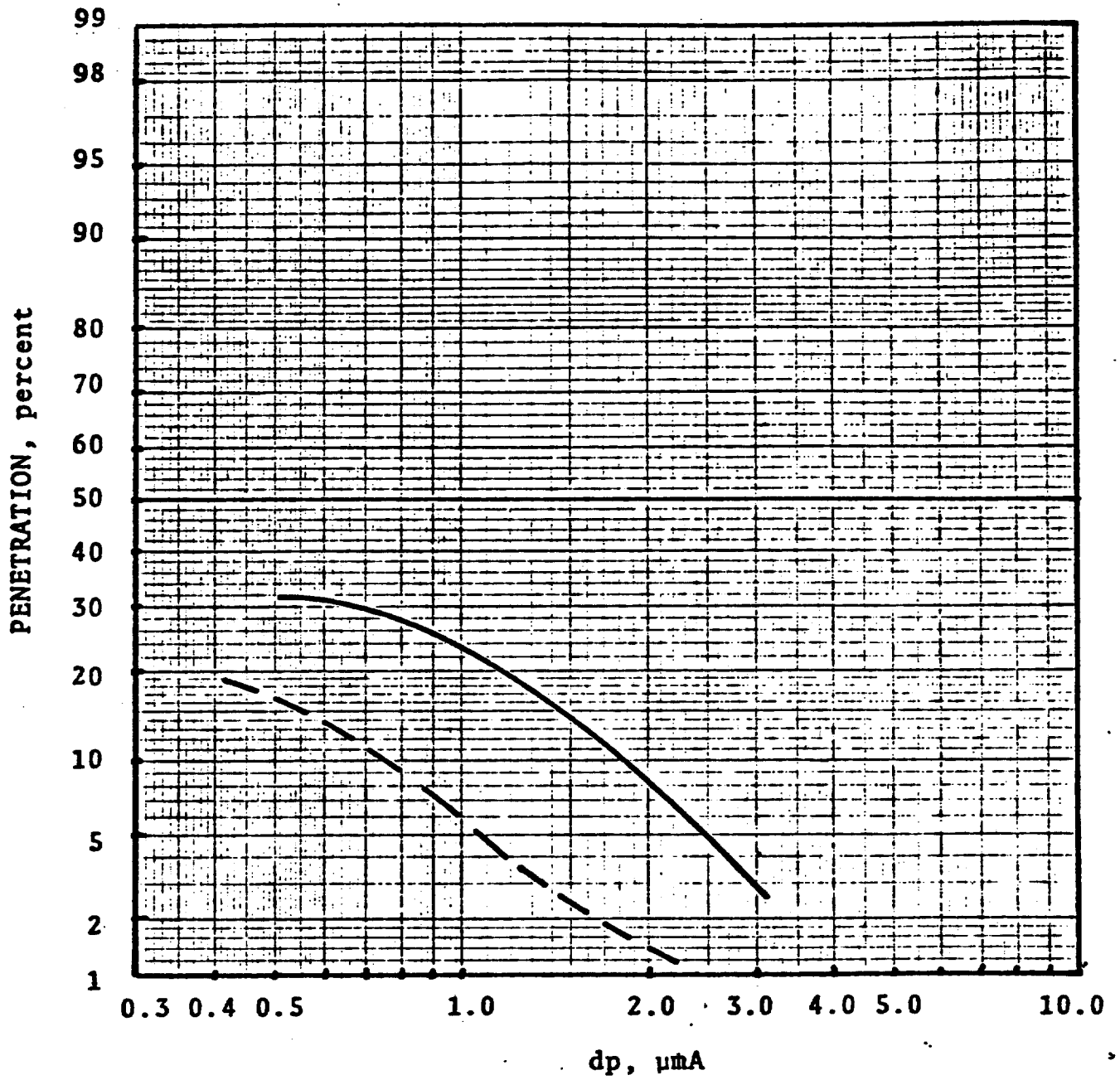


Figure 7-28 | Predicted and Experimental Penetrations Run 37/3

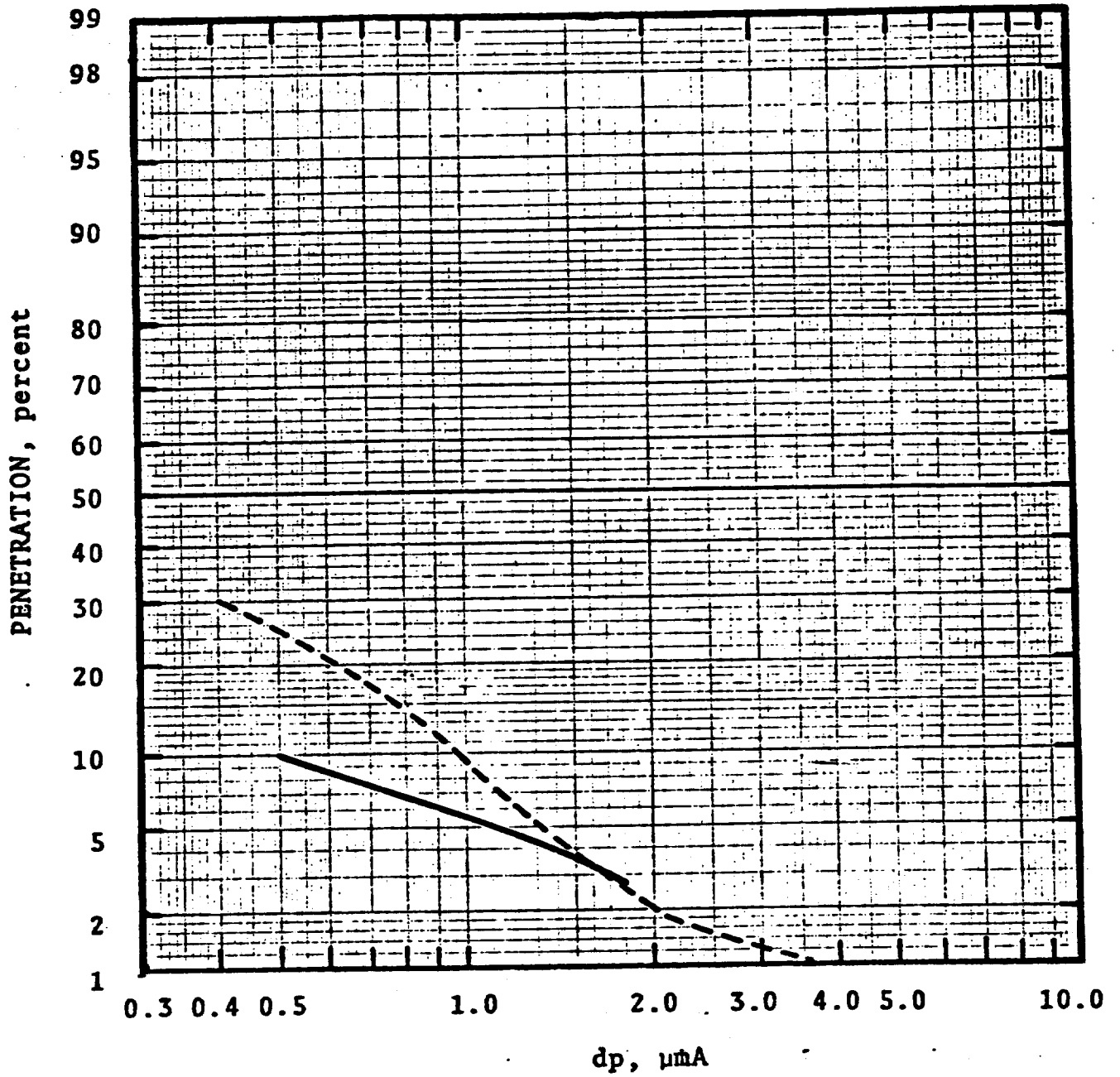


Figure 7-29 | Predicted and Experimental Penetration Run 37/4

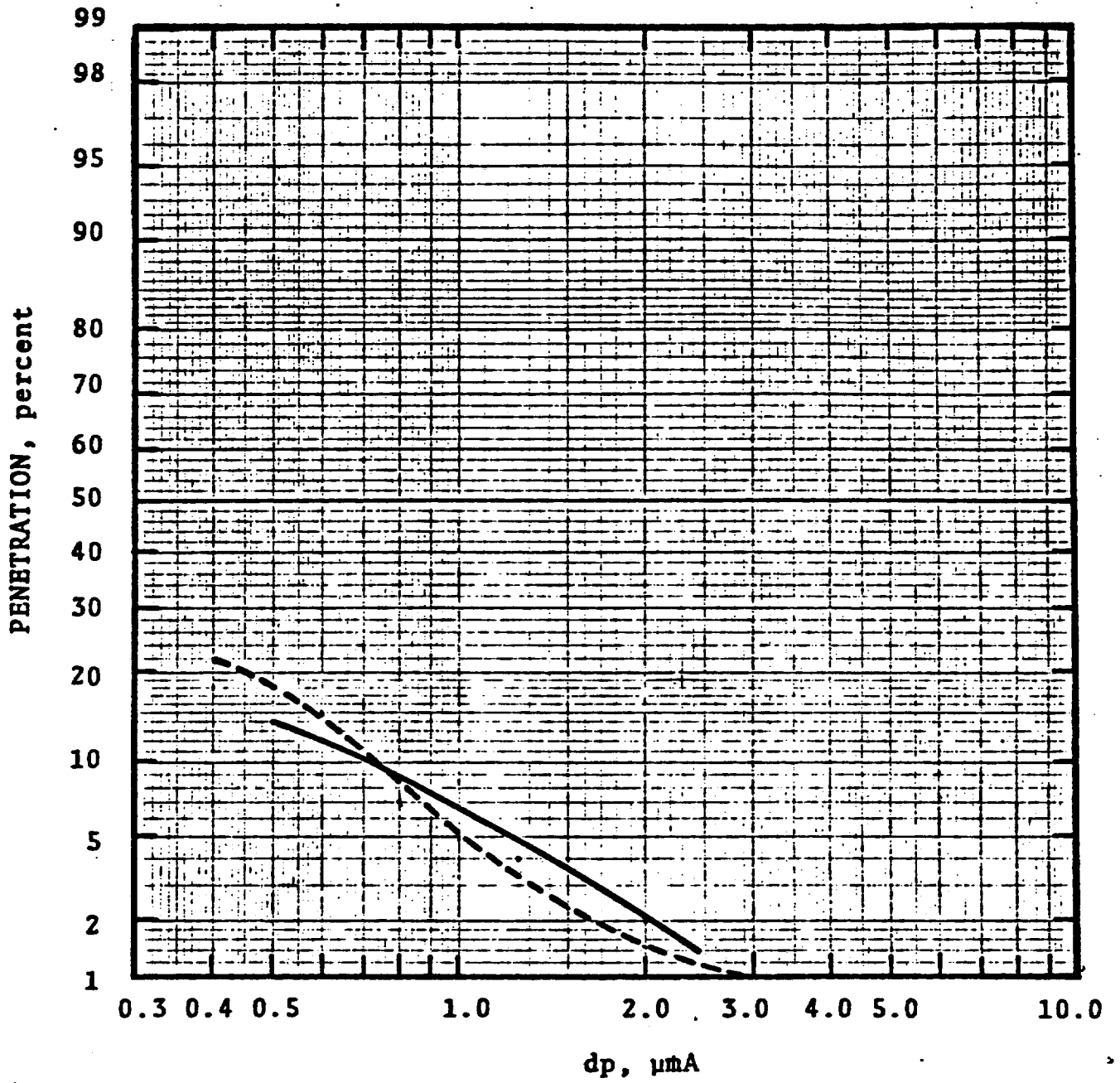


Figure 7-30 Predicted and Experimental Penetration Run 37/5

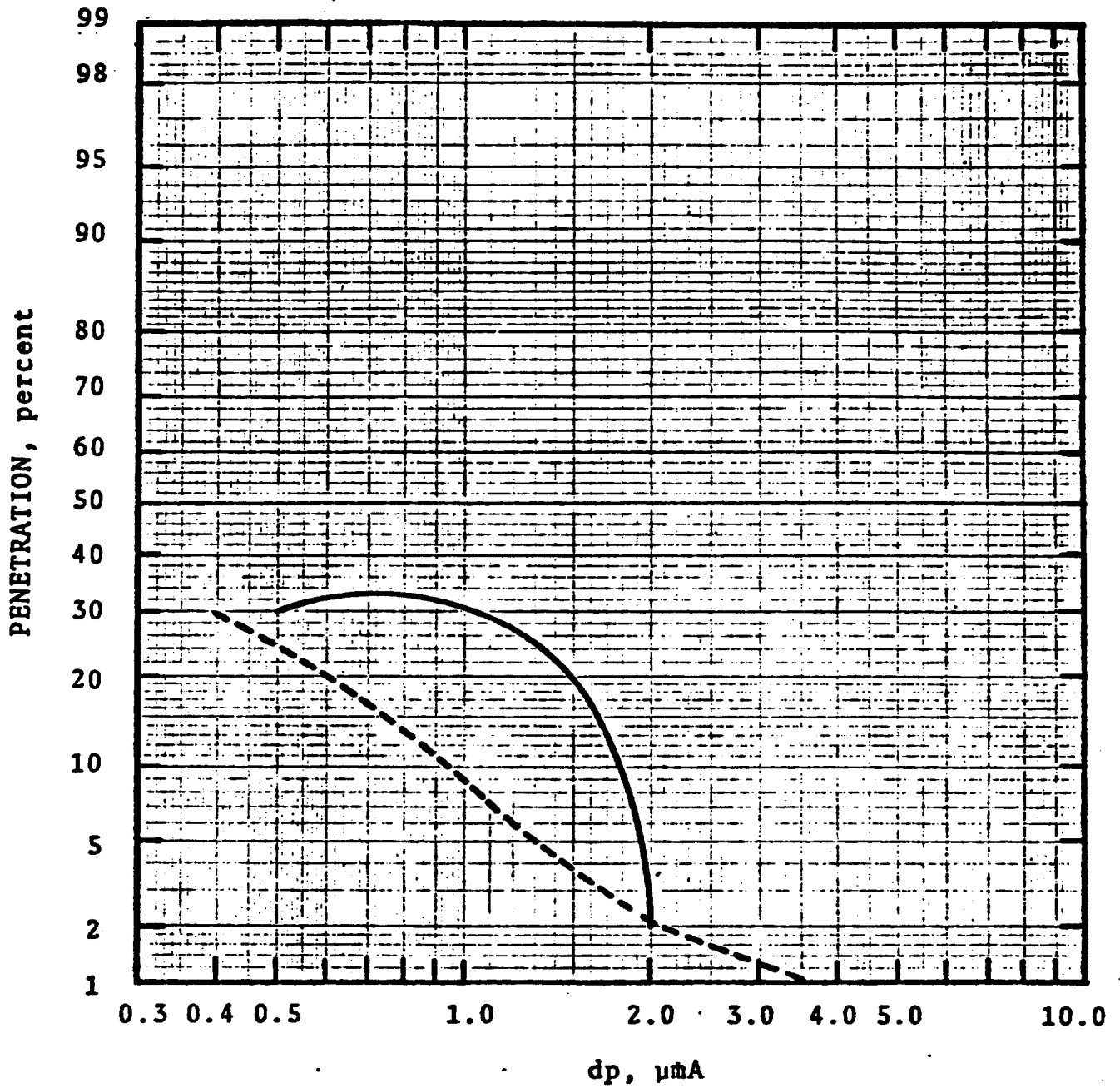


Figure 7-31 Predicted and Experimental Penetration Run 37/6

95

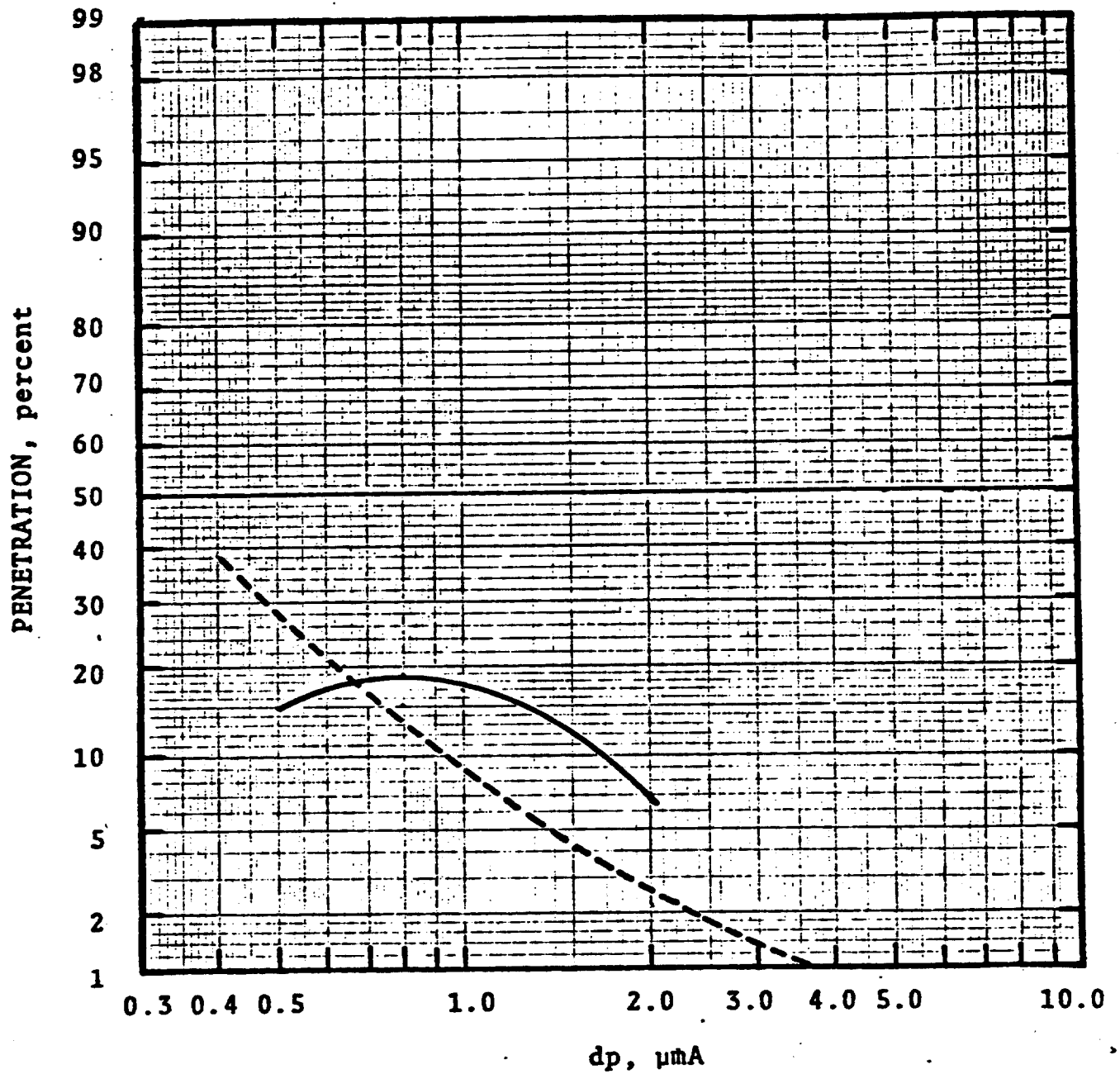


Figure 7-32 | Predicted and Experimental Penetration Run 37/7

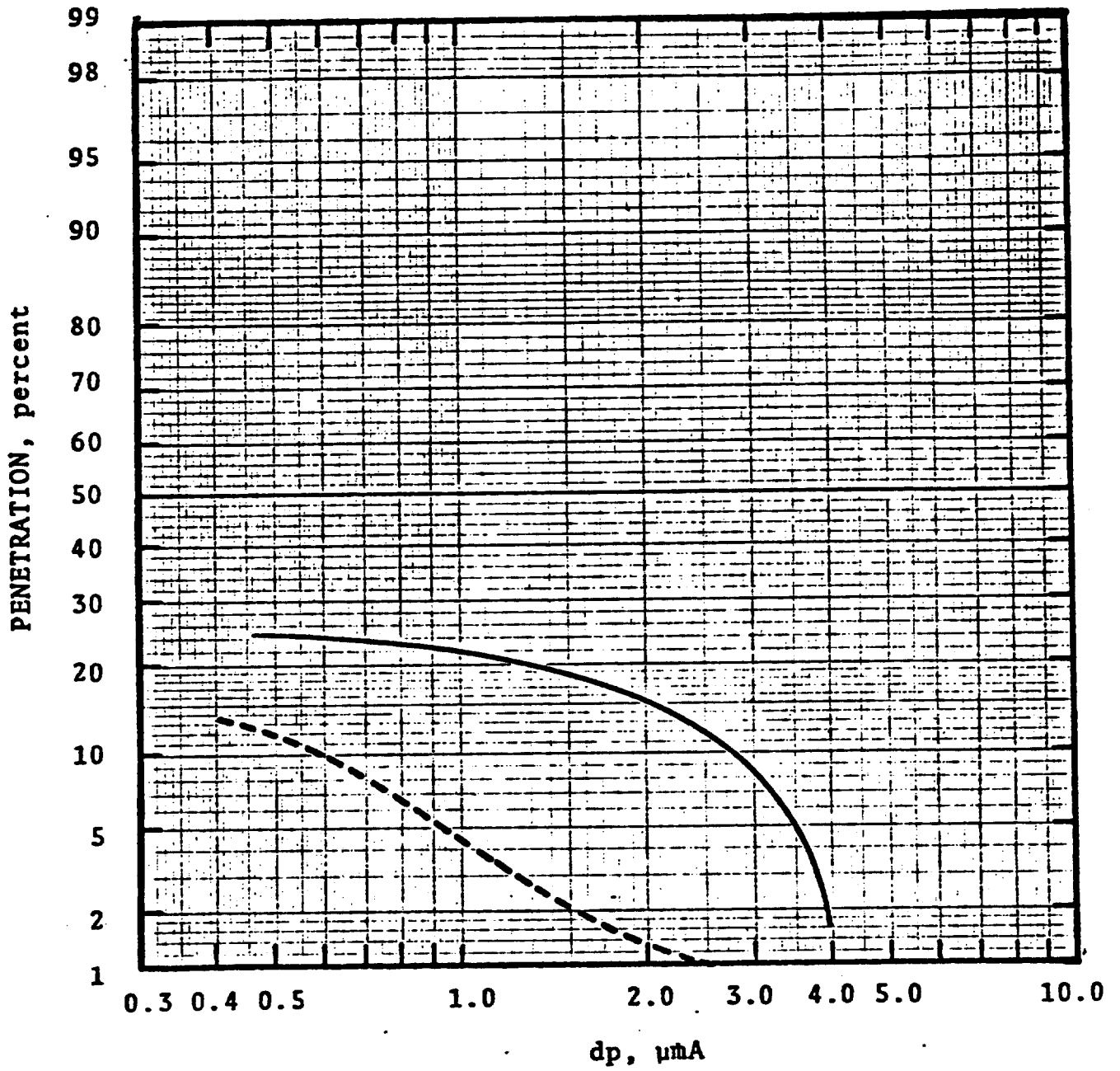


Figure 7-33 Predicted and Experimental Penetration Run 37/8

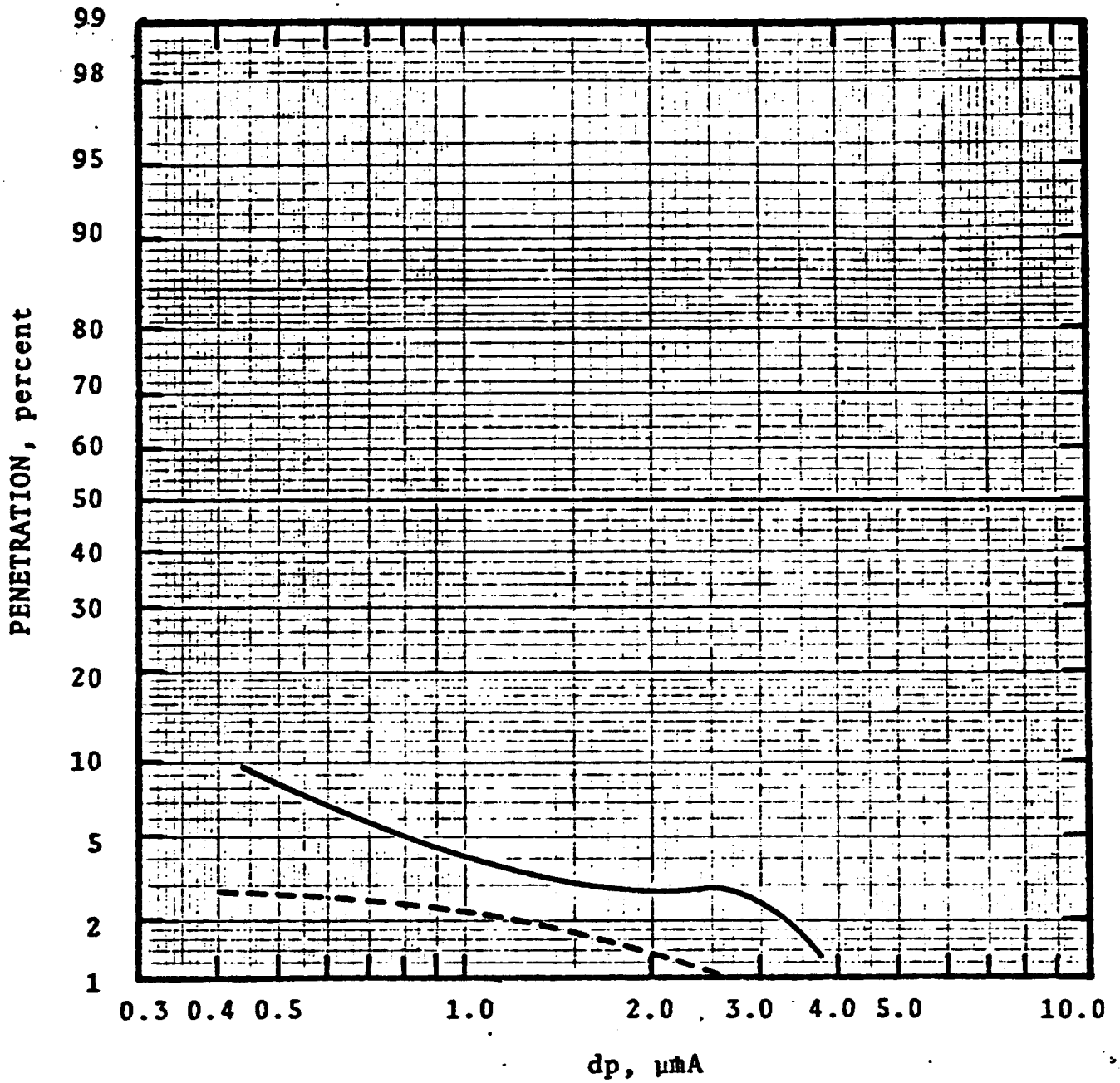


Figure 7-34; Predicted and Experimental Penetration Run 37/9

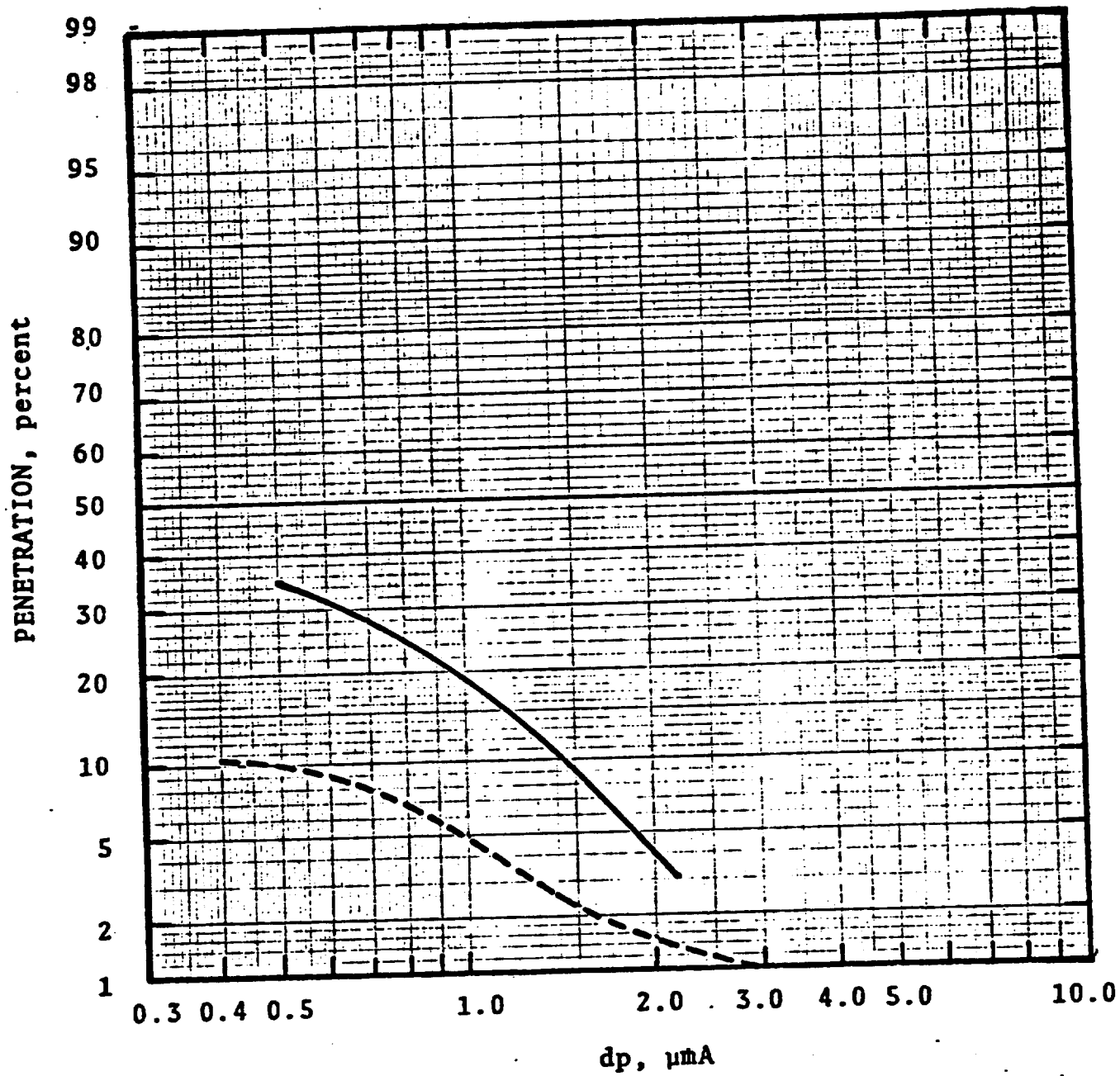


Figure 7-35: Predicted and Experimental Penetration Run 37/10

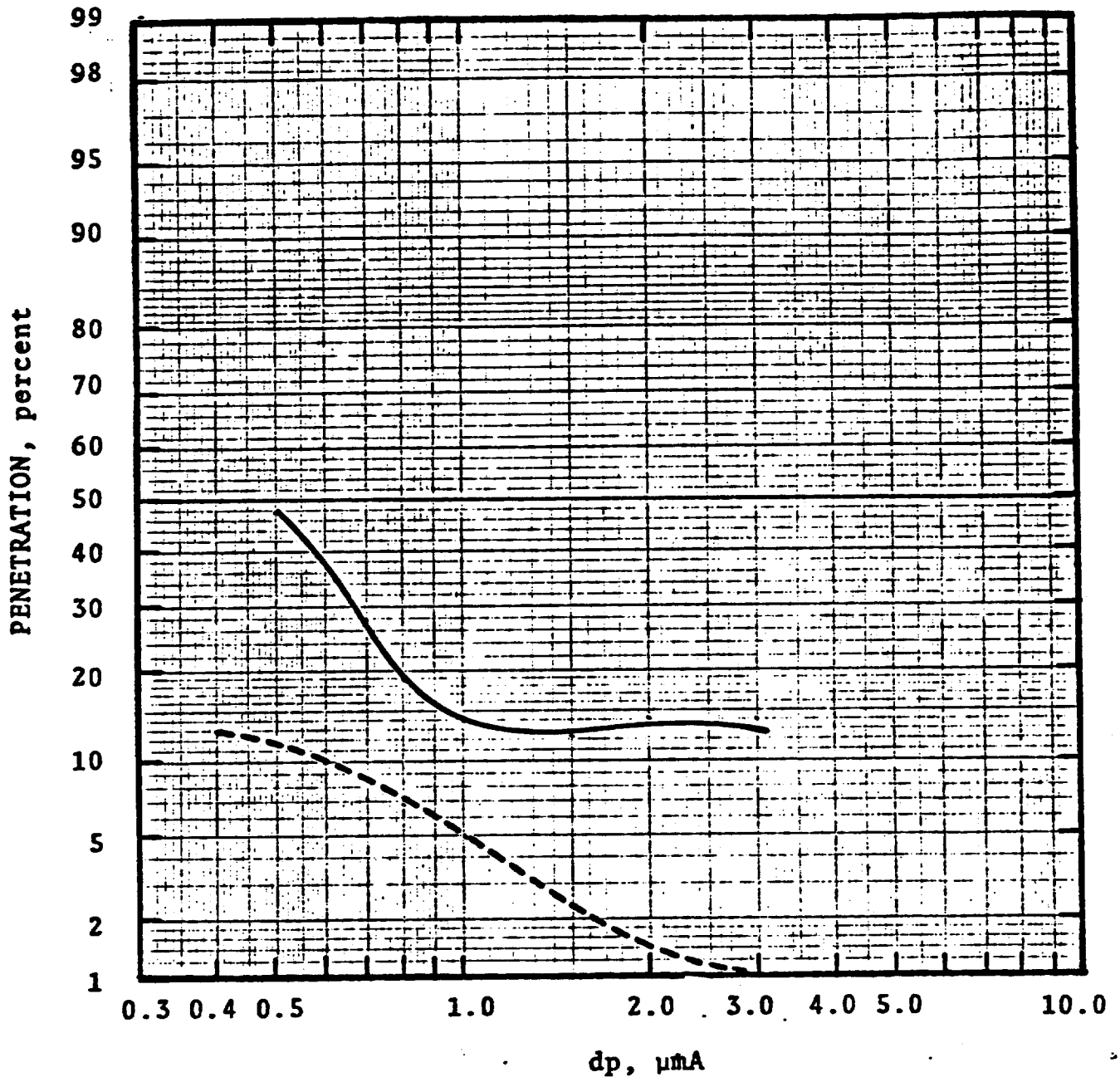


Figure 7-36 Predicted and Experimental Penetration Run 37/11

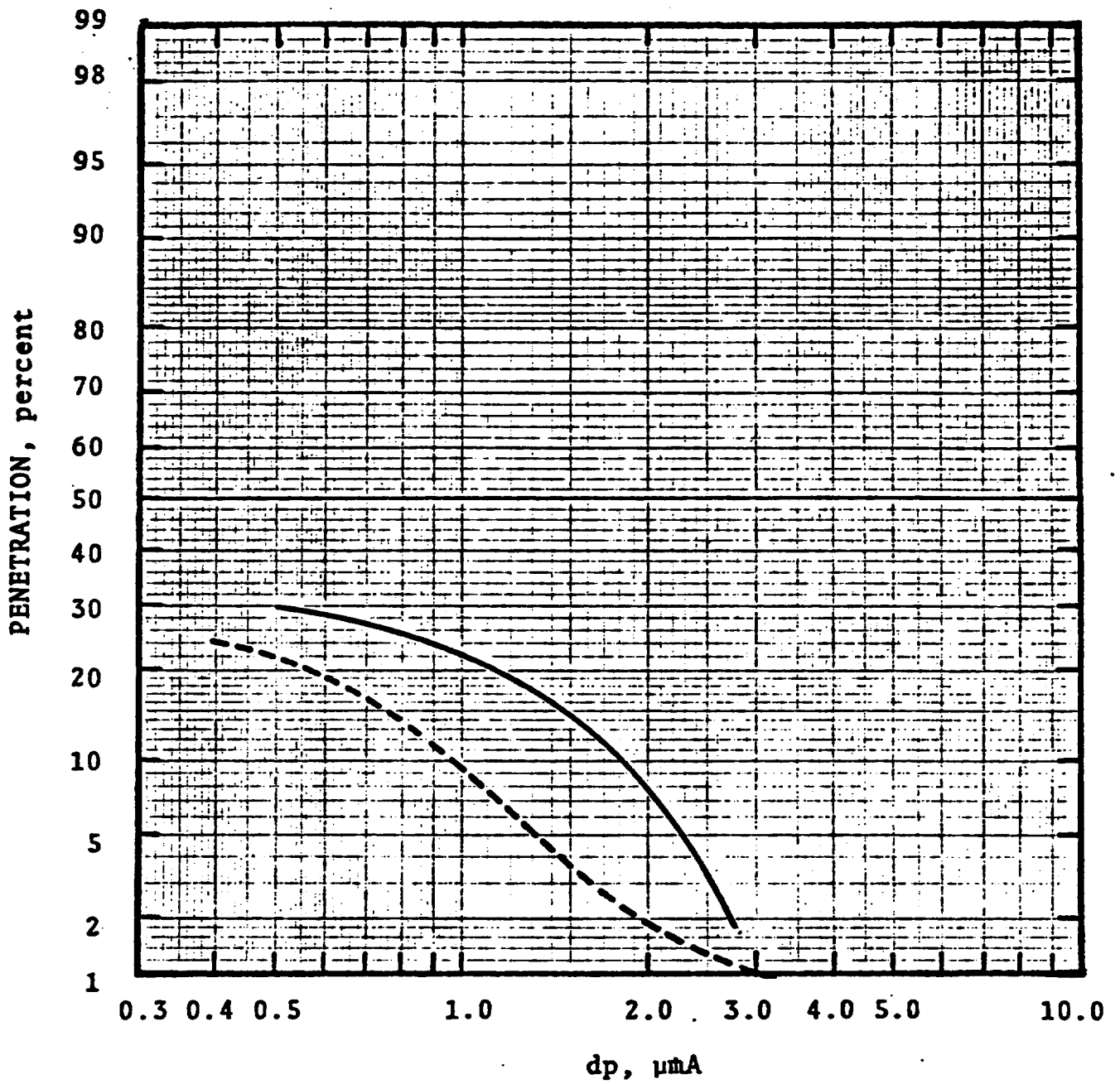


Figure 7-37 Predicted and Experimental Penetration Run 37/12

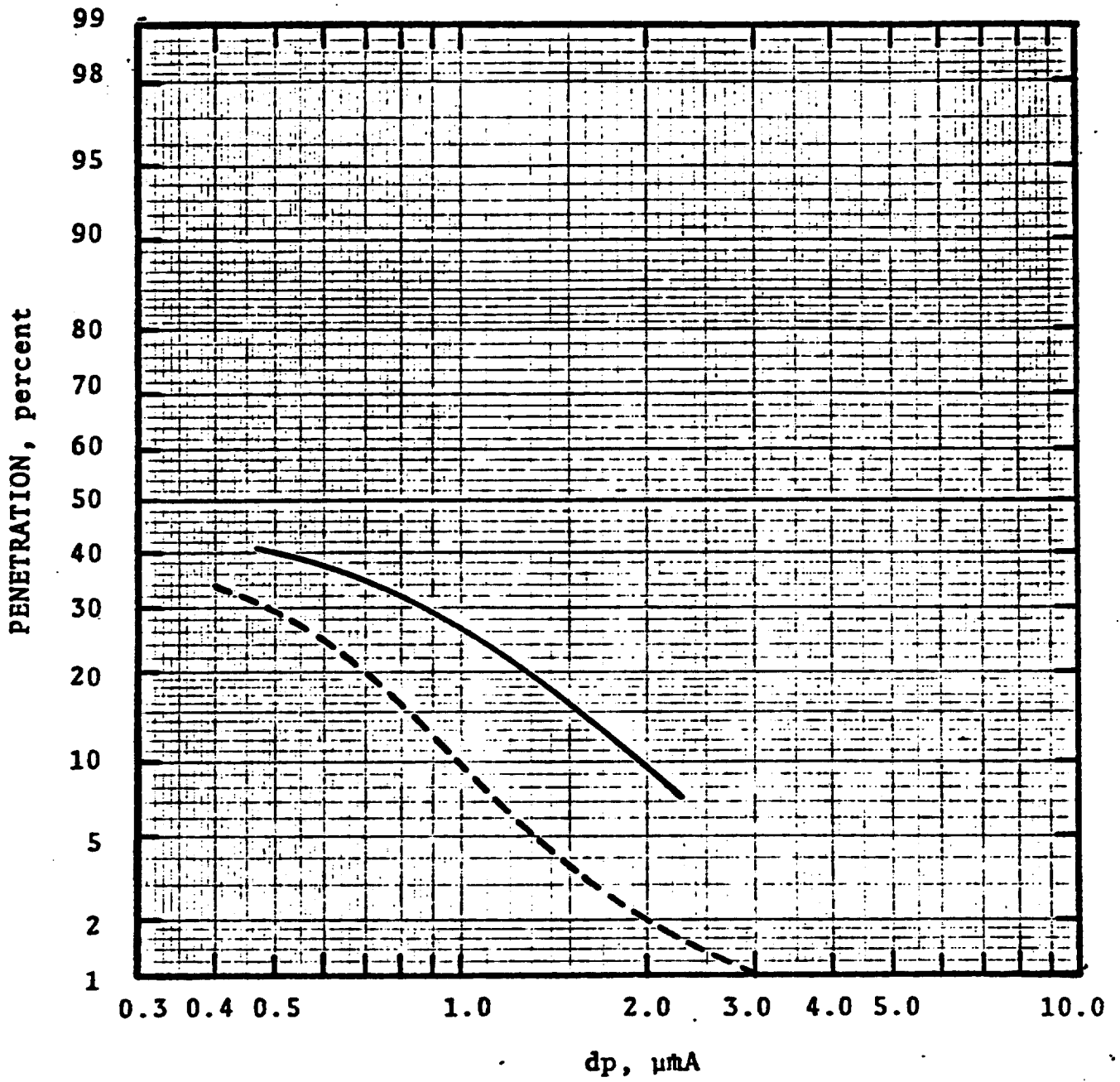


Figure 7-38 Predicted and Experimental Penetration Run 37/13

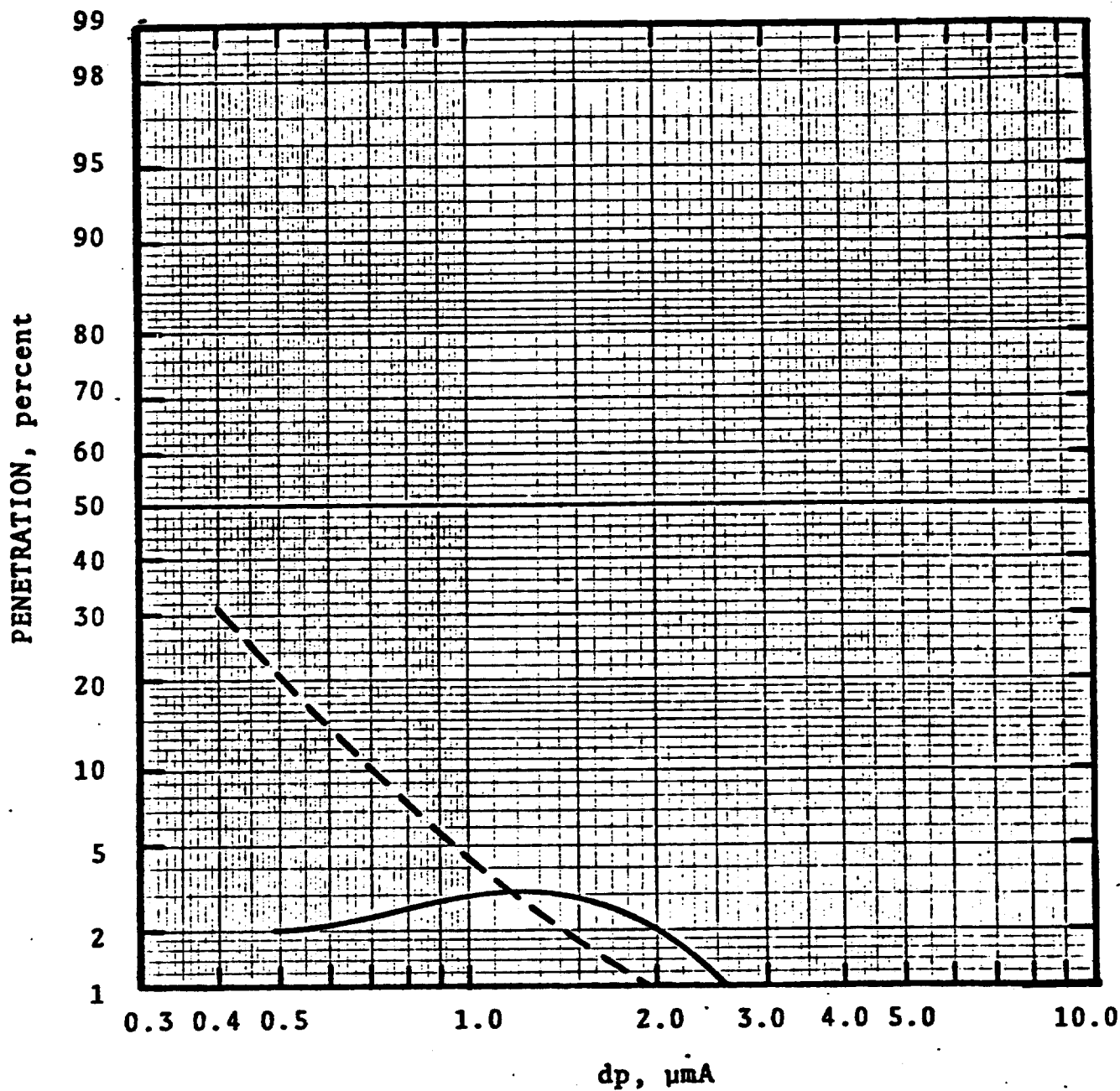


Figure 7-39 | Predicted and Experimental Penetration Run 37/15

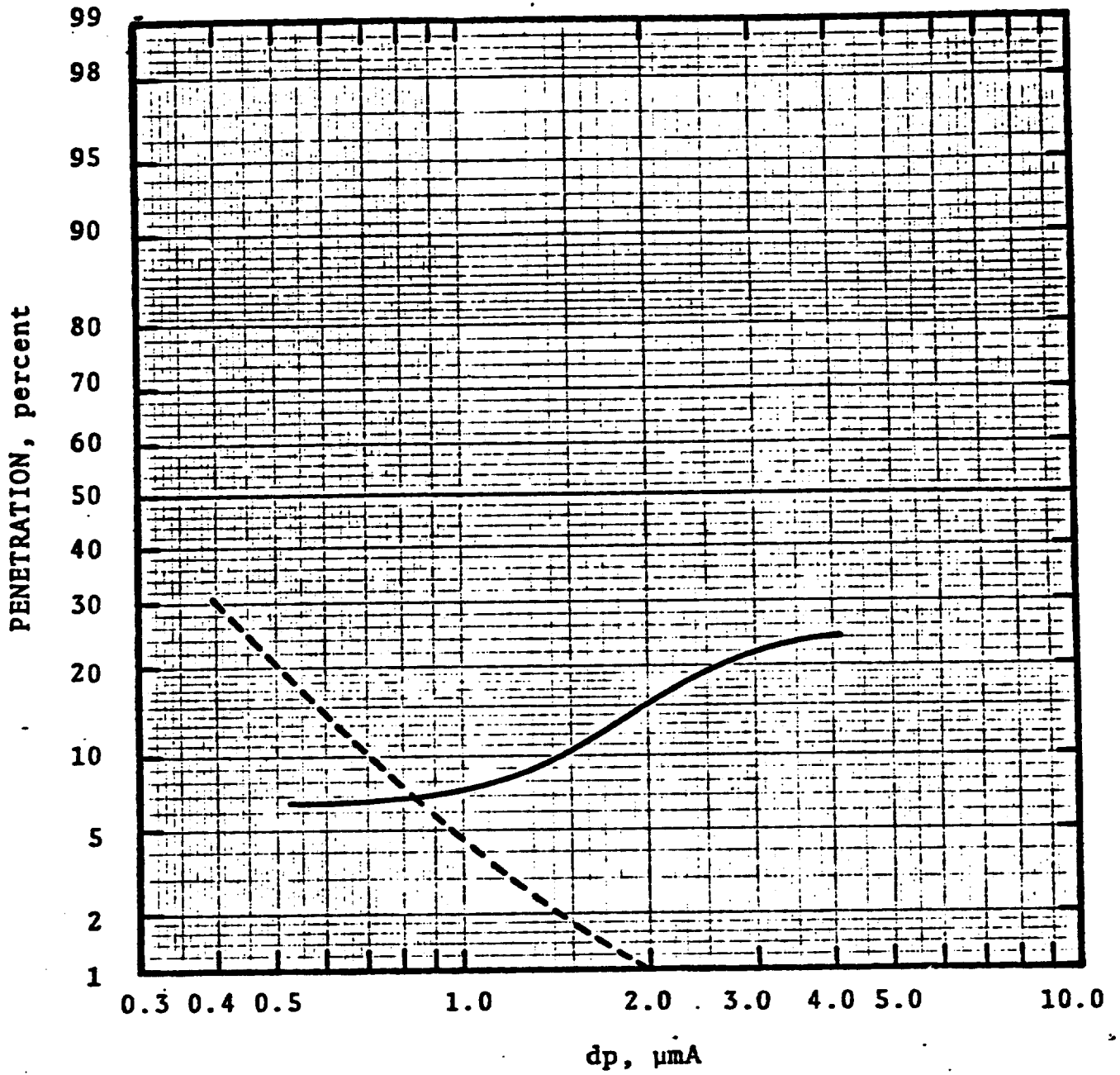


Figure 7-40 Predicted and Experimental Penetration Run 37/16

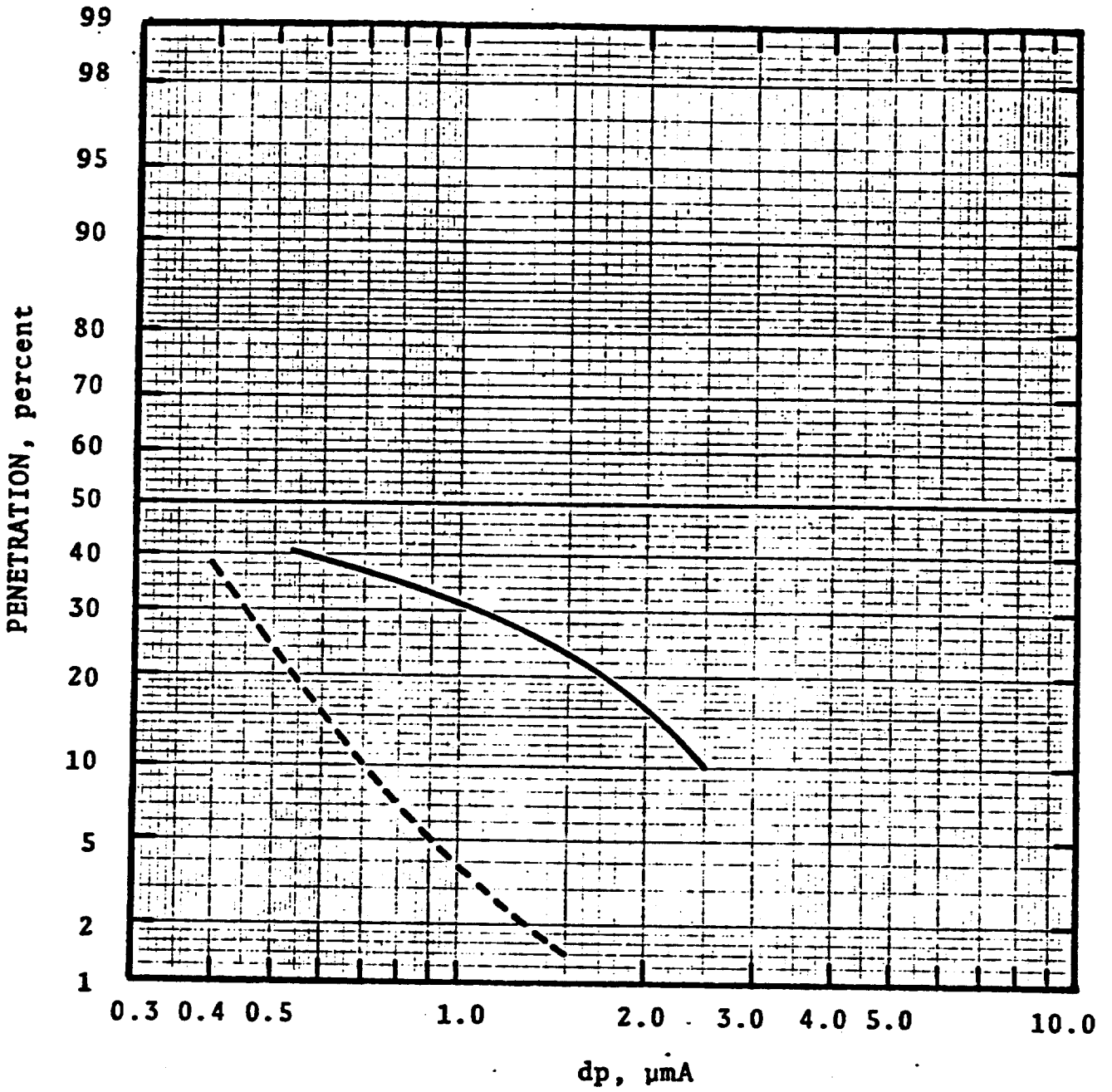


Figure 7-41 | Predicted and Experimental Penetration Run 37/17

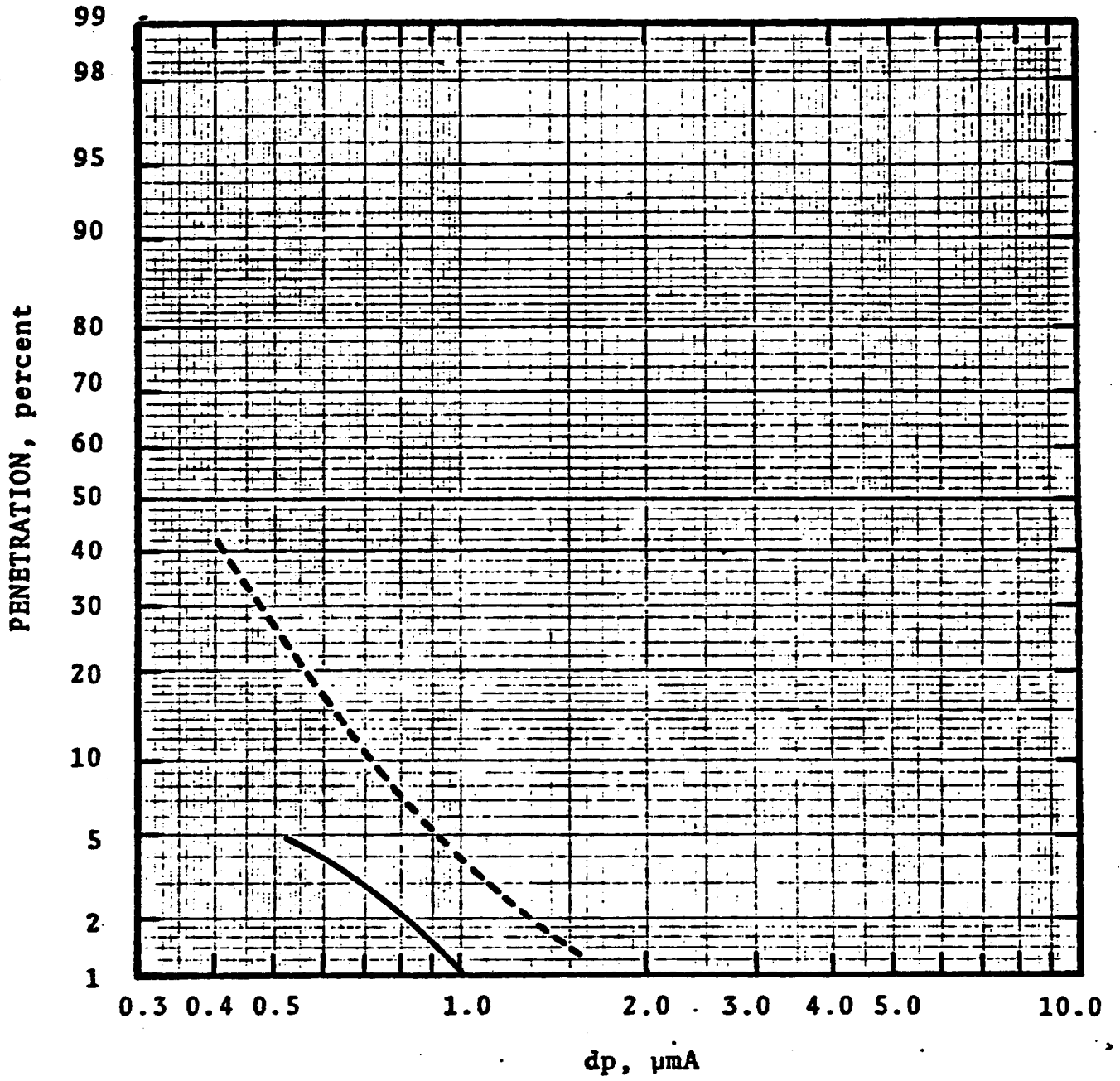


Figure 7-42 | Predicted and Experimental Penetration Run 37/18

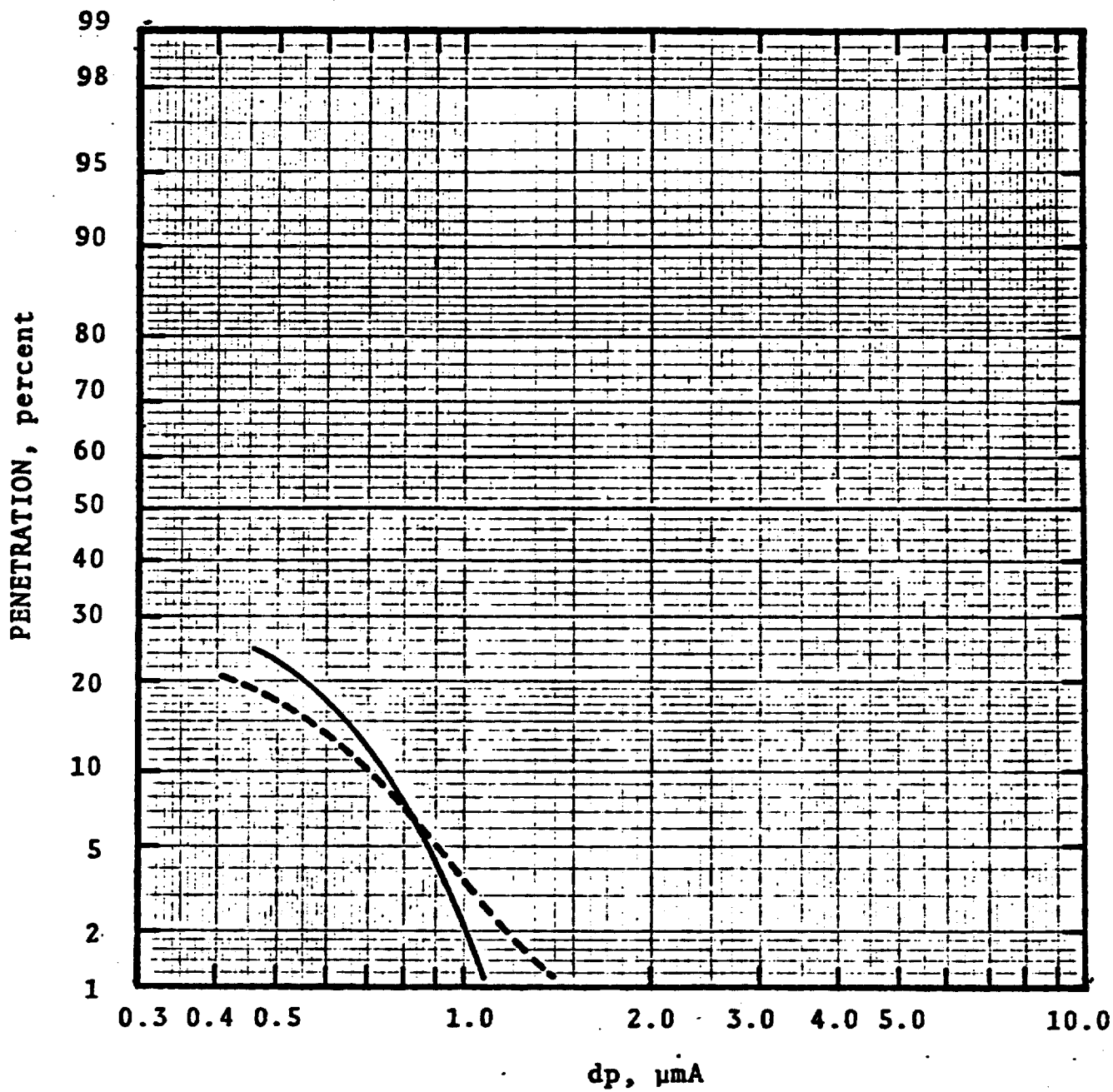


Figure 7-43 | Predicted and Experimental Penetration Run 37/19

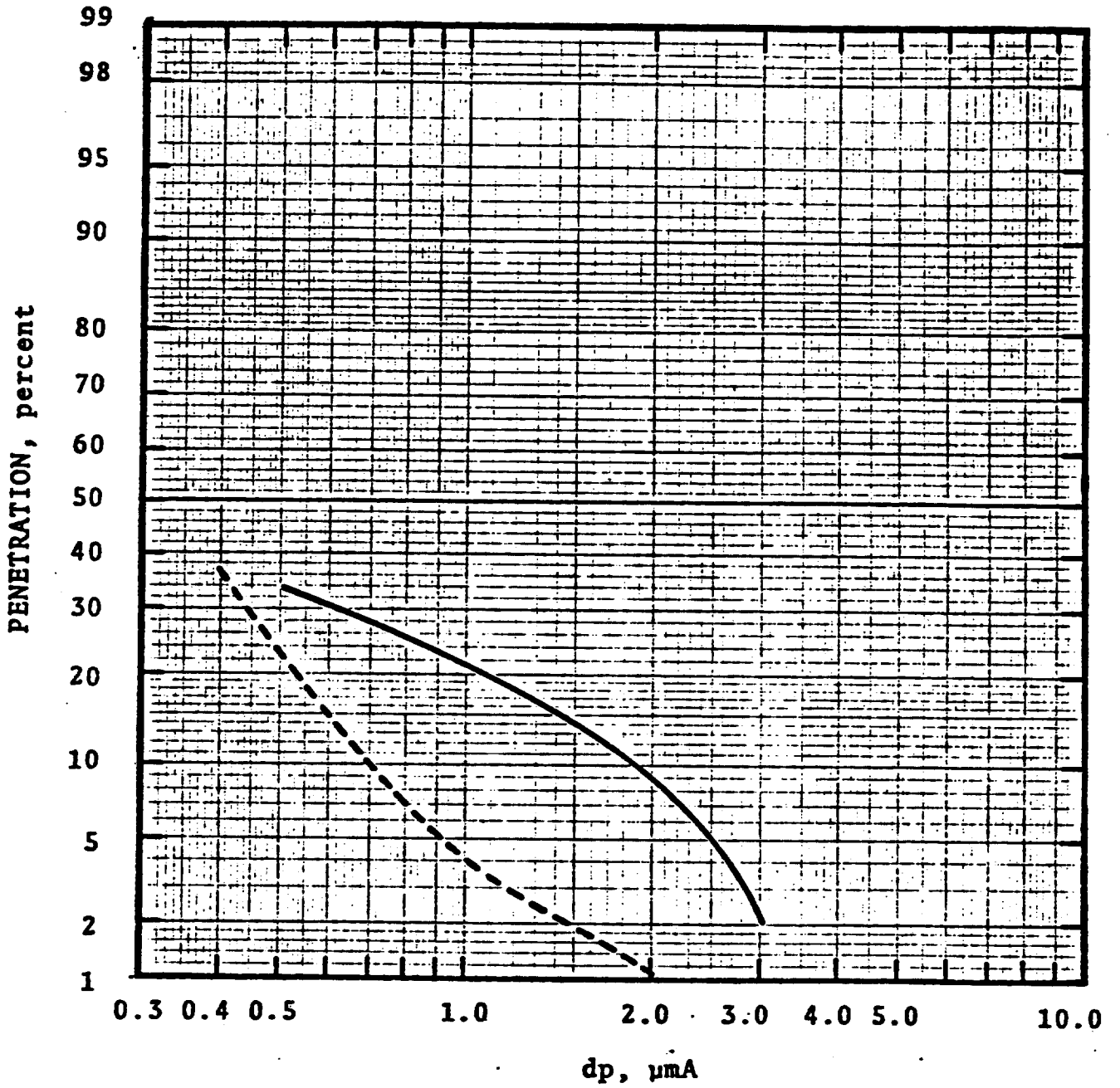


Figure 7-44 Predicted and Experimental Penetration Run 37/21

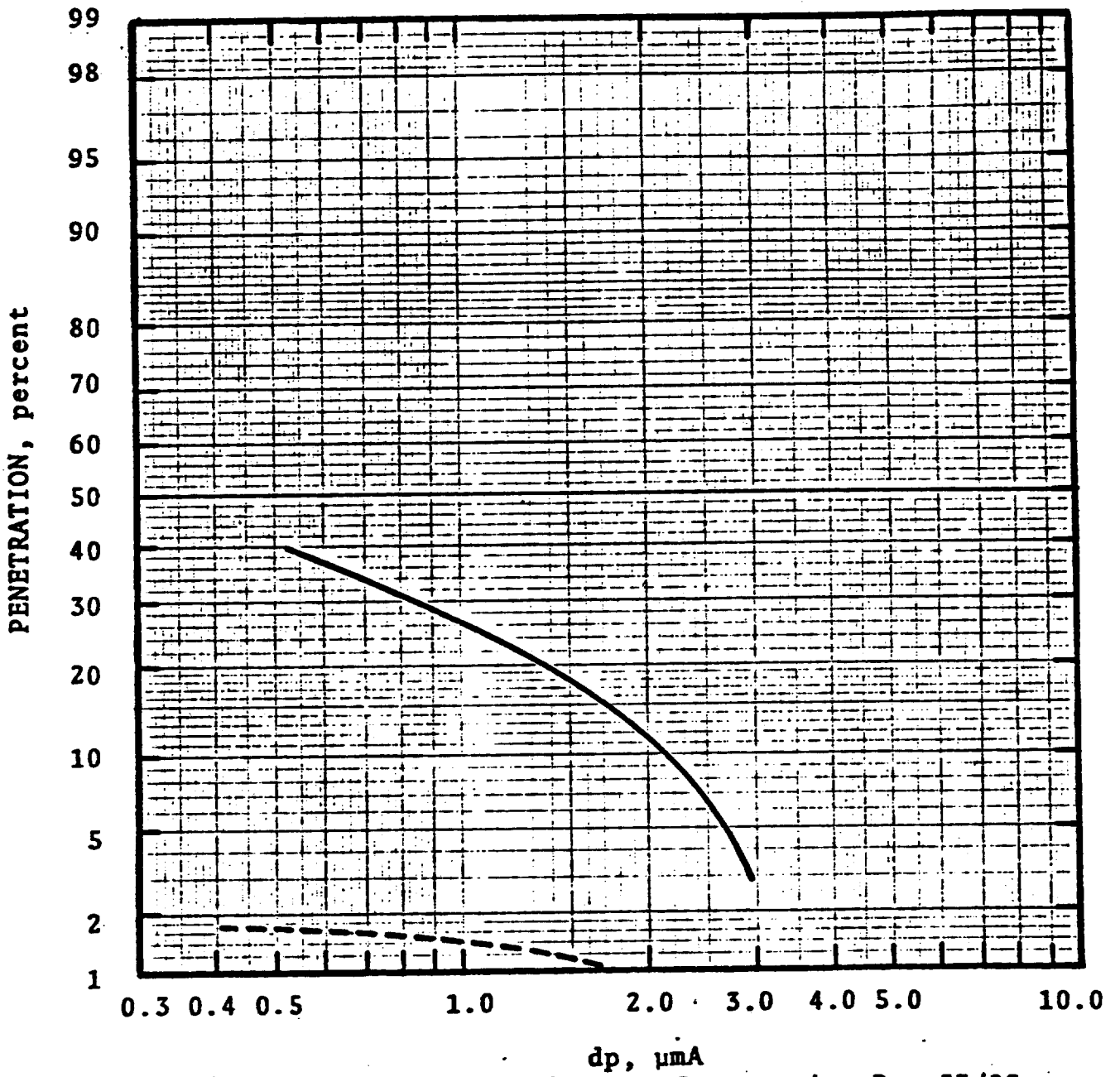


Figure 7-45 Predicted and Experimental Penetration Run 37/23

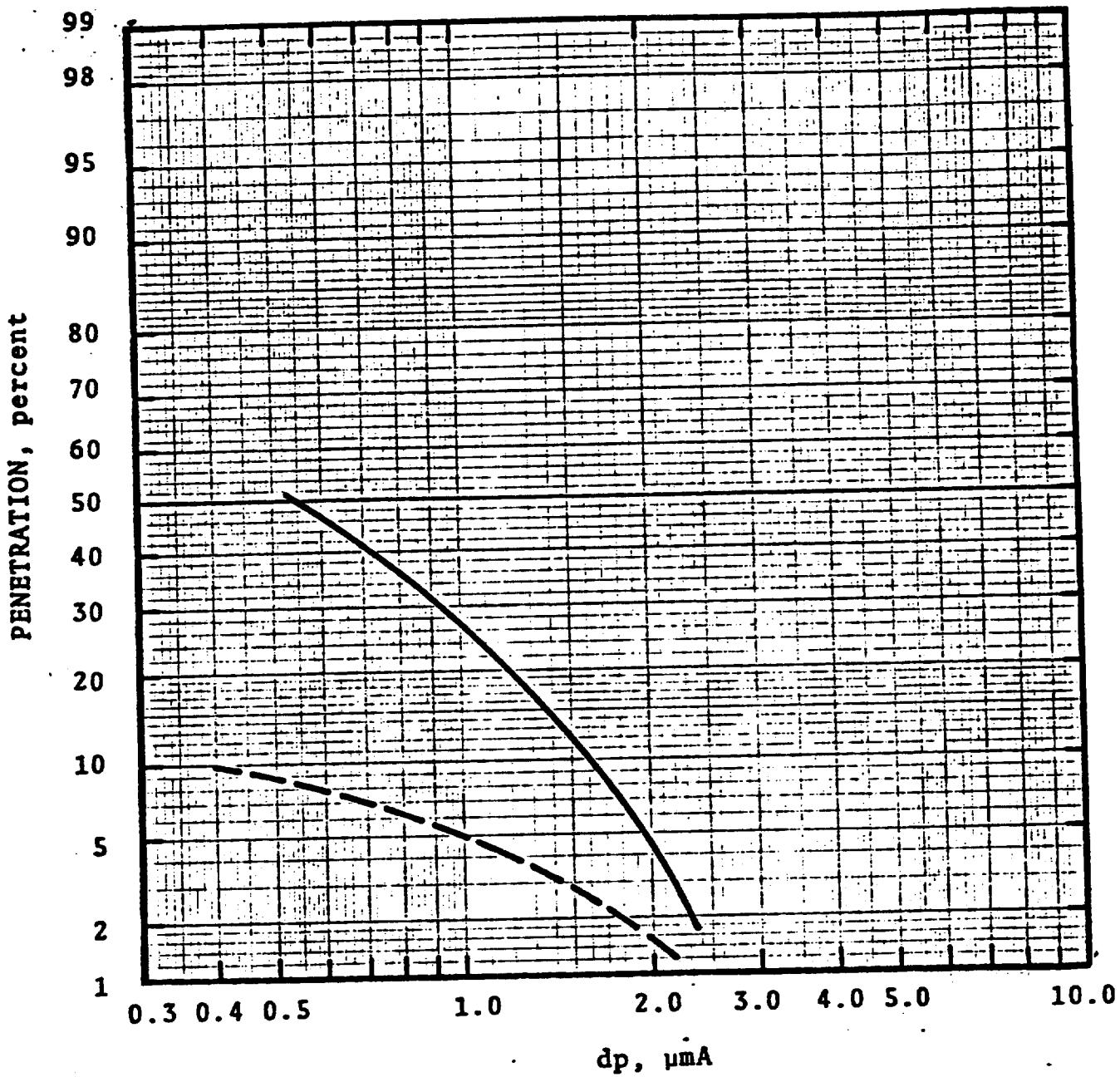


Figure 7-46 Predicted and Experimental Penetration Run 37/24

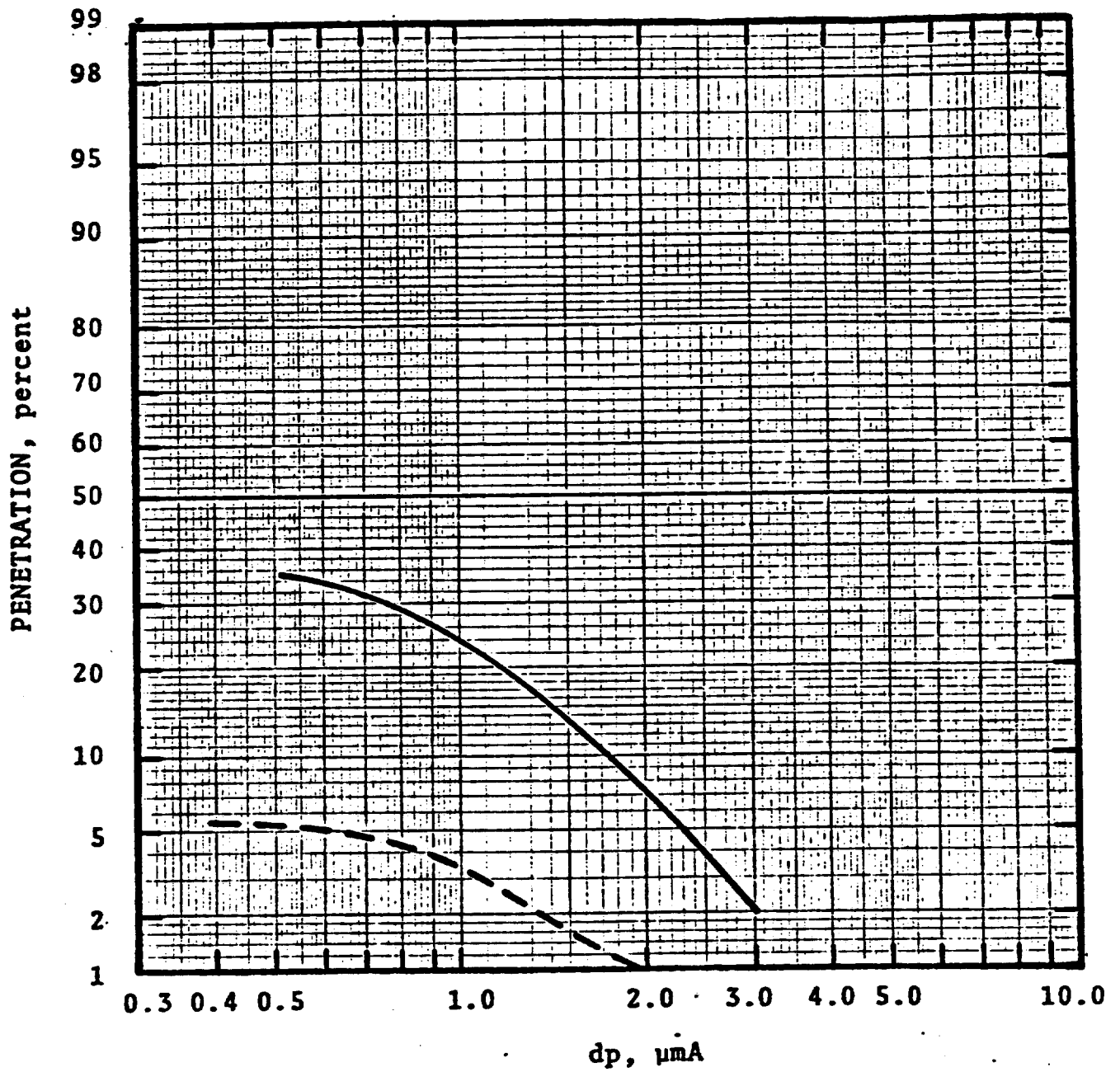


Figure 7-47 Predicted and Experimental Penetration Run 37/25

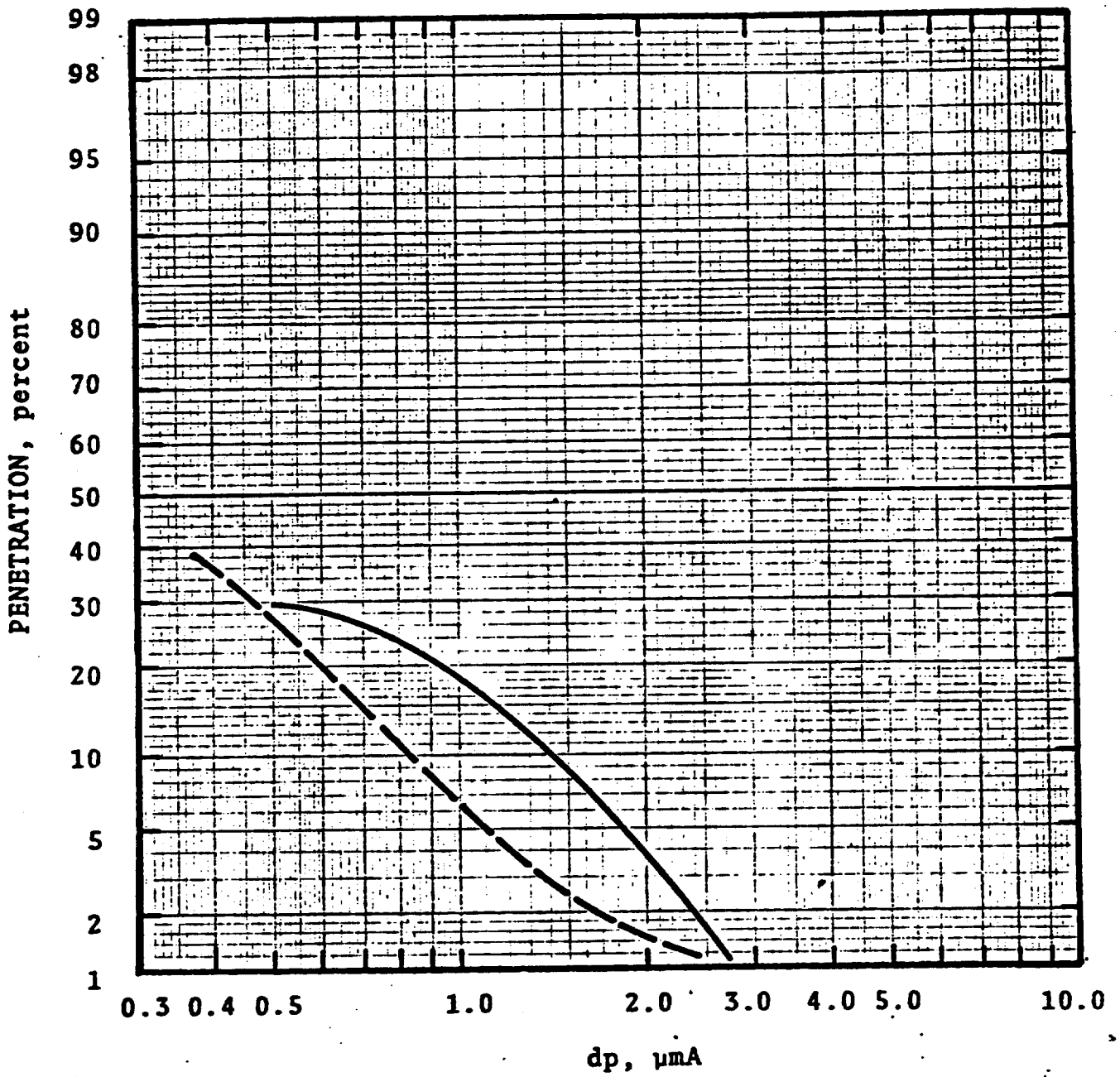


Figure 7-48 Predicted and Experimental Penetration Run 37/26

SECTION 8

ECONOMIC ANALYSIS

OPTIMUM SYSTEM DESIGN

The optimum F/C scrubber system design for this application would not be significantly different ^{from} than the demonstration plant and the process design would remain substantially unchanged. The major modifications recommended for an optimum system involve equipment redesign and specification to reduce capital expense. Figure 8-1 shows a flow sheet for an optimum system.

The major area where redesign can provide significant cost savings is a single combined condenser/scrubber vessel. The diameter can be reduced from the size of the demonstration plant by increasing the superficial velocity through the packing section. The depth of the packing can be reduced to approximately 1 m, based on the results obtained in the demonstration plant.

The second item which can result in cost savings is an alternate choice in cooling towers. The cooling tower chosen for the demonstration plant was dictated by space requirements. The cooling tower had to be elevated on a platform above the saturator and sump. Consequently the most compact tower was chosen, which was not the most economical or energy efficient.

In the course of the project bids were obtained by other manufacturers. A wood-filled cooling tower would be the most likely choice if space were not at a premium. Such a tower would require only 30 HP, compared to 60 HP for the tower used on the demonstration plant. The wood packing may have some advantage over epoxy coated steel in terms of corrosion resistance. A second circulating water pump would be required for the system but the total cost would be less ^{because} since an expensive structural

steel platform would not be needed.

The saturator design would be changed in an optimum system. The saturator was designed to allow the equipment to be fit into the available space at the foundry. An optimum system would have a smaller, more compact saturator.

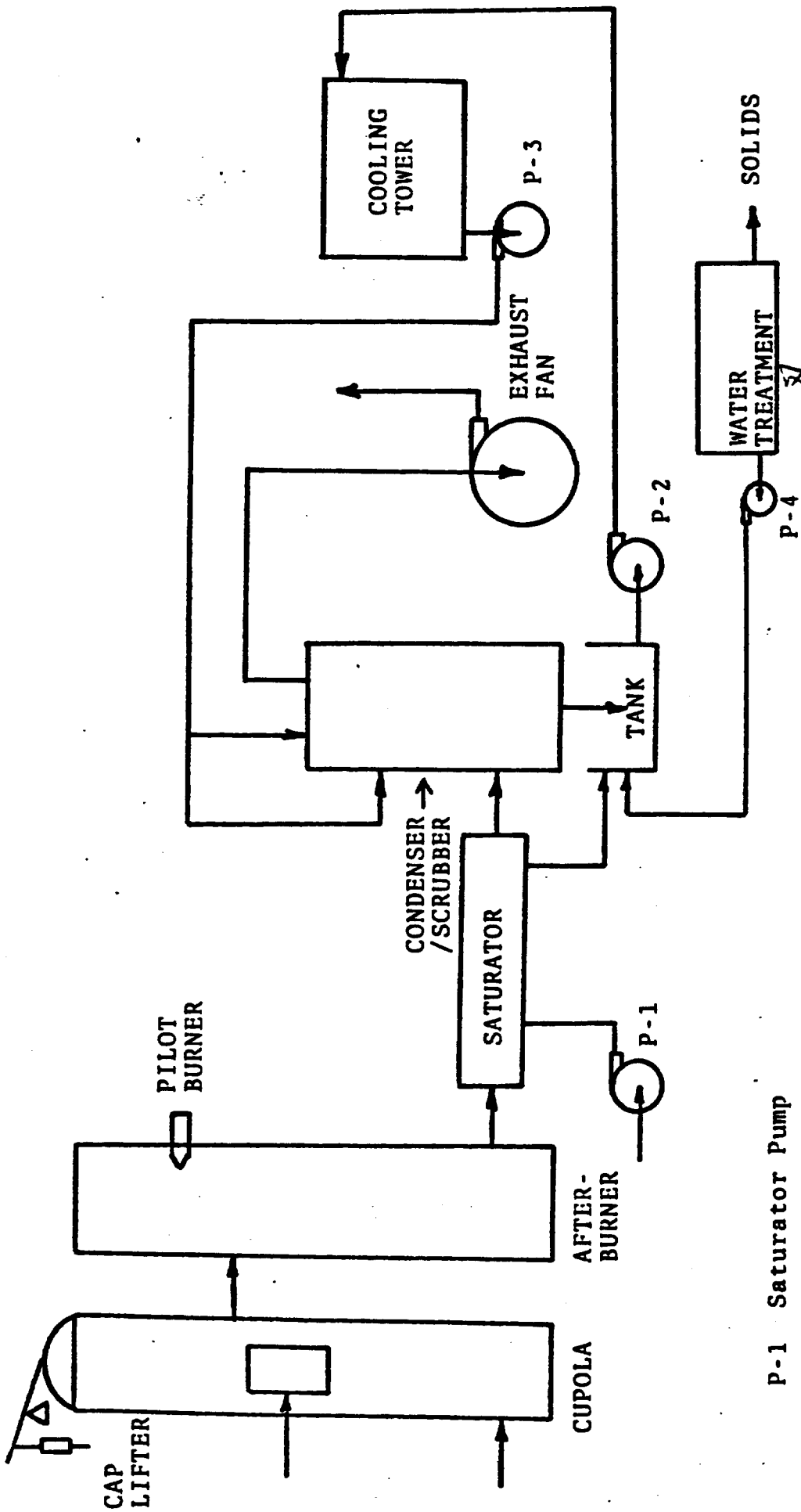
The settler used on the demonstration system provided acceptable performance, however the condenser, scrubber and sump all were subject to deposition of fine sandy material which required removal at frequent intervals. The material which settled out was fairly large, which is apparent from the fact that it settled out in these process vessels. Sloped bottoms should be used in all of these vessels.

It is also recommended that a moving belt filter be used instead of the gravity settler to remove this sandy material. These can be purchased at a lower cost than the settler which was used on the demonstration plant.

CAPITAL COST ESTIMATES

The capital cost of an optimum F/C system would consist of the total equipment costs and other direct costs such as installation, piping, electrical, etc., along with indirect costs such as engineering, construction overhead, contingencies, etc. The total equipment costs were calculated as described below. For equipment identical or similar to that purchased for the demonstration plant, costs were scaled up from those incurred for the purchased component. For the condenser/scrubber vessel, cost estimates were prepared with standard techniques and then compared to purchased cost for the demonstration plant scrubber and condenser vessels. The fan and motor costs were obtained from the data presented by Neveril et al. (1978). Tables 8-1 and 8-2 show the total equipment costs for the F/C system and high energy scubber respectively.

The other direct costs were computed by means of ratio factors obtained from Peters (1968) which are based on equipment costs. These factors were confirmed using cost data from the Demonstration Plant. The indirect costs have been estimated in the



- P-1 Saturator Pump
- P-2 Cooling Tower Pump
- P-3 Condenser Pump
- P-4 Water Treatment Pump

Figure 8-1. Optimum F/C Scrubber System Flow Diagram

TABLE 8-1. SUMMARY OF EQUIPMENT COSTS
F/C SCRUBBER SYSTEM

	<u>Unit Cost</u>	<u>Total Cost</u>
Saturator pump & motor	\$ 2,290	
starter	240	\$ 2,530
Cooling loop pumps & motors	6,950	
starters	580	7,530
Exhaust fan	3,890	
motor & starter	8,290	12,180
Cooling tower	29,370	
fan starter	280	29,650
Saturator shell	3,650	
internals	1,300	4,960
Condenser/scrubber shell	20,000	
internals	8,000	28,000
Tank	4,630	4,630
Belt filter	12,900	12,900
		<hr/>
	TOTAL EQUIPMENT COST	\$102,380

**TABLE 8-2. SUMMARY OF EQUIPMENT COSTS
CONVENTIONAL SCRUBBER**

	<u>Unit Cost</u>	<u>Total Cost</u>
Saturator pump & motor	\$ 2,290	
starter	240	\$ 2,530
Scrubber pump & motor	3,880	
starter	195	4,075
Saturator vessel	3,650	
internals	1,300	4,960
Exhaust fan	5,350	
motor & starter	18,450	23,800
Scrubber vessel	14,600	
internals	10,900	25,500
Belt filter	12,900	12,900
	TOTAL EQUIPMENT COST	\$73,765

same manner with factors suggested by Peters (1968). Tables 8-3 and 8-4 show the indirect costs for the F/C system and the high energy scrubber. All costs were adjusted to December 1979 by means of the M&S cost index.

OPERATING COSTS

The operating costs for the air pollution control system consist of the annual cost of the utilities (power and water), raw material and maintenance. Table 8-5 shows the power requirement for both the F/C scrubber system and a conventional scrubber. The F/C scrubber system is shown to require only 65% of the power of the conventional scrubber. The exhaust fan for the conventional scrubber requires more than twice the power of the F/C system.

The total operating costs are summarized in Table 8-6. The power cost was estimated at 6.5¢/Kwhr. The water cost estimate was 3.5¢/1,000ℓ. The raw materials included soda ash for neutralizing the scrubber liquor at 26.5¢/Kg and flocculant to improve water treatment at \$1.15/ℓ. The total operating cost for the F/C scrubber system was found to be \$84,361 compared to ~~\$111,503~~ for the conventional scrubber. The annual operating cost of the F/C scrubber system was about 75% of the cost for a conventional scrubber for this application.

\$139,830
Re. Table 8-6

\$123,675
Re. Table 8-6

The return on the investment, after taxes, is only 8.3%.

88%

TABLE 8-3. DIRECT AND INDIRECT COST
F/C SYSTEM

<u>Direct</u>	<u>Ratio</u>	<u>Cost, \$</u>
Equipment	1.00 ✓	\$102,380
Installation	0.40 ✓	40,952
Instruments	0.10 ✓	10,238
Piping and Ducting	0.40 ✓	40,952
Electrical	0.10 ✓	10,238
Site Preparation	0.05 ✓	5,119
Total Direct Cost	2.05 ✓	\$209,879
 <u>Indirect</u>		
Engineering	0.40 ✓	40,952
Construction Overhead	0.45 ✓	46,071
Contractors Fee	0.10 <i>low</i>	10,238
Contingency	0.40 ✓	40,952
Total Indirect Costs	1.35 ✓	\$138,213
Total Capital Investment	3.40 ✓	\$348,092

*One might argue with the numbers,
and the method is OK*

**TABLE 8-4. DIRECT AND INDIRECT COST
CONVENTIONAL SCRUBBER**

<u>Direct</u>	<u>Ratio</u>	<u>Cost, \$</u>
Equipment	1.00	\$ 73,765
Installation	0.40	29,506
Instruments	0.10	7,377
Piping and Ducting	0.40	29,506
Electrical	0.10	7,377
Site Preparation	0.05	3,687
Total Direct Cost	2.05	\$751,218
<u>Indirect</u>		
Engineering	0.40	29,506
Construction Overhead	0.45	33,194
Contractors Fee	0.10	7,377
Contingency	0.40	29,506
Total Indirect Costs	1.35	\$ 99,582
Total Capital Investment	3.40	\$250,800

TABLE 8-5. SUMMARY OF POWER REQUIREMENTS

	Power, Kw (HP)	
	<u>F/C Scrubber</u>	<u>Conventional Scrubber</u>
Exhaust fan	156 (210)	332 (445)
Saturator pump	10 (13)	10 (13)
Scrubber pump	2 (2)	3 (4)
Cooling water pumps	33 (44)	-
Cooling tower fan	<u>22 (30)</u>	<u>-</u>
Total Power Required	223 (299)	345 (462)

TABLE 8-6. SUMMARY OF ANNUAL OPERATING COSTS

<u>Item</u>	<u>Unit Cost</u>	<u>F/C Scrubber System</u>	<u>Conventional Scrubber</u>
Capital Cost	<i>Should depreciate the whole thing</i> 10 yr, S.L. depreciation	\$34,809 \$10,238	\$25,080 \$7,377
Maintenance	<i>fixed cap. investment</i> 6% of equipment cost	\$20,886 6,143	15,850 4,426
Power Cost *	6.5¢/Kwhr	57,980 ✓	89,700 ✓
Water Use	3.5¢/1,000 l	2,000	2,000
Raw Materials	soda ash 26.5¢/Kg flocculent \$1.15/l	<u>8,000</u>	<u>8,000</u>
TOTAL OPERATION COST		\$84,361	\$111,503
*Power cost estimated at 4,000 hours per year.		\$123,675	\$139,830

$$\% ROI = \frac{139,830 - 123,675}{2(348,042 - 250,800)} \times 100 = \frac{16,155 \times 100}{2 \times 97,242} = 8.3\% \text{ return after taxes}$$

88%

REFERENCES

- Calvert, S., J. Goldshmid, D. Leith, N. Jhaveri. Feasibility of Flux Force/Condensation Scrubbing for Fine Particle Collection. A.P.T., Inc. EPA Contract No. 68-02-0256. NTIS #PB 227 307. October 1973.
- Calvert, S., J. Goldshmid, D. Leith, N. Jhaveri. Scrubber Handbook. A.P.T., Inc. EPA Contract No. CPA-70-95. NTIS #PB 213 016. August 1972.
- Calvert, S., S. Gandhi. Fine Particle Collection By A Flux-Force/Condensation Scrubber: Pilot Demonstration. A.P.T., Inc. EPA Contract No. 68-02-1869. NTIS #EPA-600/2-77-238. December 1977.
- Calvert, S., N. Jhaveri, T. Huisking. Study of Flux Force/Condensation Scrubbing of Fine Particles. A.P.T., Inc. EPA Contract No. 68-02-1082. NTIS # EPA-600/2-75-018 August 1975.
- Green, H.L., W. R. Lane, Particulate Clouds E. & F. N. Spon Ltd. London, 1964.
- Neveril, R.B., J. V. Price and K. L. Engdahl, Capital and Operating Costs of Selected Air Pollution Control Systems Parts II and IV. J. Air Pollution Control Association V28 N9 P963, September 1978 and V28 N10, October 1978.
- McCain, J.D., Clinard, G.I., Felix L. G., Johnson J. W., A Data Reduction System for Cascade Impactors. EPA No. 600/7-78-132a, July 1978.
- Peters, M.S., K. D. Timmerhaus, Plant Design and Economics for Chemical Engineers, McGraw-Hill Book Company, 1968.
- Yung, S., S. Calvert, H. Barbarika, Ventrui Scrubber Performance Model. Environmental Science and Technology V 12 p.456, April 1978.